Mathematisches Forschungsinstitut Oberwolfach

Report No. 5/2020

DOI: 10.4171/OWR/2020/5

Boundary Element Methods

Organized by
Stéphanie Chaillat-Loseille, Palaiseau
Ralf Hiptmair, Zürich
Olaf Steinbach, Graz

2 February – 8 February 2020

Abstract. The field of *boundary element methods* (BEM) relies on recasting boundary value problems for (mostly linear) partial differential equations as (usually singular) integral equations on boundaries of domains or interfaces. Its main goal is the design and analysis of methods and algorithms for the stable and accurate discretization of these integral equations, the data-sparse representation of the resulting systems of equations, and their efficient direct or iterative solution.

Boundary element methods play a key role in important areas of computational engineering and physics addressing simulations in acoustics, electromagnetics, and elasticity. Thus progress in boundary element method, both theoretical and algorithmic, is definitely relevant beyond mathematics. Boundary element methods had been developed for many decades, but during the past two decades the field has seen a surge in research activity, spurred by algorithmic and theoretical breakthroughs concerning BEM for electromagnetics, time-domain methods, new approaches to eigenvalue problems, adaptivity, local low-rank matrix compression, and frequency-explicit analysis, to name only a few.

The contributions in this report give an impressive panorama of the many and diverse current research activities in BEM. They range profound mathematical analyses with striking results to new algorithmic developments. On the one hand, the results are based on a large variety of tools from many areas of mathematics. On the other hand, research in BEM blazes the trail for progress in the numerical treatment of non-local operators, a field that is rapidly gaining importance.

Mathematics Subject Classification (2010): 65N38, 65M38, 74S15, 78M15, 80M15.

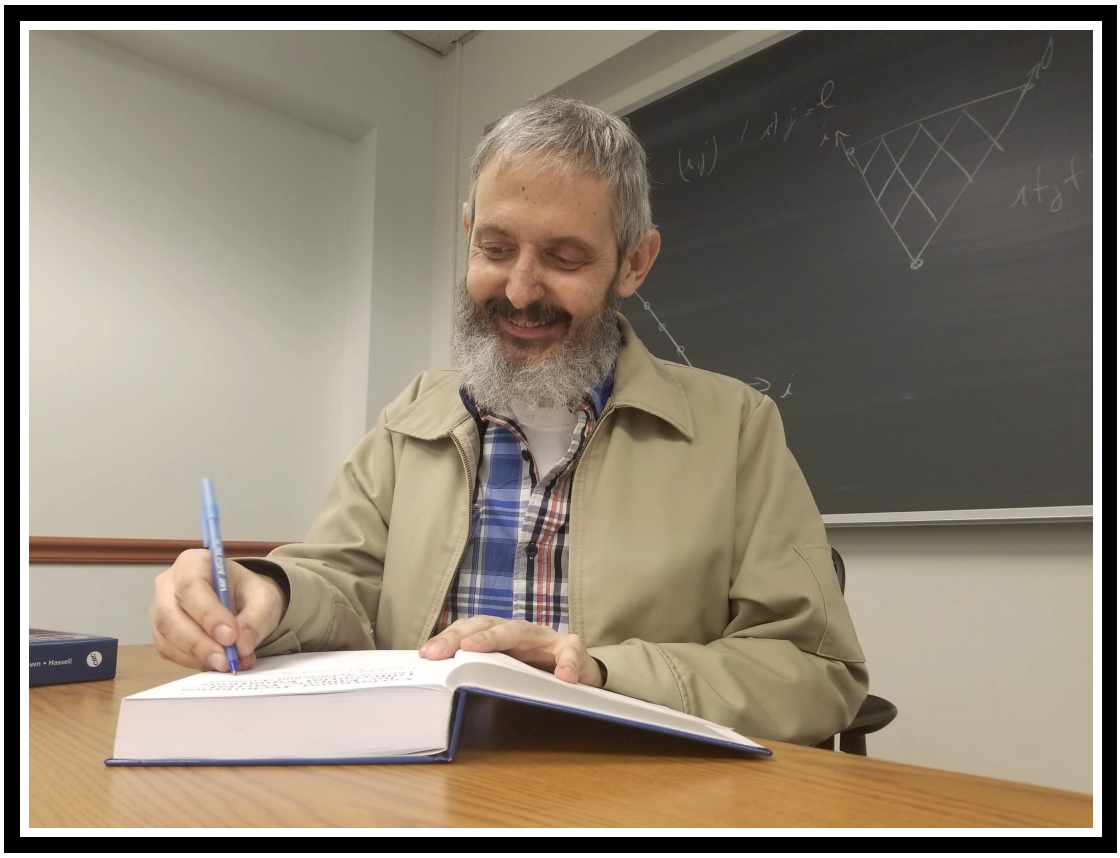

Dedicated to Francisco-Javier Sayas (1968–2019)[1]

Introduction by the Organizers

The title page tells you that this workshop on *Boundary element methods* has been organised by Stéphanie Chaillat-Loseille, Ralf Hiptmair, and Olaf Steinbach. However, it was a group of four who made plans for this event in 2018, and the one name missing now is that of our dear friend and esteemed colleague **Francisco-Javier Sayas** who prematurely passed away about a year before the beginning of the workshop, succumbing to cancer.

Yet, Francisco-Javier Sayas will live on, in our memories and, forever, in his results and contributions, since mathematics is about establishing eternal truths. No doubt, Francisco-Javier Sayas gave us plenty of these truths through his seminal, influential, and inspiring works in the field of boundary element methods, and in the wider area of numerical analysis and computational mathematics. Many contributions in this collection reference his work and rely on his ideas. We know that it was important to Francisco-Javier Sayas that he had contributed to progress in mathematics. We believe that this workshop is an impressive confirmation that this is definitely true.

[1]Picture courtesy of Hasan Eruslu and Shukai Du, PhD students of F. J. Sayas

Starting in the 1960s, the field of boundary element methods (BEM) has been developed for many decades. Dismissed as outdated for some time, breakthrough ideas have resuscitated research efforts and restored BEM as both an exciting area of numerical analysis and an important class of methods in computational science and engineering. Right now the field is brimming with activity and much progress has been made concerning, e.g., electromagnetic boundary integral equations, time-domain methods, new approaches to eigenvalue problems, a posteriori error estimators and adaptivity, local low-rank matrix compression techniques, preconditioning, and frequency-explicit analysis of boundary integral equations and boundary element methods. These and several other topics were covered in the presentations and private discussions of the 27 participants from 9 countries.

Clear evidence of timeliness and significance of research on boundary element methods in the broad field of the mathematical and numerical analysis of partial differential equations is the *John Todd Prize in Numerical Analysis* awarded to Euan Spence from the University of Bath, UK, one of the participants of the workshop. The prize ceremony took place during the workshop. The laudation of the scientific work of E. Spence was given by Simon Chandler-Wilde. In a striking scientific talk, **Euan Spence** then discussed the perennial question, if the Galerkin method converges for the standard second-kind double-layer integral equation for the Laplacian on Lipschitz domains. He gave an impressive overview of the efforts towards answering this question, and finally presented counterexamples showing that the answer is "no".

This showed that, although the numerical analysis of boundary element methods is well established, there are still new developments and results as regards the foundations of the method. Boundary integral equations for the Helmholtz equation on a fractal screen or in a domain with a fractal boundary were analyzed by **Simon Chandler-Wilde**. A rigorous theoretical analysis of a novel discretization was given by **Víctor Domínguez**. That method is a non–conforming Petrov-Galerkin scheme, which is combined with appropriate quadrature formulas to ensure stability and convergence. **Heiko Gimperlein** discussed the regularity and singular behavior of solutions of pseudo-differential equations in polyhedral domains, in particular for the integral fractional Laplacian. The numerical approximation of these equations by using *hp*-finite elements and graded meshes was then described by **Jakub Stocek**.

The optimal control of non-local operator equations by using wavelet compression techniques was the topic of the talk by **Helmut Harbrecht**. Also **Ralf Hiptmair** put BEM into a larger framework and highlighted the convergence of different formulations in the context of computing shape derivatives. New functional a posteriori error estimators to drive adaptive refinement of the boundary element approximation were proposed by **Dirk Praetorius**. The combination of topological and shape optimization tools for the solution of imaging problems subject to the electromagnetic wave equation was considered by **Frédérique Le Louër**. **Gerhard Unger** presented an overview on state of the art boundary

element methods for the numerical solution of eigenvalue problems in acoustics and electromagnetics.

Boundary element methods for acoustic and electromagnetic scattering often suffer from spurious modes which correspond to eigensolutions of related interior problems. Although there are modified or combined boundary integral equations available for stabilization, these techniques may exhibit limitations. A new approach for the solution of the magnetic field integral equation was presented by **Francesco Andriulli**. It boils down to multiplying the standard double layer magnetic field integral equation with a double layer boundary integral operator representing the solution of a Yukawa partial differential equation. **Jürgen Dölz** gave an overview on recent advances in isogeometric boundary element methods for electromagnetic scattering problems. Wave propagation in heterogeneous and unbounded media using finite and boundary element methods was discussed by **Mahadevan Ganesh**. In the case of quasi-periodic layered media one may use fast direct solvers for scattering problems, as proposed by **Adrianna Gillman**. The extension of the Wigner-Smith time delay theory characterizing the delay experienced by particles to Maxwell's equations and their potential applications in computational electromagnetics was discussed by **Eric Michielssen**.

Calderón or operator preconditioning is a well established technique for the iterative solution of huge linear systems of algebraic equations arising from the discretization of boundary integral equations. Although the spectral condition number of the preconditioned system is bounded independently of the used discretization, it may depend on the physical structure of the underlying problem, e.g., the wave number in acoustic or electromagnetic scattering, or the geometrical properties of the computational domain. In recent years, new techniques using modified kernel functions were developed to overcome those restrictions. In his talk, **Martin Averseng** has considered Helmholtz scattering problems for a thin screen in 2D, where he used weighted versions of the layer potentials to improve both the convergence of the numerical method, and the conditioning.

Domain decomposition methods are used to couple different physical models and different discretizations, as well as for parallelisation and for the construction of optimal preconditioning strategies. In the case of local Helmholtz problems, where spurious modes can appear, Robin type interface conditions have to be used to gain stability of the formulation. The optimal choice of the coupling parameters involved and modified Robin type transmission conditions using local Steklov-Poincaré operators were discussed in the talk by **Xavier Claeys**. A different strategy of domain decomposition methods using boundary integral equations are multiple trace formulations, which can be discretized by using spectral non-comforming boundary elements as discussed by **Carlos Jerez-Hanckes**.

The acceleration of boundary element methods by "fast methods" is mandatory to end up with competitive algorithms. **Steffen Börm** discussed two hybrid compression algorithms, the hybrid cross approximation, and the Green cross approximation, which both result in low rank approximations of admissible blocks.

The sparse approximation of integral operators related to the lossy Helmholtz (Yukawa) equation was the topic of the talk by **Stefan Sauter**.

The numerical analysis and efficient implementation of boundary integral equations and boundary element methods in the time domain turned out to be one of the most important and most challenging topics of the workshop. **Stéphanie Chaillat** discussed the use of fast solvers in the frequency domain to simulate fluid structure interaction problems in the time domain, in particular for large structures and high frequencies. High-frequency scattering problems in 3D elastodynamics using standard and preconditioned combined field integral equations were considered in the talk by **Marion Darbas**. The time, space, and velocity distribution for collisionless electron plasma described by the Vlasov-Poisson system and the combination of boundary element methods with a particle method for its numerical solution was discussed by **Sergej Rjasanow**. **Olaf Steinbach** gave an overview on recent results on coercive variational formulations for the heat equation, and on the analysis of related space-time finite and boundary element methods. The extension of this approach to a new setting of boundary integral equations for the wave equation was then given by **Carolina Urzúa-Torres**. In the particular case of moving boundaries, **Johannes Tausch** discussed appropriate quadrature rules.

Acknowledgement: The workshop organizers appreciate the support of the MFO for J. Dölz and M. Averseng in the framework of the "Oberwolfach Leibniz Graduate Students" program. The MFO and the workshop organizers would like to thank the National Science Foundation for supporting the participation of junior researchers in the workshop by the grant DMS-1641185, "US Junior Oberwolfach Fellows". Moreover, the MFO and the workshop organizers would like to thank the Simons Foundation for supporting M. Ganesh and J. Tausch in the "Simons Visiting Professors" program at the MFO.

Workshop: Boundary Element Methods

Table of Contents

Abstracts

Boundary Element Methods in Electromagnetics Leveraging the Quasi-Helmholtz Projectors

Francesco P. Andriulli
(joint work with Adrien Merlini, Yves Beghein, Kristof Cools, Eric Michielssen)

The analysis of electromagnetic scattering by perfect electrically conducting (PEC) objects can be performed via boundary element method (BEM) formulations, that have significant advantages with respect to other methods in that they only require the boundary of the scatterer to be discretized and they automatically enforce radiation conditions. Two of the most widely employed BEM formulations, the electric and magnetic field integral equations (EFIE and MFIE) suffer from several stability issues that impede their usage in realistic scenarios. The limitations include ill-conditioning (i) at low frequencies, (ii) at dense refinements, (iii) on multiply connected geometries, in addition to (iv) a loss of significant digits at low frequencies and (v) non-physical resonances. While the problems (i), (ii) and (iii) plaguing the EFIE have been successfully addressed using Calderón approaches and quasi-Helmholtz projectors [2], the MFIE still has to be stabilized. This is critical because, to obtain a formulation immune from (v) the EFIE and MFIE must be combined into a combined field integral formulation (CFIE), that inherits the flaws of the electric and magnetic formulations it is based on. This is why we propose a new magnetic equation that is immune from the problems (i), (iii), and (iv) of its standard counterpart, to form a new CFIE immune to problems (i) to (v). Missing details and an extended treatment can be found in [1].

The EFIE and MFIE

$$(1)\qquad \left(\boldsymbol{\mathcal{T}}_k \boldsymbol{j}\right)(\boldsymbol{r}) = \hat{\boldsymbol{n}} \times \boldsymbol{E}^i(\boldsymbol{r}) \quad \text{and} \quad \left(\left(\frac{\boldsymbol{\mathcal{I}}}{2} + \boldsymbol{\mathcal{K}}_k\right)\boldsymbol{j}\right)(\boldsymbol{r}) = \hat{\boldsymbol{n}} \times \boldsymbol{H}^i(\boldsymbol{r})\,,$$

where

$$(2)\qquad \left(\boldsymbol{\mathcal{T}}_k \boldsymbol{j}\right)(\boldsymbol{r}) = \left(\boldsymbol{\mathcal{T}}_{\mathrm{s},k} \boldsymbol{j}\right)(\boldsymbol{r}) + \left(\boldsymbol{\mathcal{T}}_{\mathrm{h},k} \boldsymbol{j}\right)(\boldsymbol{r})\,,$$

$$(3)\qquad \left(\boldsymbol{\mathcal{T}}_{\mathrm{s},k} \boldsymbol{j}\right)(\boldsymbol{r}) = \mathrm{j}k\eta\hat{\boldsymbol{n}} \times \int_\Gamma \frac{\mathrm{e}^{-\mathrm{j}kR}}{4\pi R}\boldsymbol{j}(\boldsymbol{r}')\mathrm{d}s'\,,$$

$$(4)\qquad \left(\boldsymbol{\mathcal{T}}_{\mathrm{h},k} \boldsymbol{j}\right)(\boldsymbol{r}) = -\frac{\eta}{\mathrm{j}k}\hat{\boldsymbol{n}} \times \nabla \int_\Gamma \frac{\mathrm{e}^{-\mathrm{j}kR}}{4\pi R}\nabla' \cdot \boldsymbol{j}(\boldsymbol{r}')\mathrm{d}s'\,,$$

$$(5)\qquad \left(\boldsymbol{\mathcal{K}}_k \boldsymbol{j}\right)(\boldsymbol{r}) = -\hat{\boldsymbol{n}} \times p.v. \int_\Gamma \nabla \times \frac{\mathrm{e}^{-\mathrm{j}kR}}{4\pi R}\boldsymbol{j}(\boldsymbol{r}')\mathrm{d}s'\,,$$

relate the impinging electromagnetic wave $(\boldsymbol{E}^i, \boldsymbol{H}^i)$ with wavenumber k to the surface current density $\boldsymbol{j}(\boldsymbol{r})$ it induces on the boundary Γ of the scatterer with outwards pointing normal $\hat{\boldsymbol{n}}$, characterized by the medium parameter η. To proceed with a numerical resolution of the problem following a Petrov-Galerkin approach, the unknown $\boldsymbol{j}(\boldsymbol{r})$ is expanded with with N zeroth order Raviart–Thomas (RT)

functions $\{\boldsymbol{f}_m\}$ and the EFIE is tested with rotated RT functions while the MFIE is tested with rotated Buffa-Christiansen (BC) $\{\hat{\boldsymbol{n}} \times \boldsymbol{g}_m\}$ function (refer to [1] for further details). The resulting linear systems are

$$\boldsymbol{T}\boldsymbol{j} = (\boldsymbol{T}_{\mathrm{s}} + \boldsymbol{T}_{\mathrm{h}})\,\boldsymbol{j} = \boldsymbol{v}_e \quad \text{and} \quad \left(\frac{\boldsymbol{G}^{\mathrm{T}}}{2} + \boldsymbol{K}_k\right)\boldsymbol{j} = \boldsymbol{v}_h\,, \tag{6}$$

where the matrix elements are $[\boldsymbol{T}]_{ij} = (\hat{\boldsymbol{n}} \times \boldsymbol{f}_i, \boldsymbol{\mathcal{T}}_k \boldsymbol{f}_j)$, $[\boldsymbol{T}_{\mathrm{s}}]_{ij} = (\hat{\boldsymbol{n}} \times \boldsymbol{f}_i, \boldsymbol{\mathcal{T}}_{\mathrm{s},k} \boldsymbol{f}_j)$, $[\boldsymbol{T}_{\mathrm{h}}]_{ij} = (\hat{\boldsymbol{n}} \times \boldsymbol{f}_i, \boldsymbol{\mathcal{T}}_{\mathrm{h},k} \boldsymbol{f}_j)$, $[\boldsymbol{K}_k]_{ij} = (\hat{\boldsymbol{n}} \times \boldsymbol{g}_i, \boldsymbol{\mathcal{K}}_k \boldsymbol{f}_j)$, $[\boldsymbol{G}]_{ij} = (\boldsymbol{f}_i, \hat{\boldsymbol{n}} \times \boldsymbol{g}_j)$, $[\boldsymbol{v}_e]_i = \left(\hat{\boldsymbol{n}} \times \boldsymbol{f}_i, \hat{\boldsymbol{n}} \times \boldsymbol{E}^i\right)$, and $[\boldsymbol{v}_h]_i = \left(\hat{\boldsymbol{n}} \times \boldsymbol{g}_i, \hat{\boldsymbol{n}} \times \boldsymbol{H}^i\right)$. These discretizations correspond to the standard approaches that suffer from a combination of the problems (i) to (v). In particular, this discretization of the MFIE fails to accurately represent the static ($k = 0$) nullspace of the MFIE on multiply connected geometries, which is a symptom of its lack of accuracy in finite-precision. In this form, the problem can only be mitigated by employing prohibitively expensive integration rules to compute the numerical integrals, which renders the overall scheme unpractical. At low frequencies, the accuracy of the standard MFIE is further compromised by a loss of significant digits in the non-solenoidal part of the solution, which scales as $\mathcal{O}(k)$ while the solenoidal part scales as $\mathcal{O}(1)$. This ill-scaling leads to a loss of digits in the non-solenoidal part of the solution and will cause the far field computation, which relies on both part of the solution, to amplify numerical noise for a large class of right-hand-sides.

To address these issues we propose a new MFIE equation

$$\left(\frac{\boldsymbol{\mathcal{I}}}{2} - \boldsymbol{\mathcal{K}}_{\mathrm{i}k}\right)\left(\frac{\boldsymbol{\mathcal{I}}}{2} + \boldsymbol{\mathcal{K}}_k\right)(\boldsymbol{j}) = \left(\frac{\boldsymbol{\mathcal{I}}}{2} - \boldsymbol{\mathcal{K}}_{\mathrm{i}k}\right)\left(\hat{\boldsymbol{n}}_r \times \boldsymbol{H}^i\right)\,, \tag{7}$$

which a corresponding discretization and low-frequency stabilization which reads

$$\boldsymbol{M}^{\mathrm{T}}\left(\frac{\boldsymbol{G}^{\mathrm{T}}}{2} - \boldsymbol{K}_{\mathrm{i}k}\right)\boldsymbol{G}^{-\mathrm{T}}\left(\frac{\boldsymbol{G}^{\mathrm{T}}}{2} + \boldsymbol{K}_k\right)\boldsymbol{M}\boldsymbol{i} = \boldsymbol{M}^{\mathrm{T}}\left(\frac{\boldsymbol{G}^{\mathrm{T}}}{2} - \boldsymbol{K}_{\mathrm{i}k}\right)\boldsymbol{G}^{-\mathrm{T}}\boldsymbol{v}_h \tag{8}$$

where

$$\boldsymbol{M} = \boldsymbol{P}^{\boldsymbol{\Lambda H}}\alpha^{-1} - \mathrm{i}\boldsymbol{P}^{\boldsymbol{\Sigma}}\alpha\,, \quad \boldsymbol{M} = \boldsymbol{P}^{\boldsymbol{\Sigma H}}\alpha^{-1} - \mathrm{i}\boldsymbol{P}^{\boldsymbol{\Lambda}}\alpha\,, \tag{9}$$

with $\boldsymbol{M}\boldsymbol{i} = \boldsymbol{j}$ and where $\boldsymbol{P}^{\boldsymbol{\Sigma}} = \boldsymbol{\Sigma}(\boldsymbol{\Sigma}^{\mathrm{T}}\boldsymbol{\Sigma})^{+}\boldsymbol{\Sigma}^{\mathrm{T}}$ and $\boldsymbol{P}^{\boldsymbol{\Lambda H}} = \mathbf{I} - \boldsymbol{P}^{\boldsymbol{\Sigma}}$ are the projector to the non-solenoidal and solenoidal RT subspaces and $\boldsymbol{P}^{\boldsymbol{\Lambda}} = \boldsymbol{\Lambda}(\boldsymbol{\Lambda}^{\mathrm{T}}\boldsymbol{\Lambda})\boldsymbol{\Lambda}^{\mathrm{T}}$ and $\boldsymbol{P}^{\boldsymbol{\Sigma H}} = \mathbf{I} - \boldsymbol{P}^{\boldsymbol{\Lambda}}$, the corresponding projectors in the dual (BC) space. The matrix $\boldsymbol{\Sigma}^{\mathrm{T}}$is a discretization of the divergence operator defined on the RT space normalized such that $(\boldsymbol{\Sigma}^{\mathrm{T}}\boldsymbol{\Sigma})$ is the cell-based mesh graph Laplacian, while $\boldsymbol{\Lambda}$ is a discretization of the $\hat{\boldsymbol{n}} \times \nabla$ operator and normalized such that $(\boldsymbol{\Lambda}^{\mathrm{T}}\boldsymbol{\Lambda})$ is the vertex-based mesh graph Laplacian [2]. The stability of the new formulation relies on the fundamental matrix property

$$\boldsymbol{P}^{\boldsymbol{\Sigma H}}(\boldsymbol{G}^{\mathrm{T}}/2 - \boldsymbol{K}_{\mathrm{i}k})\boldsymbol{G}^{-\mathrm{T}}(\boldsymbol{G}^{\mathrm{T}}/2 + \boldsymbol{K}_k)\boldsymbol{P}^{\boldsymbol{\Lambda H}} = \mathbf{0}\,, \tag{10}$$

which we have proved in [1]. The above property can then be used to prove that the ill-scaling of the solenoidal and non-solenoidal parts of the solution can be addressed with adequately scaled projectors. In addition, the same property allows

for a stable discretization of the equation even with finite precision quadrature rules [1].

The problem of the spurious resonances plaguing both the EFIE and the MFIE, can be tackled by forming a combined field formulation out of the stabilized versions of the EFIE from [2] and the new MFIE. The resulting formulation, like its underlying components, is immune to issues (i) to (iv) and can be proven to be immune from spurious resonances. Because $\left(\frac{\boldsymbol{\mathcal{I}}}{2} - \boldsymbol{\mathcal{K}}_{ik}\right)$ is always invertible, this proof amounts to proving that

$$\left(\frac{\boldsymbol{\mathcal{I}}}{2} + \boldsymbol{\mathcal{K}}_{k}\right) + \left(\frac{\boldsymbol{\mathcal{I}}}{2} - \boldsymbol{\mathcal{K}}_{ik}\right)^{-1} \boldsymbol{\mathcal{T}}_{ik} \boldsymbol{\mathcal{T}}_{k} \tag{11}$$

is also always invertible. This follows from the symmetry of $\left(\hat{\boldsymbol{n}} \times \left(\frac{\boldsymbol{\mathcal{I}}}{2} - \boldsymbol{\mathcal{K}}_{ik}\right)^{-1} \boldsymbol{\mathcal{T}}_{ik}\right)^{\mathrm{T}}$ and from a straightforward extension of [4, Theorem 3.1].

In addition to the theoretical developments, the validity of the new MFIE and CFIE has been further verified via numerical examples computed on a multiply connected geometry (torus). The stability of the conditioning of the new schemes is compared against well-established formulations (Fig. 1). In particular, these results confirm the resilience of the new CFIE to spurious resonances (v) and the stability of the new MFIE and CFIE to h-refinement ill-conditioning (ii). The first set of tests shows the stability of the new formulations at low frequencies (i) and (iii) (left in Fig. 2). The second test compares the accuracy of the toroidal and poloidal nullspaces of the new MFIE and mixed MFIEs, showing a clear advantage for the proposed approach.

References

[1] A. Merlini, Y. Beghein, K. Cools, E. Michielssen, and F. P. Andriulli, "Magnetic and Combined Field Integral Equations Based on the Quasi-Helmholtz Projectors", *in press, available online.*

[2] F. P. Andriulli, K. Cools, H. Bagci, F. Olyslager, A. Buffa, S. Christiansen, and E. Michielssen, "A Multiplicative Calderon Preconditioner for the Electric Field Integral Equation",IEEE Transactions on Antennas and Propagation, vol. 56, no. 8, pp. 2398–2412, Aug. 2008.

[3] M. Darbas, "Generalized combined field integral equations for the iterative solution of the three-dimensional Maxwell equations", Applied Mathematics Letters, vol. 19, no. 8, pp. 834–839, 2006.

[4] O. Bruno, T. Elling, R. Paffenroth, and C. Turc, "Electromagnetic integral equations requiring small numbers of Krylov-subspace iterations", Journal of Computational Physics, vol. 228, no. 17, pp. 6169–6183, Sep. 2009.

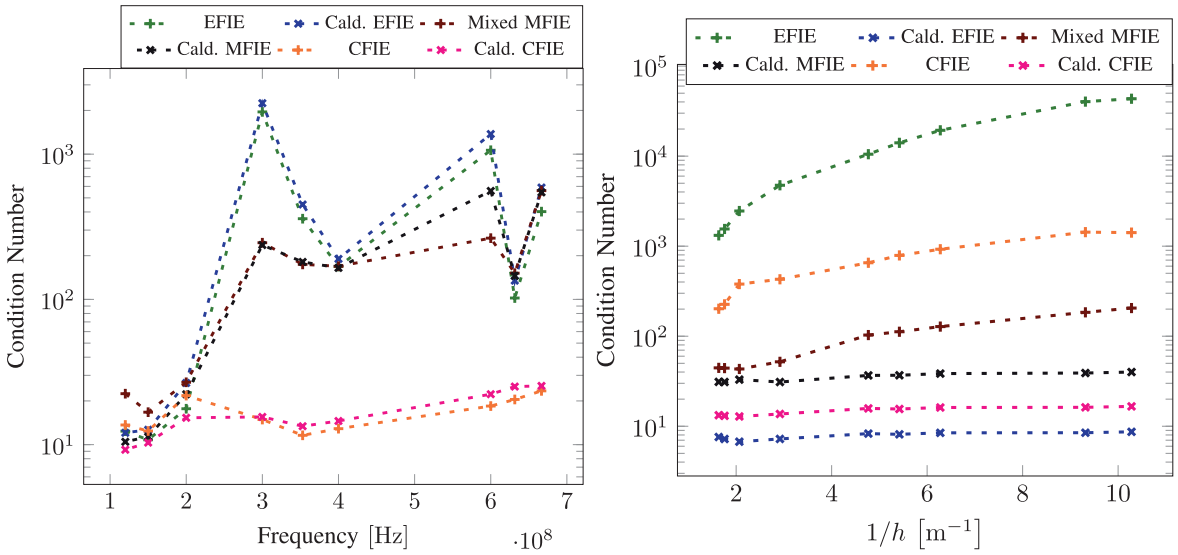

FIGURE 1. Conditioning of different (new and traditional) formulations with respect to frequency (left) and refinement (right), respectively showing that the new CFIE is immune from spurious resonances and that the new MFIE and CFIE are well-conditioning also for increasing h-refinements. The simulated geometry is a torus of radius 0.5 m and tube radius 0.25 m.

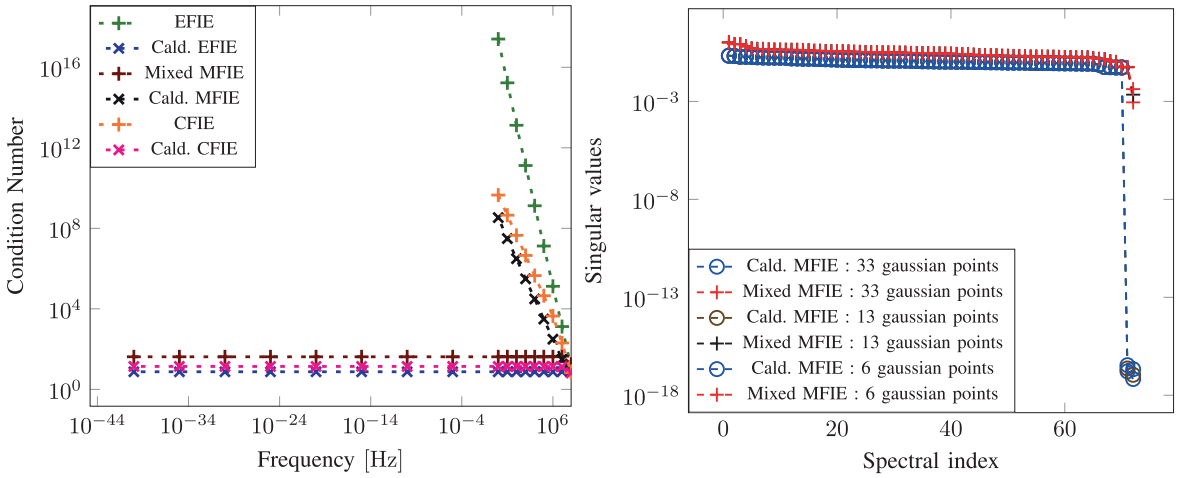

FIGURE 2. (left) Conditioning of different (new and traditional) formulations at low frequency showing the stability of the new schemes. (right) Comparison of the accuracy of the static nullspaces of the mixed and Calderón MFIEs as a function of the number of gaussian integration points used to compute the discrete operators. These results correspond to a torus 0.5 m and tube radius 0.25 m simulated.

Preconditioning integral equations on singular geometries

Martin Averseng
(joint work with François Alouges)

This work is concerned with the integral equations arising from the resolution of the Helmholtz scattering problems by a thin screen in 2D with Dirichlet or Neumann conditions, namely the single-layer and hypersingular integral equations

$$V\lambda = f \quad \text{in } H^{1/2}(\Gamma)\,, \quad W\mu = g \quad \text{in } H^{-1/2}(\Gamma)\,,$$

with the notation of [12]. We focus on the case where Γ is a smooth Jordan curve in $\mathbb{R}^2$ (in particular, **not a Lipschitz domain**). Many theoretical results are well-established for those integral equations. Since the work of Stephan and Wendland [15], we know that they are well-posed, and the operators

$$V : \tilde{H}^{-1/2}(\Gamma) \to H^{1/2}(\Gamma)\,, \quad W : \tilde{H}^{1/2}(\Gamma) \to H^{-1/2}(\Gamma)$$

satisfy Garding type inequalities. The numerical resolution can be performed using the standard Galerkin method with piecewise linear trial functions, on a polygonal mesh of Γ_h, where h denotes the length of the largest segment. Nevertheless, the singularity of the geometry raises two main issues.

Singularity of the solutions:
The solutions λ and μ have edge singularities, making them unsuited to approximation by piecewise polynomials. In fact, if f and g are smooth, it is known that there exist smooth functions α and β such that

$$\lambda = \frac{\alpha}{\omega}, \quad \mu = \omega\beta$$

where $\omega(x) = \sqrt{d(x, \partial\Gamma)}$ is the square root of the distance to the edges of Γ [6]. It is well-known that choosing a uniform mesh in the Galerkin method results in $O(\sqrt{h})$ convergence rate only. This problem can be overcome in several way, including mesh refinement [11], addition of special singular functions in the Galerkin space [15], or cosine change of variables [14, 16].

Ill-conditioned linear systems:
On the other hand, with screens, the usual second kind formulations degenerate, so one has no choice but deal with the first-kind formulations. This is well-known to lead to ill-conditioned linear systems. The popular Calderón preconditioning technique is unfortunately haunted by the duality mismatch, i.e. the fact that for a screen, $(H^{1/2}(\Gamma))' \neq H^{-1/2}(\Gamma)$, leading to poly-logarithmic grows of the condition numbers of the preconditioned systems. The analytic preconditioners method of Darbas and Antoine [7], which are built from discrete approximations of the operator

$$P = \sqrt{-\Delta_\Gamma - k^2 I_d}\,. \tag{1}$$

where Δ_Γ is the Laplace-Beltrami operator on Γ and I_d is the identity, also suffers similar issues. Many recent works are concerned with the question of preconditioning integral equations on open arcs, e.g. [5, 9].

Here we present a new approach that overcomes both difficulties (convergence and conditioning) at the same time. As in [5], we consider weighted versions of the layer potentials, namely

$$V_\omega : \varphi \mapsto V\left(\frac{\varphi}{\omega}\right), \quad W_\omega : \varphi \mapsto W(\omega\varphi).$$

They act naturally in weighted L^2 spaces and in a scale of Sobolev-like spaces built on Chebyshev polynomials of the first and second kind respectively. More precisely, let T_n and U_n be the first and second kind Chebyshev polynomials respectively. Every function $f \in L^2_{\frac{1}{\omega}}$ and $g \in L^2_\omega$ can be be decomposed in Fourier-Chebyshev series

$$f = \sum_{n=0}^{+\infty} \hat{f}_n T_n, \quad g = \sum_{n=0}^{+\infty} \check{g}_n U_n.$$

The coefficients $(\hat{f}_n)_n$ and $(\check{g}_n)_n$ are obtained by orthogonal projections in the spaces $L^2_{\frac{1}{\omega}}$ and L^2_ω. Defining some Sobolev-like scales,

$$T^s = \{f \in L^2_{\frac{1}{\omega}} \mid \sum_n (1+n^2)^s \mid \hat{f}_n|^2 < +\infty\},$$

$$U^s = \{g \in L^2_\omega \mid \sum_n (1+n^2)^s |\check{g}_n|^2 < +\infty\},$$

one finds that $V_\omega : T^s \to T^{s+1}$ and $W_\omega : U^s \to U^{s+1}$ are isomorphisms for all $s \in \mathbb{R}$. We propose to discretize V_ω and W_ω with a Galerkin method in their natural, weighted L^2 scalar product. The Galerkin solutions are then shown to converge quasi-optimally to the exact solutions in energy norm. With piecewise linear trial functions, the maximal order of convergence (wich is the same as for smooth scatterers) is reached when the mesh is quadratically refined, a mild refinement compared to standard methods [3, Thm 2.29, 2.30].

The weighted layer potentials are known to satisfy a Calderón-type identity, generalizing the situation that occurs in smooth geometries [5], so that optimal preconditioning can be achieved in this setting by simply composing the two operators. Here, we propose a new, alternative approach, which generalizes the method of Darbas and Antoine [7].

We start by transplanting a simple pseudo-differential calculus on the segment $\Gamma = [-1, 1]$ (the generalization to a smooth jordan curve is straightforward), by transporting the so-called "periodic pseudo-differential operators" (PPDO) available on a torus (for more details, see [14]). A linear continuous operator $A : T^\infty \to T^{-\infty}$ is called a pseudo-differential operator on the segment (ψDOS) if there exists a "symbol pair" of functions $a_1(x, n)$ and $a_2(x, n)$, smooth in x, such that

$$\forall n \in \mathbb{N}, \quad Au(x) = \sum_{n=0}^{+\infty} a_1(x, n)\hat{u}_n T_n(x) - \omega^2 a_2(x, n)\hat{u}_n U_{n-1}$$

(with the convention $U_{-1} = 0$). In particular, this is the case for V_ω when $k = 0$ since in this case

$$V_\omega T_n = \frac{1}{2_n} T_n \,.$$

The operator A is of order σ if it maps continuously T^s to $T^{s+\sigma}$ for all real s. We establish simple necessary and sufficient conditions on a_1 and a_2 for A to be of order σ. We also prove that the ψDOS form an algebra, i.e. if A is a ψDOS of order α and B of order β, then AB is a ψDOS of order $\alpha + \beta$ and an asymptotic expansion of the symbol pair of AB can be computed from the symbol pairs of A and B. A similar construction is also developed based on the second-kind Chebyshev polynomials U_n. We refer to [2] for more details.

The operators V_ω and W_ω are ψDOS of orders 1 and -1 in this new sense. In view of operator preconditioning [8, 13], we introduce two (low-order) parametrices, P and Q, defined by

$$P = 2\sqrt{-(\omega\partial_\tau)^2 - k^2\omega^2}\,, \quad Q = 2\left[-(\partial_\tau\omega)^2 - k^2\omega^2\right]^{-1/2}$$

where ∂_τ is the tangential derivative on Γ and ω abusively denotes the operator $\phi \mapsto \omega(x)\phi(x)$. One can observe a clear connection with (1). We establish that P and Q are ψDOS of order 1 and -1 in [2, Lem. 18] and that they commute respectively with V_ω and W_ω in [1, Thm 3]. We show that PV_ω and QW_ω are second-kind operators [2, Thms 4, 5]. For $k \neq 0$, the symbolic calculus that we introduce allows to show that $-k^2\omega^2$ is the best correction among other possible first order operators [2, Cor. 10, 12], in some sense. The numerical results exposed in [1] clearly show that the k-dependent correction allows for very significant gains in the numbers of GMRES iterations, with little sensitivity to the parameter k. We also discuss some possible extensions of this work to polygonal domains and to screens in dimension 3.

References

[1] F. Alouges, M. Aversneg: New preconditioners for Laplace and Helmholtz integral equations on open curves: Analytical framework and Numerical results. *arXiv preprint* arXiv:1905.13602 (2019)

[2] M. Averseng: Pseudo-differential analysis of the Helmholtz layer potentials on open curves. *arXiv preprint* arXiv:1905.13604 (2019)

[3] M. Averseng: *Efficient methods for acoustic scattering in 2 and 3 dimensions: preconditioning on singular geometries and fast convolution* (PhD dissertation) Ecole Polytechnique, Paris-Saclay (2019)

[4] S. H. Christiansen, J.-C. Nédélec: Des préconditionneurs pour la résolution numérique des équations intégrales de frontière de l'acoustique. *Comptes Rendus de l'Académie des Sciences, series I: mathématiques* 330(7), 617-622 (2000)

[5] O. P. Bruno, S. K. Lintner: Second-kind integral solvers for TE and TM problems of diffraction by open arcs. *Radio Science* 47(06), 1-13 (2012)

[6] M. Costabel, M. Dauge, R. Duduchava: Asymptotics Without Logarithmic Terms for Crack Problems *Comm. P.D.E.* 28(5-6), 869-926 (2003)

[7] X. Antoine, M. Darbas: Generalized combined field integral equations for the iterative solution of the three-dimensional Helmholtz equation. *ESAIM: Mathematical Modelling and Numerical Analysis* 41(1), 147-167 (2007)

[8] Hiptmair, R.: Operator preconditioning. *Computers and mathematics with Applications* 52(5), 699-706 (2006)
[9] R. Hiptmair, C. Jerez-Hanckes, C. Urzúa-Torres: Closed-form inverses of the weakly singular and hypersingular operators on disks. *Integral Equations and Operator Theory* 90: 4 (2018)
[10] W. McLean, O. Steinbach: Boundary element preconditioners for a hypersingular integral equation on an interval. *Advances in Computational Mathematics* 11(4), 271-286 (1999)
[11] F. V. Postell, E. P. Stephan: On the h-, p-and hp versions of the boundary element method: numerical results. *Computer methods in applied mechanics and engineering* 83(1), 69-89 (1990)
[12] S. A. Sauter, C. Schwab: *Boundary element methods.* Springer, Berlin, Heidelberg (2010)
[13] O. Steinbach, W. L. Wendland: The construction of some efficient preconditioners in the boundary element method. *Advances in Computational Mathematics* 9(1-2), 191-216 (1998)
[14] V. Turunen, G. Vainikko: On Symbol Analysis of Periodic Pseudo differential Operators. *Zeitschrift fúr Analysis und ihre Anwendungen* 17(1), 9–22 (1998)
[15] E. P. Stephan, W. L. Wendland: An augmented Galerkin procedure for the boundary integral method applied to two-dimensional screen and crack problems. *Applicable Analysis* 18(3), 183-219 (1984)
[16] Y. Yan: Cosine change of variable for Symm's integral equation on open arcs. *IMA journal of numerical analysis* 10(4), 521-535 (1990)

Fast large-scale boundary element methods

Steffen Börm
(joint work with Sven Christophersen and Jessica Gördes)

Introduction. Given a domain $\Omega \subseteq \mathbb{R}^3$ and the Green's function

$$g(x,y) = \frac{1}{4\pi\|x-y\|}$$

of Laplace's partial differential operator $-\Delta$, we consider numerical methods for solving either the Dirichlet-to-Neumann boundary integral equation

$$\int_{\partial\Omega} g(x,y)u(y)\,dy = \frac{1}{2}f(x) + \int_{\partial\Omega} \frac{\partial g}{\partial n_y}(x,y)f(y)\,dy$$

with given Dirichlet data f and Neumann data u or the Neumann-to-Dirichlet boundary integral equation

$$-\int_{\partial\Omega} \frac{\partial^2 g}{\partial n_x \partial n_y}(x,y)u(y)\,dy = \frac{1}{2}f(x) - \int_{\partial\Omega} \frac{\partial g}{\partial n_x}(x,y)f(y)\,dy$$

with given Neumann data f and Dirichlet data u.

Applying Galerkin's method allows us to replace the integral operators by matrices, and solving the resulting linear systems yields approximations of the solution.

If a highly accurate approximation is required, standard boundary element methods lead to very large and dense matrices, and compression schemes like panel clustering [14] or fast multipole approximation [16, 10] have to be used to obtain efficient algorithms.

In this talk, we have focused on two hybrid compression algorithms: the *hybrid cross approximation* (HCA) and the *Green cross approximation* (GCA). Both start

with an analytically-derived approximation of the kernel function g that is refined using algebraic techniques in order to reduce the storage requirements and improve the efficiency of iterative solvers for the resulting linear system. We are particularly interested in ensuring that the optimal rate of convergence of the underlying Galerkin scheme is preserved despite the various approximation steps involved in the practical procedure, i.e., numerical quadrature, matrix compression, and the iterative solver.

Hybrid cross approximation. In order to construct an approximation of a submatrix $G|_{t\times s}$ with suitable subsets t and s of rows and column indices, both techniques rely on axis-parallel *bounding boxes* $\mathcal{B}_t$, $\mathcal{B}_s$ that contain the supports of the basis functions or functionals corresponding to t and s, respectively.

The hybrid cross approximation (HCA) [7] method relies on interpolation: using interpolation points $(\xi_{t,\nu})_{\nu=1}^k$ and $(\xi_{s,\mu})_{\mu=1}^k$ for t and s, respectively, with corresponding Lagrange polynomials $(\mathcal{L}_{t,\nu})_{\nu=1}^k$ and $(\mathcal{L}_{s,\mu})_{\mu=1}^k$, the first approximation step is given by

$$g(x,y) \approx \sum_{\nu=1}^{k}\sum_{\mu=1}^{k} \mathcal{L}_{t,\nu}(x) g(\xi_{t,\nu},\xi_{s,\mu}) \mathcal{L}_{s,\mu}(y). \tag{1}$$

In order to take advantage of the special properties of the kernel function g, we introduce the matrix $S \in \mathbb{R}^{k\times k}$ of the interpolation coefficients

$$s_{\nu\mu} := g(\xi_{t,\nu},\xi_{s,\mu})$$

and apply the *adaptive cross approximation* algorithm [1, 2] to find subsets $\tau \subseteq [1:k]$ and $\sigma \subseteq [1:k]$ such that $S|_{\tau\times\sigma}$ is invertible and

$$S \approx S|_{[1:k]\times\sigma} (S|_{\tau\times\sigma})^{-1} S|_{\tau\times[1:k]}.$$

Substituting this approximation in (1) yields

$$\begin{aligned} g(x,y) &\approx \sum_{\nu=1}^{k}\sum_{\mu=1}^{k}\sum_{\kappa\in\tau}\sum_{\lambda\in\sigma} \mathcal{L}_{t,\nu}(x) s_{\nu\lambda} (S|_{\tau\times\sigma})^{-1}_{\lambda\kappa} s_{\kappa\mu} \mathcal{L}_{s,\mu}(y) \\ &= \sum_{\kappa\in\tau}\sum_{\lambda\in\sigma} \left(\sum_{\nu=1}^{k} \mathcal{L}_{t,\nu}(x) g(\xi_{t,\nu},\xi_{s,\lambda}) \right) (S|_{\tau\times\sigma})^{-1}_{\lambda\kappa} \left(\sum_{\mu=1}^{k} g(\xi_{t,\kappa},\xi_{s,\mu}) \mathcal{L}_{s,\mu}(y) \right). \end{aligned}$$

In the last step, we "take back" the interpolation

$$\sum_{\nu=1}^{k} \mathcal{L}_{t,\nu}(x) g(\xi_{t,\nu},\xi_{s,\lambda}) \approx g(x,\xi_{s,\lambda}), \qquad \sum_{\mu=1}^{k} g(\xi_{t,\kappa},\xi_{s,\mu}) \mathcal{L}_{s,\mu}(y) \approx g(\xi_{t,\kappa},y),$$

to obtain the final approximation

$$g(x,y) \approx \sum_{\kappa\in\tau}\sum_{\lambda\in\sigma} g(x,\xi_{s,\lambda}) (S|_{\tau\times\sigma})^{-1}_{\lambda\kappa} g(\xi_{t,\kappa},y).$$

It can be proven that this approximation converges if the interpolation order is sufficiently high and the cross approximation is sufficiently accurate [7].

This approach immediately leads to an approximation of G by a *hierarchical matrix* [11, 9]. In order to obtain a more efficient $\mathcal{H}^2$*-matrix* [13, 8, 4], we have to apply an algebraic re-compression algorithm [3].

Green cross approximation. The *Green cross approximation* (GCA) [6] aims at constructing an efficient $\mathcal{H}^2$-matrix approximation directly. We choose a domain $\omega_t \supseteq \mathcal{B}_t$ such that

$$\operatorname{dist}(\partial\omega_t, \partial\mathcal{B}_t) \sim \operatorname{diam}(\omega_t), \qquad \operatorname{dist}(\omega_t, \mathcal{B}_s) \sim \operatorname{diam}(\omega_t)$$

hold. The second condition ensures that for any $y \in \mathcal{B}_s$, the function $x \mapsto g(x,y)$ is harmonic for all $x \in \mathcal{B}_t$, and Green's representation theorem yields

$$g(x,y) = \int_{\partial\omega_t} g(x,z)\frac{\partial g}{\partial n_z}(z,y)\,dz - \int_{\partial\omega_t} \frac{\partial g}{\partial n_z}(x,z)g(z,y)\,dz.$$

Since $\partial\omega_t$ is well-separated from $\mathcal{B}_t$ and $\mathcal{B}_s$, the integrands are smooth and the integrals can be approximated by quadrature. Denoting quadrature points on $\partial\omega_t$ by $(z_\kappa)_{\kappa=1}^{\ell}$ and the corresponding weights by $(w_\kappa)_{\kappa=1}^{\ell}$, we find the approximation

$$g(x,y) \approx \sum_{\kappa=1}^{\ell} w_\kappa g(x,z_\kappa)\frac{\partial g}{\partial n_z}(z_\kappa,y) - \sum_{\kappa=1}^{\ell} w_\kappa \frac{\partial g}{\partial n_z}(x,z_\kappa)g(z_\kappa,y) \tag{2}$$

of the kernel function g. It can be proven that this approximation converges exponentially when the quadrature order is increased [6], but numerical experiments suggest that the storage requirements are unattractively high.

This issue can be remedied by applying cross approximation: the discretization of (2) leads to the low-rank factorization

$$G|_{t\times s} \approx A_t B_{ts}^*,$$

where the matrix $A_t \in \mathbb{R}^{t\times[1:2\ell]}$ depends only on t, but not on s. Cross approximation yields subsets $\tau \subseteq t$ and $\sigma \subseteq [1:2\ell]$ such that $A_t|_{\tau\times\sigma}$ is invertible and

$$A_t \approx A_t|_{t\times\sigma}(A_t|_{\tau\times\sigma})^{-1}A_t|_{\tau\times[1:\ell]}.$$

If we define $V_t := A_t|_{t\times\sigma}(A_t|_{\tau\times\sigma})^{-1} \in \mathbb{R}^{t\times\tau}$, we arrive at $A_t \approx V_t A_t|_{\tau\times[1:\ell]}$, and "taking back" the quadrature approximation gives us

$$G|_{t\times s} \approx A_t B_{ts}^* \approx V_t A_t|_{\tau\times[1:\ell]} B_{ts}^* \approx V_t G|_{\tau\times s}.$$

We can apply the same procedure to the columns instead of the rows of G in order to obtain an approximation that only requires a small number of rows and columns of G in order to approximate entire submatrices. In order to find an $\mathcal{H}^2$-matrix approximation, we can use a recursive algorithm that chooses the pivot elements for parent clusters among those of the children in order to ensure the nested structure that allows us to reduce both the storage requirements and the computing time.

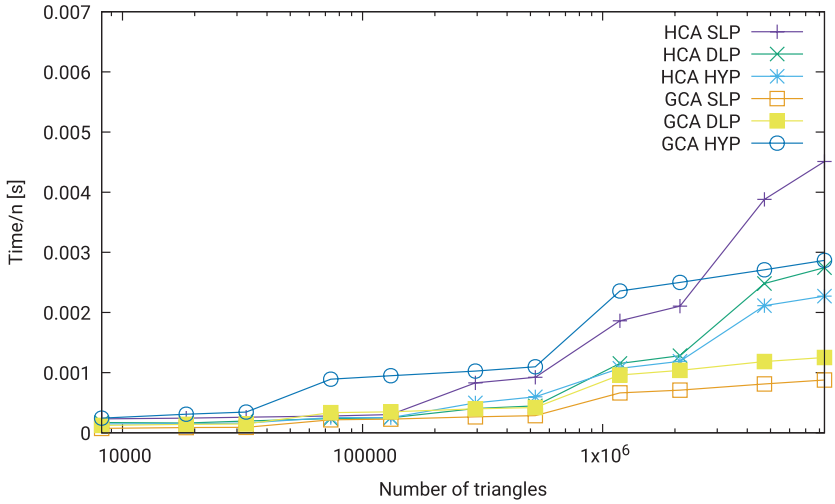

FIGURE 1. Setup times per triangle using HCA and GCA

Numerical experiments. We examine the performance of HCA and GCA by discretizing the Dirichlet-to-Neumann and Neumann-to-Dirichlet problems for the Laplace equation on the unit ball. Its surface is split into between 8 192 and 8 388 608 triangles. We use continuous piecewise linear basis functions for the Dirichlet data and discontinuous piecewise constants for the Neumann data. The nearfield integrals are evaluated using Sauter-Schwab quadrature [17].

The setup times per triangle for single-layer, double-layer and hypersingular operators are reported in Figure 1. We can see that GCA is very fast for the single- and double-layer operators, but that HCA is superior for the hypersingular operator.

REFERENCES

[1] M. Bebendorf. Approximation of boundary element matrices. *Numer. Math.*, 86(4):565–589, 2000.

[2] M. Bebendorf and S. Rjasanow. Adaptive low-rank approximation of collocation matrices. *Computing*, 70(1):1–24, 2003.

[3] S. Börm. Construction of data-sparse $\mathcal{H}^2$-matrices by hierarchical compression. *SIAM J. Sci. Comp.*, 31(3):1820–1839, 2009.

[4] S. Börm. *Efficient Numerical Methods for Non-local Operators: $\mathcal{H}^2$-Matrix Compression, Algorithms and Analysis*, volume 14 of *EMS Tracts in Mathematics*. EMS, 2010.

[5] S. Börm. Hierarchical matrix arithmetic with accumulated updates. *Comp. Vis. Sci.*, 20(3):71–84, 2019.

[6] S. Börm and S. Christophersen. Approximation of integral operators by Green quadrature and nested cross approximation. *Numer. Math.*, 133(3):409–442, 2016.

[7] S. Börm and L. Grasedyck. Hybrid cross approximation of integral operators. *Numer. Math.*, 101:221–249, 2005.

[8] S. Börm and W. Hackbusch. Data-sparse approximation by adaptive $\mathcal{H}^2$-matrices. *Computing*, 69:1–35, 2002.

[9] L. Grasedyck and W. Hackbusch. Construction and arithmetics of $\mathcal{H}$-matrices. *Computing*, 70:295–334, 2003.

[10] L. Greengard and V. Rokhlin. A fast algorithm for particle simulations. *J. Comp. Phys.*, 73:325–348, 1987.

[11] W. Hackbusch. A sparse matrix arithmetic based on $\mathcal{H}$-matrices. Part I: Introduction to $\mathcal{H}$-matrices. *Computing*, 62(2):89–108, 1999.
[12] W. Hackbusch. *Hierarchical Matrices: Algorithms and Analysis*. Springer, 2015.
[13] W. Hackbusch, B. N. Khoromskij, and S. A. Sauter. On $\mathcal{H}^2$-matrices. In H. Bungartz, R. Hoppe, and C. Zenger, editors, *Lectures on Applied Mathematics*, pages 9–29. Springer-Verlag, Berlin, 2000.
[14] W. Hackbusch and Z. P. Nowak. On the fast matrix multiplication in the boundary element method by panel clustering. *Numer. Math.*, 54(4):463–491, 1989.
[15] M. R. Hestenes and E. Stiefel. Methods of conjugate gradients for solving linear systems. *J. Res. Nat. B. Stand.*, 49(6), 1952.
[16] V. Rokhlin. Rapid solution of integral equations of classical potential theory. *J. Comp. Phys.*, 60:187–207, 1985.
[17] S. A. Sauter. Cubature techniques for 3-d Galerkin BEM. In W. Hackbusch and G. Wittum, editors, *Boundary Elements: Implementation and Analysis of Advanced Algorithms*, pages 29–44. Vieweg-Verlag, 1996.

On the efficiency of fast BEM solvers in the frequency domain to simulate fluid-structure interactions in the time domain

Stéphanie Chaillat
(joint work with Damien Mavaleix-Marchessoux, Marc Bonnet, Bruno Leblé)

Assessing the impact of underwater explosions on submerged structures (submarines) is an important naval engineering problem. An underwater explosion mainly induces two distinct phenomena: a "shock wave" (fast acoustic perturbation) followed by an oscillating bubble of gas (slow incompressible flow) [4]. Our overall goal is to create an efficient numerical method that accounts for the effects of both phenomena on submerged structures.

This contribution focuses on the interaction for the shock wave phenomenon. Computational challenges arise: (a) the relevant structures are large, and (b) the interaction is fast (lasting a few milliseconds) and hence involves high frequencies. The inherent transient nature of the shock wave phenomenon compels us to carry out a FEM-BEM coupling in the time domain (see Figure 1).

There exist various time-domain BEMs. The Convolution Quadrature Method (CQM) based BEM is a type of time-domain BEMs that allows to solve transient time problems by solving frequency BEM problems. CQM-BEMs then permit to profit from the improvements of frequency fast BEMs, while offering results numerically more stable than the ones usually obtained with Fourier or Laplace syntheses. Moreover, since the method relies on a reformulation in the frequency domain, it allows the use of a high frequency approximation (HFA) to drastically speed up the overall solving.

Formulation of the problem, radiated and reflected pressures. Consider a structure Ω_s of surface Γ submerged in an infinite fluid domain Ω_f. The fluid and the structure are both at initial rest. At $t = 0$, a known spherical wave emerges from an explosion (remote point source). At a distance r far from the explosion,

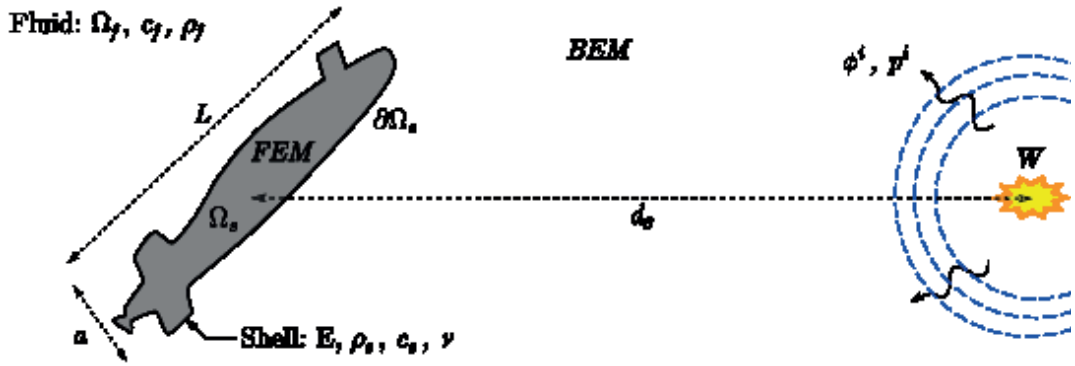

FIGURE 1. Shell submerged in an acoustic medium, submitted to a far-field underwater explosions.

the incident pressure p^{inc} is given by an empirical law[4]:

$$p^{\text{inc}}(r,t) = p_m(r)\exp\Big(-\frac{t-r/c}{\tau(r)}\Big)H\big(t-r/c\big)\,,$$

where $p_m(r)$ and $\tau(r)$ depend on parameters of the explosive material, and H is the Heaviside step function. The velocity potential ϕ is such that

$$\vec{v} = \vec{\nabla}\phi\,, \quad p = -\rho\frac{\partial\phi}{\partial t}\,, \quad \Delta\phi - \frac{1}{c^2}\frac{\partial^2\phi}{\partial t^2} = 0\,.$$

A set of structure equations, not specified here, governs the dynamical response of the structure. The fluid and structure equations are coupled by requiring the continuity of the normal velocity and the normal stress on Γ. For the fluid-structure interaction (FSI) problem, the potential p is decomposed upon three parts [6] (see Fig. 2):

$$p^{\text{tot}} = p^{\text{inc}} + p^{\text{ref}} + p^{\text{rad}}.$$

The incident field p^{inc} defines the acoustic field in the absence of the structure. The reflected field p^{ref} is the perturbation that would be observed in the fluid if the structure were motionless. The radiated field p^{rad} corresponds to the modification of the fluid state due to the motion of the structure, which radiates an acoustic wave into the fluid. On Γ, the boundary conditions verified by $p^{\text{ref}}, p^{\text{rad}}$ stem from the required continuity of the normal velocity The potentials $p^{\text{ref}}, p^{\text{rad}}$ are to be computed using the boundary element method.

Convolution quadrature based fast boundary element method. The BEM [1, 9] allows to solve 3D linear problems by discretising only a 2D surface (such as Γ), making it very suitable for unbounded propagation domains. Combining the CQM [8] and the $\mathcal{Z}$-transform, a time-marching solution algorithm can be set up using a set of suitably chosen Laplace-domain BEM solutions.

We focus on problems where the numbers N of spatial degrees of freedom (DOFs) and of time steps are both large. The large-DOF aspect is addressed by applying the fast multipole method (FMM) [7, 2] to the frequency-domain boundary integral equations (BIEs) arising in the CQM-BEM. Then, large numbers M of time steps may also overwhelm available computational resources, as the

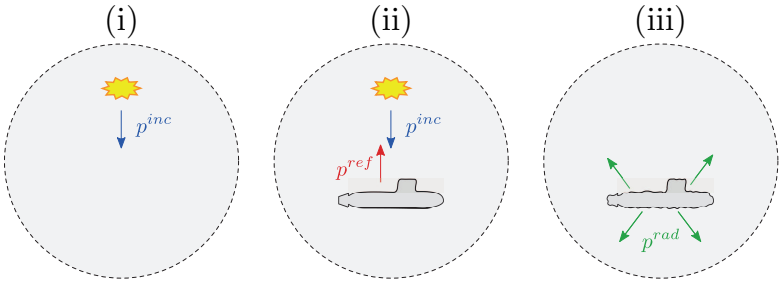

FIGURE 2. Decomposition of the field in the fluid-structure interaction context.

CQM-BEM a priori requires O(M) BEM solutions in the frequency domain. To address this issue, we propose to resort to a high-frequency approximation (HFA) for all BEM problems at frequencies above a certain threshold frequency f_{HFA}.

The main issue then is whether and how a HFA and a threshold f_{HFA} can be satisfactorily defined. For the case (iii) of waves radiated into a fluid by a moving structure, a simple HFA consists in setting that the radiated pressure is approximately that of a vibrating infinite plate. The starting point for finding approximate solutions to scattering problems (ii) is the Kirchhoff HFA. To define a more accurate approximation of the same type, ensuring a similarly low computation time we look for a coefficient $C = C(\mathbf{y})$, depending on the evaluation point $\mathbf{y} \in \Gamma$, such that $p_{HFA} = Cp^{\text{inc}}$.

HFA yields $O(1)$ complexity in time. The spatial complexity of the FM-BEM is $O(N \log N)$. Asymptotically, the time complexity of our procedure is given by the complexity of the $\mathcal{Z}$-transform, computed with an FFT, so $O(M \log M)$. However, performing the FFT is much faster than solving a BEM problem. Then, in practice, for reasonable values of M, the time complexity of the procedure depends on the number of frequency-domain BEM problems N_B actually solved. Without recourse to a HFA, we have $N_B = M + 1$. By contrast, the availability of a HFA such that BEM problems are actually solved only when the frequency is smaller than a fixed threshold f_{HFA} has the remarkable consequence of making the overall complexity in time constant (instead of linear). More precisely, we can show that for any large enough M, the number of complex frequencies with modulus smaller than a chosen HFA threshold is at most $2K - 1$ where the parameter K only depends on f_{HFA} (and is in particular independent of the time step).

Numerical validations. We have validated our fast procedure on various examples representative of our intended applications. As an illustration, we consider the case of the scattering of a wave by an infinite cylinder. Importantly, meshes for BEM problems are adapted to the frequency in order to take advantage of the FM-BEM. For this example, the most refined mesh has $N \approx 10^6$ DOFs and the number of time steps is $M = 10^4$. Table 1 reports the number of BEM problems to be solved for various choices of f_{HFA} and the consequences on the time-domain solution (with respect to a semi-analytic solution). The fast CQM-BEM is seen to provide accurate results while drastically reducing the computational cost.

f_{HFA} (kHz)	$k_{HFA}a/\pi$	$k_{HFA}L/\pi$	N_B	Time error (%)
20.0	13.3	133	32	3.6
25.0	16.7	167	40	3.4
30.0	20.0	200	48	3.4
35.0	23.3	233	56	3.3
40.0	26.7	267	64	3.3
45.0	30.0	300	72	3.3

TABLE 1. Scattering by a small cylinder ($a = 0.5\,\mathrm{m}$, $L = 5\,\mathrm{m}$): influence of f_{HFA} on time-domain solution accuracy.

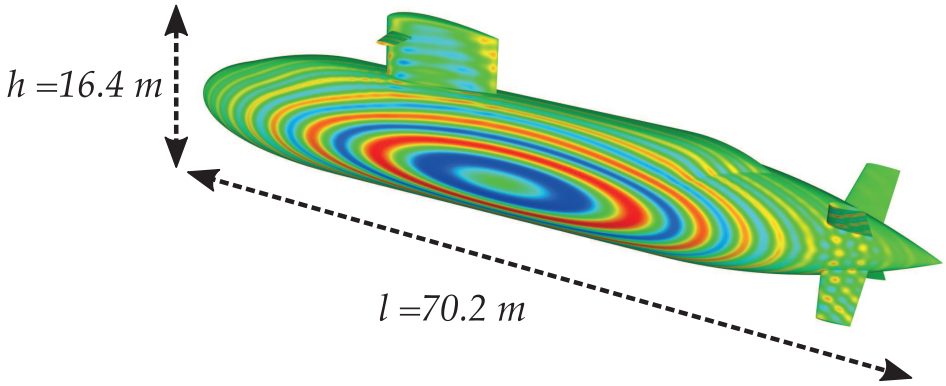

FIGURE 3. Example of wave scattering by a submarine.

We have also considered the three-dimensional scattering of a spherical wave by a complex submarine-shaped structure referred to as BB2 (see Fig. 3). Its geometry, corresponds to a realistic submarine. As before, the CQM-BEM procedure entails the solution of a large number of frequency-domain problems, using either the FM-BEM or a HFA. We show again on this example with $N \approx 3\ 10^6$ and $M = 10^4$ that the availability and exploitation of a HFA reduces the BEM solution burden to $O(1)$.

REFERENCES

[1] M. Bonnet. *Boundary integral equation methods in solids and fluids*. John Wiley & sons, 1999.

[2] S. Chaillat, M. Bonnet, and J.-F. Semblat. A multi-level fast multipole BEM for 3-D elastodynamics in the frequency domain. *Comput. Methods Appl. Mech. Engrg.*, 197(49):4233 – 4249, 2008.

[3] S. Chaillat, *uma.ensta-paristech.fr/soft/COFFEE/*

[4] R. H. Cole. *Underwater explosions*. Princeton University Press, 1948.

[5] T. L. Geers and C. A. Felippa. Doubly asymptotic approximations for vibration analysis of submerged structures, *J. Acoust. Soc. Am.* 73:1152–1159, 1983.

[6] M. C. Junger and D. Feit. *Sound, structures, and their interaction*. The MIT Press, 2nd edition, 1986.

[7] N. Nishimura. Fast multipole accelerated boundary integral equation methods. *Appl. Mech. Rev.*, 55:299 – 324, 2002.
[8] F. J. Sayas. *Retarded Potentials and Time Domain Boundary Integral Equations. A Road Map*. Springer International Publishing, 2016.
[9] S. Sauter and C. Schwab. *Boundary element methods*. Springer, 2010.

Convergence of boundary element methods on fractals

Simon N. Chandler-Wilde
(joint work with David P. Hewett, Andrea Moiola, Jeanne Besson)

This talk is concerned with BEM for time-harmonic acoustic scattering by infinitely thin, bounded planar screens. This is a classical subject [8]: our substantial and novel twist is that we consider the case where the screen is fractal or has fractal boundary. One motivation is the application of fractal antennae in electromagnetics [9]. For details, including numerical examples, see the preprint [5].

We work in n dimensions ($n = 2$ or 3), and suppose that the screen Γ is a bounded subset of $\Gamma_\infty := \{x = (x_1, ..., x_n) \in \mathbb{R}^n : x_n = 0\}$, which we identify with $\mathbb{R}^{n-1}$. We restrict attention to the case that Γ is either a closed or an open[1] subset of Γ_∞, and set $D := \mathbb{R}^n \setminus \overline{\Gamma}$. We suppose that an incident wave u^i, to be concrete the plane wave $u^i(x) = \exp(\mathrm{i}kx \cdot d)$, where d is a unit vector, is incident on the screen Γ. This incident wave is a solution of the Helmholtz equation

$$\Delta u + k^2 u = 0 \tag{1}$$

for wavenumber $k > 0$. We focus on the case of a sound soft screen (see [3] for the sound hard case). The scattering problem that we consider is the following:

Given the incident field u^i, find the total field $u \in C^2(D) \cap W_0^{1,\mathrm{loc}}(D)$ *such that* (1) *holds in D, and $u^s := u - u^i$ satisfies the standard Sommerfeld radiation condition.*

Here $\phi \in W_0^{1,\mathrm{loc}}(D)$ if $\chi\phi \in W_0^1(D)$, for every $\chi \in C_0^\infty(\mathbb{R}^n)$; and $W_0^1(D)$ is the closure of $C_0^\infty(D)$ in $W^1(D)$, where $W^1(D) := \{\phi \in L^2(D) : \nabla\phi \in L^2(D)\}$.

Our numerical scheme is: approximate the screen Γ by a sequence Γ_j of more regular screens; compute the solution for Γ_j by a conventional BEM with some maximum element diameter h_j. BEM computations for fractals have been carried out previously using this methodology, for example in potential theory [6]. Our main novelty is that we present the first results, conditions on the sequences Γ_j and h_j, that guarantee convergence in the limit $j \to \infty$. Our focus is concrete fractal scattering problems, but our numerical analysis ideas are widely applicable, to general classes of BIEs/pseudo-differential equations on rough sets approximated by sequences of more regular sets.

BIE and Variational Formulations. Our Sobolev space notations are those of [7], and we identify $H^s(\Gamma_\infty)$ with $H^s(\mathbb{R}^{n-1})$ in the obvious way. In particular, for a closed set $F \subset \Gamma_\infty$, H_F^s is the set of those $\phi \in H^s(\Gamma_\infty)$ with support in F and, for an open set $O \subset \Gamma_\infty$, $\widetilde{H}^s(O) \subset H^s(\Gamma_\infty)$ is the closure of $C_0^\infty(O)$ in the

[1] Strictly speaking 'relatively open', which we abbreviate as 'open' throughout.

$H^s(\Gamma_\infty)$ norm. Both H^s_F and $\widetilde{H}^s(O)$ are closed subspaces of $H^s(\Gamma_\infty)$. Further, $\widetilde{H}^s(O) \subset H^s_{\overline{O}}$, with equality if: O is C^0 [7]; $|s| \leq 1/2$ and O is C^0 except at a set of countably many points in ∂O that has only finitely many limit points [4]; ∂O has $(n-1)$-dimensional Lebesgue measure zero, and O is 'thick' in the sense of Triebel, the case for many open O with fractal boundaries, for example the interior of the Koch snowflake [1]. See [4] for examples where equality does not hold.

In the case when the screen Γ is some C^∞ open subset of Γ_∞, it is well-known [8, 2] that u satisfies the above scattering problem iff

$$u(x) = u^i(x) - \int_\Gamma \Phi(x,y) \left[\frac{\partial u}{\partial n}\right](y) \mathrm{d}s(y), \quad x \in D, \tag{2}$$

and

$$S[\partial u/\partial n] = g := u^i|_\Gamma. \tag{3}$$

Here $[\partial u/\partial n] = [\partial u/\partial x_n] \in H^{-1/2}_{\overline{\Gamma}} = \widetilde{H}^{-1/2}(\Gamma)$ is the jump in the normal derivative across Γ_∞ and S is the standard acoustic single-layer potential operator on Γ. S is an isomorphism from $\widetilde{H}^{-1/2}(\Gamma)$ to its dual space $H^{1/2}(\Gamma)$, indeed is coercive [2]. In particular, in the case that $\Gamma = \Gamma_R := \{x \in \Gamma_\infty : |x| < R\}$, it holds that

$$|\langle S\phi, \phi\rangle| \;\geq\; C_R \|\phi\|^2_{\widetilde{H}^{-1/2}(\Gamma_R)}, \tag{4}$$

for $\phi \in \widetilde{H}^{-1/2}(\Gamma_R)$, where $\langle\cdot,\cdot\rangle$ is the usual extension of the inner product on $L^2(\Gamma_\infty)$ to a sesquilinear form on $H^s(\Gamma_\infty) \times H^{-s}(\Gamma_\infty)$ and $C_R > 0$ depends only on k and R. This implies, by Lax-Milgram, that the variational form of (3) has exactly one solution. Where $a(\phi,\psi) := \langle S\phi, \psi\rangle$, for $\phi, \psi \in \widetilde{H}^{-1/2}(\Gamma_R)$, this variational form is to find $[\partial u/\partial n] \in \widetilde{H}^{-1/2}(\Gamma_R)$ such that

$$a\left([\partial u/\partial n], \psi\right) = \langle g, \psi\rangle, \quad \forall \psi \in \widetilde{H}^{-1/2}(\Gamma_R). \tag{5}$$

These observations immediately give us well-posedness of variational formulations of integral equations on *arbitrary* bounded open or closed subsets of Γ_∞. For any such subset Γ is contained in Γ_R for some $R > 0$. These variational formulations are (5) with $\widetilde{H}^{-1/2}(\Gamma_R)$ replaced by the closed subspace $V \subset \widetilde{H}^{-1/2}(\Gamma_R)$, where $V := H^{-1/2}_\Gamma$ if Γ is closed, $V := \widetilde{H}^{-1/2}(\Gamma)$ if Γ is open. It is immediate from (4) and the Lax-Milgram lemma that these variational formulations are well-posed. This is part of the proof of the following theorem.

Theorem 1. [3, 5] *If $\Gamma \subset \Gamma_R$ is closed,* (5)*, with $\widetilde{H}^{-1/2}(\Gamma_R)$ replaced by $V = H^{-1/2}_\Gamma$, has exactly one solution, and u given by* (2) *is the unique solution of the above scattering problem. If $\Gamma \subset \Gamma_R$ is open,* (5)*, with $\widetilde{H}^{-1/2}(\Gamma_R)$ replaced by $V = \widetilde{H}^{-1/2}(\Gamma)$, has exactly one solution. Further, u given by* (2) *is the unique solution of the above scattering problem, provided $\widetilde{H}^{-1/2}(\Gamma) = H^{-1/2}_{\overline{\Gamma}}$.*

Generally the integral in (2) has to be interpreted as a duality pairing, in particular if Γ is closed with empty interior, when the solution of (5) is zero iff $H^{-1/2}_\Gamma = \{0\}$, but $H^{-1/2}_\Gamma \neq \{0\}$ if the Hausdorff dimension of Γ exceeds $n-2$ [4].

BEM and Mosco convergence. In our BEM we approximate Γ by a sequence of (more regular) open sets $\Gamma_j \subset \Gamma_R$, and we mesh Γ_j with what we call a *pre-convex* mesh $M_j = \{T_{j,1}, ..., T_{j,N_j}\}$, meaning that: each element $T_{j,\ell} \subset \Gamma_j$ is open; Γ_j is the interior of the union of the closures of the elements $T_{j,\ell}$; the convex hulls of the elements are pairwise disjoint; and each $\partial T_{j,\ell}$ has $(n-1)$-dimensional Lebesgue measure zero. Let $h_j := \max_\ell \operatorname{diam}(T_{j,\ell})$ and let $V_j^h \subset L^2(\Gamma_j) \subset \tilde{H}^{-1/2}(\Gamma_j)$ denote the piecewise constant BEM approximation space, the set of functions that are constant on each element $T_{j,\ell}$. Then the solution $\phi := [\partial u/\partial n] \in V$ and its BEM approximation $\phi_j^h \in V_j^h$ are defined by

$$a(\phi, \psi) = \langle g, \psi \rangle, \ \ \forall \psi \in V, \quad a(\phi_j^h, \psi) = \langle g, \psi \rangle, \ \ \forall \psi \in V_j^h. \tag{6}$$

In contrast to usual BEM analysis, it need not be the case that $V_j^h \subset V$, in particular this cannot be the case if Γ is closed with empty interior. However, V and V_j^h are both subsets of the larger Hilbert space $H := \widetilde{H}^{-1/2}(\Gamma_R)$.

The following results are a partial extension to this case of the standard Céa's lemma. In these results we suppose temporarily that: H is any Hilbert space; $\langle \cdot, \cdot \rangle$ is the duality pairing on $H^* \times H$; $a(\cdot, \cdot)$ is any continuous sesquilinear form on H; $V \subset H$ and $V_j^h \subset H$, for $j \in \mathbb{N}$, are closed subspaces; and $\phi \in V$ and $\phi_j^h \in V_j^h$ are defined by (6), with $g \in H^*$. Further, $\to$ is norm and $\rightharpoonup$ weak convergence in H.

Theorem 2. *Suppose that $a(\cdot, \cdot)$ is invertible on V and, for some $J \in \mathbb{N}$, on V_j^h for $j \geq J$ (meaning that, for every $g \in H^*$, the problems (6) have exactly one solution $\phi \in V$ and $\phi_j^h \in V_j^h$, for $j \geq J$). Suppose also, for every $g \in H^*$, that $\phi_j^h \to \phi$ as $j \to \infty$. Then V_j^h* Mosco-converges *to V ($V_j^h \xrightarrow{\mathcal{M}} V$), meaning that*

(i) for every $v \in V$ and $j \in \mathbb{N}$ there exists $v_j \in V_j^h$ such that $v_j \to v$;

(ii) if j_m is a subsequence of $\mathbb{N}$, $w_{j_m} \in V_{j_m}^h$, and $w_{j_m} \rightharpoonup w \in H$, then $w \in V$.

Proof. Suppose $v \in V$ and define $g \in H^*$ on V by $\langle g, \psi \rangle = a(v, \psi)$, for all $\psi \in V$, and then extend g to a linear functional on H by Hahn-Banach. Then, where ϕ, ϕ_j^h are the solutions of (6), $\phi_j^h \to \phi$, but also $\phi = v$ by construction, so that (i) holds. To see that (ii) holds suppose that a weakly convergent sequence w_{j_m} exists as in (ii), but that its limit $w \notin V$. Define $g \in H^*$ on $\mathbb{C}w + V$ by $\langle g, cw + v \rangle = c$, for $c \in \mathbb{C}$ and $v \in V$, and extend g to H by Hahn-Banach. Then, where ϕ, ϕ_j^h are the solutions of (6), $\phi_j^h \to \phi$ as $j \to \infty$ and $\phi = 0$ as $\langle g, \psi \rangle = 0$, $\psi \in V$. Thus $a(\phi_{j_m}^h, w_{j_m}) \to 0$ as $m \to \infty$, but also $a(\phi_{j_m}^h, w_{j_m}) = \langle g, w_{j_m} \rangle \to \langle g, w \rangle = 1$. □

Theorem 3. [5] *Suppose that $a(\cdot, \cdot)$ is invertible on V and is a compact perturbation of a coercive form on H. Then, for every sequence of closed subspaces $V_j^h \subset H$ such that $V_j^h \xrightarrow{\mathcal{M}} V$, there exists $J \in \mathbb{N}$ such that $a(\cdot, \cdot)$ is invertible on V_j^h for $j \geq J$, and, for every $g \in H^*$, $\phi_j^h \to \phi$, where ϕ and ϕ_j^h are the solutions of (6).*

In the case that $H = V$ (so $V_j^h \subset V$): (ii) holds automatically in Theorem 2; $V_j^h \xrightarrow{\mathcal{M}} V$ iff $m_j(v) := \inf_{\psi \in V_j^h} \|v - \psi\| \to 0$ as $j \to \infty$ for every $v \in V$; Theorem 3 reduces to (part of) a generalised Céa's lemma. An **open problem** is what should

replace the standard Céa's lemma quasi-optimality bound that $\|\phi-\phi_j^h\| \leq Cm_j(\phi)$ in cases where $V_j^h \not\subset V$?

Returning to the case in which (6) is the BIE variational problem and its BEM approximation, with V_j^h the piecewise constant BEM approximation space on a pre-convex mesh M_j, it follows from the above theorems that the BEM approximation $\phi_j^h \to \phi = [\partial u/\partial n]$ in $\widetilde{H}^{-1/2}(\Gamma_R)$, for every incident wave direction d, iff $V_j^h \xrightarrow{\mathcal{M}} V$. The following theorem gives conditions in the case when Γ is compact (see [5] for the case Γ open) that guarantee that $V_j^h \xrightarrow{\mathcal{M}} V$. For $\epsilon > 0$, $\Gamma(\epsilon) := \{x \in \Gamma_\infty : \mathrm{dist}(x, \Gamma) < \epsilon\}$.

Theorem 4. *Let Γ_j be a sequence of open subsets of Γ_R such that $\Gamma \subset \Gamma(\epsilon_j) \subset \Gamma_j \subset \Gamma(\eta_j)$, for some $0 < \epsilon_j < \eta_j$, with $\eta_j \to 0$ as $j \to \infty$. If H_Γ^t is dense in $H_\Gamma^{-1/2}$ for some $t \in [-1/2, 0]$ (always true for $t = -1/2$), and $h_j = o((\epsilon_j)^{-2t})$, then $V_j^h \xrightarrow{\mathcal{M}} V$ so that $\phi_j^h \to \phi$ as $j \to \infty$.*

As an example, consider the $n = 2$ case when $\Gamma = C \times \{0\} \subset \mathbb{R}^2$, where $C \subset [0, 1]$ is the Cantor set, with Hausdorff dimension $d = \log(2)/\log(1/\alpha)$, that is the attractor of the iterated function system $\{s_1, s_2\}$, where, for some $\alpha \in (0, 1/2)$, $s_1(t) := \alpha t$, $s_2(t) := \alpha t + 1 - \alpha$, for $t \in \mathbb{R}$. Choose $\delta \in (0, -1 + 1/(2\alpha))$, set $C_0 := (-\delta, 1 + \delta)$, $C_j := s_1(C_{j-1}) \cup s_2(C_{j-1})$, for $j \in \mathbb{N}$. Then $C_0 \supset C_1 \supset ... \supset C$, $C = \cap_j C_j$, and C_j is the disjoint union of 2^j intervals of length $H_j := \alpha^j(1 + 2\delta)$. Define $\Gamma_j := C_j \times \{0\}$, for $j \in \mathbb{N}$, choose $i = i(j) \in \{1, ..., j\}$ and mesh Γ_j with a pre-convex mesh M_j of $N_j = 2^i$ elements, each element comprising 2^{j-i} intervals of length H_j, and each element having diameter $h_j = \alpha^i(1 + 2\delta\alpha^{j-i})$. It is shown in [1] that H_Γ^t is dense in $H_\Gamma^{-1/2}$ for $-1/2 \leq t < (d-1)/2$, so that it follows from the above theorem [5] that $\phi_j^h \to \phi$ in $\widetilde{H}^{-1/2}(\Gamma_R)$ provided $i(j) > \mu j$ for some $\mu > 1 - \log(2)/\log(1/\alpha)$. An **open problem** is to prove convergence, even in the case when $i(j) = j$, when $\delta = 0$ and C_j is the standard prefractal sequence for C.

References

[1] A. Caetano, D. P. Hewett, and A. Moiola, *Density results for Sobolev, Besov and Triebel-Lizorkin spaces on rough sets*, arXiv:1904.05420, (2018).

[2] S. N. Chandler-Wilde and D. P. Hewett, *Wavenumber-explicit continuity and coercivity estimates in acoustic scattering by planar screens*, Integr. Equat. Oper. Th., **82** (2015), 423–449.

[3] S. N. Chandler-Wilde and D. P. Hewett, *Well-posed PDE and integral equation formulations for scattering by fractal screens*, SIAM J. Math. Anal., **50** (2018), 677–717.

[4] S. N. Chandler-Wilde, D. P. Hewett, and A. Moiola, *Sobolev spaces on non-Lipschitz subsets of $\mathbb{R}^n$ with application to boundary integral equations on fractal screens*, Integr. Equat. Operat. Th., **87** (2017), 179–224.

[5] S. N. Chandler-Wilde, D. P. Hewett, A. Moiola, and J. Besson, *Boundary element methods for acoustic scattering by fractal screens*, arXiv:1909.05547, (2019).

[6] P. Jones, J. Ma, and V. Rokhlin, *A fast direct algorithm for the solution of the Laplace equation on regions with fractal boundaries*, J. Comput. Phys., **113** (1994), 35–51.

[7] W. McLean, *Strongly Elliptic Systems and Boundary Integral Equations*, CUP, 2000.

[8] E. P. Stephan, *Boundary integral equations for screen problems in* $\mathbb{R}^3$, Integral Equations and Operator Theory **10** (1987), 236–257.
[9] D. H. Werner and S. Ganguly, *An overview of fractal antenna engineering research*, IEEE Antenn. Propag. M., **45** (2003), 38–57.

Generalized Optimised Schwarz Method for arbitrary non-overlapping sub-domain partitions

Xavier Claeys
(joint work with Emile Parolin)

We wish to solve a time harmonic Helmholtz problem in an infinite medium: find $u \in H^1_{\mathrm{loc}}(\mathbb{R}^d)$ such that $\mathrm{div}(\mu\nabla u) + \kappa^2 u = f$ in $\mathbb{R}^d$ and u outgoing radiating. The coefficients a priori admit (boundedly supported) heterogeneity. We are interested in domain decomposition (DDM) strategies so we introduce a non-overlapping partition $\mathbb{R}^d = \cup_{j=0}^{\mathrm{J}} \overline{\Omega}_j$ into Lipschitz subdomains, with Ω_j bounded if $j \neq 0$.

We do not make any further assumption regarding the geometric partitionning. This allows the presence of *junctions*, also commonly called *cross points*, where (at least) three subdomains abut. Consider traces taken from the interior of subdomains, let $\boldsymbol{n}_j$ be the orthonormal vector field at $\Gamma_j := \partial\Omega_j$ pointing outside Ω_j. Our problem then rewrites

$$(1)\qquad \begin{array}{ll} \textbf{local subproblems:} & \textbf{transmission conditions:} \\ \left\{\begin{array}{l} \mathrm{div}(\mu\nabla u) + \kappa^2 u = f \ \text{ in } \Omega_j \\ u \text{ is outgoing radiating} \\ \forall j = 0 \dots \mathrm{J} \end{array}\right. & \left\{\begin{array}{l} \partial_{\boldsymbol{n}_j} u|_{\Gamma_j} = -\partial_{\boldsymbol{n}_k} u|_{\Gamma_k} \\ u|_{\Gamma_j} = u|_{\Gamma_k} \ \text{ on } \ \Gamma_j \cap \Gamma_k \\ \forall j,k = 0 \dots \mathrm{J}, j \neq k \end{array}\right. \end{array}$$

1. Standard Optimized Schwarz Method

The Optimized Schwarz Method (OSM) [3] is one of the most established DDM approach for waves. This strategy relies on two ingredients. First, transmission conditions are reformulated in terms of Robin traces $\partial_{\boldsymbol{n}_j} u|_{\Gamma_j} - \imath\Lambda u|_{\Gamma_j} = -\partial_{\boldsymbol{n}_k} u|_{\Gamma_k} - \imath\Lambda u|_{\Gamma_k}$ on $\Gamma_j \cap \Gamma_k$ for $\forall j,k, j \neq k$, where $\Lambda > 0$ is a tuning parameter, which can be rewritten in a vector manner as follows

$$(2)\qquad (\partial_{\boldsymbol{n}_j} u|_{\Gamma_j} - \imath\Lambda u|_{\Gamma_j})_{j=0}^{\mathrm{J}} = -\Pi_0((\partial_{\boldsymbol{n}_k} u|_{\Gamma_k} + \imath\Lambda u|_{\Gamma_k})_{k=0}^{\mathrm{J}})$$

where $(p_0, \dots, p_{\mathrm{J}}) = \Pi_0(q_0, \dots, q_{\mathrm{J}}) \iff p_j = q_k$ on $\Gamma_j \cap \Gamma_k$. The operator Π_0 is usually referred to as *exchange operator* and simply consists in swapping the traces from both sides of each interface. The second ingredient of OSM is a scattering operator $\mathrm{S}_0(p_0, \dots, p_{\mathrm{J}}) = (\mathrm{S}^0_{\Gamma_0}(p_0), \dots, \mathrm{S}^0_{\Gamma_{\mathrm{J}}}(p_{\mathrm{J}}))$ defined by

$$\begin{aligned} &\mathrm{S}^0_{\Gamma_j}(\partial_{\boldsymbol{n}_j}\psi|_{\Gamma_j} - \imath\Lambda\psi|_{\Gamma_j}) := \partial_{\boldsymbol{n}_j}\psi|_{\Gamma_j} + \imath\Lambda\psi|_{\Gamma_j}, \\ &\text{for all } \psi \in H^1_{\mathrm{loc}}(\overline{\Omega}_j) \text{ satisfying} \\ &\mathrm{div}(\mu\nabla\psi) + \kappa^2\psi = 0 \text{ in } \Omega_j \text{ and } \psi \text{ outgoing radiating.} \end{aligned}$$

This scattering operator is used to reformulate the local subproblems as identities written on the Γ_j's in terms of Robin traces

$$(3) \qquad (\partial_{\boldsymbol{n}_j} u|_{\Gamma_j} + \imath\Lambda u|_{\Gamma_j})_{j=0}^{\mathrm{J}} = \mathrm{S}_0((\partial_{\boldsymbol{n}_k} u|_{\Gamma_k} - \imath\Lambda u|_{\Gamma_k})_{k=0}^{\mathrm{J}}) + \mathfrak{f}$$

where $\mathfrak{f}$ is a tuple of traces stemming from the source term f of (1). The whole boundary value problem (1) is then reformulated as an equation on the skeleton $\Sigma = \cup_{j=0}^{\mathrm{J}} \Gamma_j$ by combining (2) and (3),

$$(4) \qquad (\mathrm{Id} + \Pi_0 \mathrm{S}_0)\mathfrak{p} = -\Pi_0(\mathfrak{f}) \quad \text{where} \quad \mathfrak{p} = (\partial_{\boldsymbol{n}_j} u|_{\Gamma_j} - \imath\Lambda u|_{\Gamma_j})_{j=0\ldots\mathrm{J}}.$$

Classical linear solvers such as Richardson's method were proved to converge for (4) with general subdomain partitions. But available litterature has so far not offered any sharp estimate on the decrease rate of the error and numerical results show that geometric convergence of linear solvers does not hold anymore in the presence of cross points.

2. Enforcing transmission conditions in a new way

The exchange operator Π_0 is continuous in trace spaces only if there is no cross point. This seems to be the key issue spoiling geometric convergence. Thus we propose a regularized exchange operator that remains continuous no matter the presence of cross points. Let us introduce an appropriate functionnal setting

$$\mathbb{H}_{\mathrm{D}} := H^{+1/2}(\Gamma_0) \times \cdots \times H^{+1/2}(\Gamma_{\mathrm{J}})$$
$$\mathbb{H}_{\mathrm{N}} := H^{-1/2}(\Gamma_0) \times \cdots \times H^{-1/2}(\Gamma_{\mathrm{J}})$$

The bilinear form $\langle\!\langle (v_j)_{j=0}^{\mathrm{J}}, (q_j)_{j=0}^{\mathrm{J}} \rangle\!\rangle := \langle v_0, q_0 \rangle_{\Gamma_0} + \cdots + \langle v_{\mathrm{J}}, q_{\mathrm{J}} \rangle_{\Gamma_{\mathrm{J}}}$ puts these two spaces in duality. Given $\delta > 0$, we also define $\mathrm{T}_\delta(v_0, \ldots, v_{\mathrm{J}}) := (\mathrm{T}_\delta^{\Gamma_0}(v_0), \ldots, \mathrm{T}_\delta^{\Gamma_{\mathrm{J}}}(v_{\mathrm{J}}))$ where each $\mathrm{T}_\delta^{\Gamma_j} : H^{+1/2}(\Gamma_j) \to H^{-1/2}(\Gamma_j)$ is a Stecklov-Poincaré operator defined by

$$\mathrm{T}_\delta^{\Gamma_j}(v) := \delta \partial_{\boldsymbol{n}_j} \phi|_{\Gamma_j}$$
$$\text{where } \phi \in H^1(\Omega_j) \text{ satisfies}$$
$$\phi|_{\Gamma_j} = v \text{ and } -\Delta\phi + \delta^{-2}\phi = 0 \text{ in } \Omega_j.$$

The problem defining T_δ is variationnally reformulated in a strongly coercive form with constant coefficients, and is a priori unrelated to (1). We consider $(\mathfrak{p}, \mathfrak{q})_{\mathbb{H}_{\mathrm{N}}} := \langle\!\langle \mathrm{T}_\delta^{-1}(\mathfrak{p}), \mathfrak{q} \rangle\!\rangle$ as scalar product on $\mathbb{H}_{\mathrm{N}}$, and denote $\| \ \|_{\mathbb{H}_{\mathrm{N}}}$ the associated norm. We also introduce single-trace spaces

$$\mathbb{X}_{\mathrm{D}} := \{(\varphi|_{\Gamma_0}, \ldots, \varphi|_{\Gamma_{\mathrm{J}}}),\ \varphi \in H^1(\mathbb{R}^d)\}$$
$$\mathbb{X}_{\mathrm{N}} := \{(\boldsymbol{n}_0 \cdot \boldsymbol{\psi}|_{\Gamma_0}, \ldots, \boldsymbol{n}_{\mathrm{J}} \cdot \boldsymbol{\psi}|_{\Gamma_{\mathrm{J}}}),\ \boldsymbol{\psi} \in H(\mathrm{div}, \mathbb{R}^d)\}$$

which are two closed subspaces of $\mathbb{H}_{\mathrm{D}}$ and $\mathbb{H}_{\mathrm{N}}$ that consist in tuples of traces complying with transmission conditions. As a consequence, the transmission conditions in (1) can be rewritten $(u|_{\Gamma_j})_{j=0}^{\mathrm{J}} \in \mathbb{X}_{\mathrm{D}}$ and $(\partial_{\boldsymbol{n}_j} u|_{\Gamma_j})_{j=0}^{\mathrm{J}} \in \mathbb{X}_{\mathrm{N}}$.

Theorem 1. $\mathbb{H}_{\mathrm{N}} = \mathbb{X}_{\mathrm{N}} \oplus \mathrm{T}_\delta(\mathbb{X}_{\mathrm{D}})$ *with orthogonality, and the orthogonal projection* $\mathrm{P}_\delta : \mathbb{H}_{\mathrm{N}} \to \mathrm{T}_\delta(\mathbb{X}_{\mathrm{D}})$ *is given by* $\mathrm{P}_\delta(\mathfrak{q}) = (\partial_{\boldsymbol{n}_0}\Psi(\mathfrak{q})|_{\Gamma_0}, \dots, \partial_{\boldsymbol{n}_{\mathrm{J}}}\Psi(\mathfrak{q})|_{\Gamma_{\mathrm{J}}})$ *where*

$$\Psi(q_0, \dots, q_{\mathrm{J}})(\boldsymbol{x}) := \sum_{j=0}^{\mathrm{J}} \int_{\Gamma_j} \frac{\exp(-\imath|\boldsymbol{x}-\boldsymbol{y}|/\delta)}{4\pi|\boldsymbol{x}-\boldsymbol{y}|} q_j(\boldsymbol{y}) d\sigma(\boldsymbol{y}).$$

Theorem 2. *Define* $\Pi_\delta := 2\mathrm{P}_\delta - \mathrm{Id}$. *Then for any pair* $(\mathfrak{v}, \mathfrak{q}) \in \mathbb{H}_{\mathrm{D}} \times \mathbb{H}_{\mathrm{N}}$, *we have* $(\mathfrak{v}, \mathfrak{q}) \in \mathbb{X}_{\mathrm{D}} \times \mathbb{X}_{\mathrm{N}} \iff \mathfrak{q} - \imath\Lambda\mathrm{T}_\delta(\mathfrak{v}) = -\Pi_\delta(\mathfrak{q} + \imath\Lambda\mathrm{T}_\delta(\mathfrak{v}))$.

In the present analysis, Π_δ plays the role of a non-local exchange operator that is systematically continuous and satisfies $\|\Pi_\delta(\mathfrak{p})\|_{\mathbb{H}_{\mathrm{N}}} \leq \|\mathfrak{p}\|_{\mathbb{H}_{\mathrm{N}}}$. The previous theorem yields a new manner to enforce the transmission conditions of (1),

$$(\partial_{\boldsymbol{n}_j} u|_{\Gamma_j} - \imath\Lambda\mathrm{T}_\delta^{\Gamma_j}(u))_{j=0}^{\mathrm{J}} = -\Pi_\delta((\partial_{\boldsymbol{n}_j} u|_{\Gamma_j} + \imath\Lambda\mathrm{T}_\delta^{\Gamma_j}(u))_{j=0}^{\mathrm{J}}) \tag{5}$$

3. Reformulation of the scattering problem

Next we need to reformulate the wave equation local to each subdomain. We rely once again on a scattering operator taking $\Lambda\mathrm{T}_\delta^{\Gamma_j}$ instead of Λ as an (operator valued) impedance factor. We define $\mathrm{S}_\delta(p_0, \dots, p_{\mathrm{J}}) = (\mathrm{S}_{\Gamma_0}^\delta(p_0), \dots, \mathrm{S}_{\Gamma_{\mathrm{J}}}^\delta(p_{\mathrm{J}}))$ by

$$\mathrm{S}_{\Gamma_j}^\delta(\partial_{\boldsymbol{n}_j}\psi|_{\Gamma_j} - \imath\Lambda\mathrm{T}_\delta^{\Gamma_j}(\psi)) := \partial_{\boldsymbol{n}_j}\psi|_{\Gamma_j} + \imath\Lambda\mathrm{T}_\delta^{\Gamma_j}(\psi)$$

for all $\psi \in H^1_{\mathrm{loc}}(\overline{\Omega}_j)$ satisfying $\mathrm{div}(\mu\nabla\psi) + \kappa^2\psi = 0$ in Ω_j and ψ outgoing radiating. Conservation of energy in each subdomain yields $\|\mathrm{S}_\delta(\mathfrak{p})\|_{\mathbb{H}_{\mathrm{N}}} \leq \|\mathfrak{p}\|_{\mathbb{H}_{\mathrm{N}}}$ for all $\mathfrak{p} \in \mathbb{H}_{\mathrm{N}}$. Local wave equations are then rewritten under the form

$$(\partial_{\boldsymbol{n}_j} u|_{\Gamma_j} + \imath\Lambda\mathrm{T}_\delta^{\Gamma_j}(u))_{j=0}^{\mathrm{J}} = \mathrm{S}^0((\partial_{\boldsymbol{n}_k} u|_{\Gamma_k} - \imath\Lambda\mathrm{T}_\delta^{\Gamma_k}(u))_{k=0}^{\mathrm{J}}) + \tilde{\mathfrak{f}} \tag{6}$$

where $\tilde{\mathfrak{f}}$ stems from the source term of (1). Combining (5) and (6), we finally obtain an equation posed on the skeleton $\cup_{j=0}^{\mathrm{J}}\Gamma_j$,

$$\begin{aligned} &(\mathrm{Id} + \Pi_\delta\mathrm{S}_\delta)\mathfrak{p} = -\Pi_\delta(\tilde{\mathfrak{f}}) \\ &\mathfrak{p} = (\partial_{\boldsymbol{n}_k} u|_{\Gamma_k} - \imath\Lambda\mathrm{T}_\delta^{\Gamma_k}(u))_{k=0\dots\mathrm{J}} \end{aligned} \tag{7}$$

Due to the continuity properties of the nonlocal exchange operator and the scattering operator we have $\|(\mathrm{Id} + \Pi_\delta\mathrm{S}_\delta)\mathfrak{q}\|_{\mathbb{H}_{\mathrm{N}}} \leq 2\|\mathfrak{q}\|_{\mathbb{H}_{\mathrm{N}}}$ for all $\mathfrak{q} \in \mathbb{H}_{\mathrm{N}}$. On the other hand we have the coercivity result.

Theorem 3. *There exists* $\alpha > 0$ *such that, for all* $\mathfrak{q} \in \mathbb{H}_{\mathrm{N}}$,

$$\Re e\{(\mathfrak{q}, (\mathrm{Id} + \Pi_\delta\mathrm{S}_\delta)\mathfrak{q})_{\mathbb{H}_{\mathrm{N}}}\} \geq \alpha\|\mathfrak{q}\|^2_{\mathbb{H}_{\mathrm{N}}}.$$

In passing, this exhibits a strongly coercive formulation of Problem (1). This leads to a convergence estimate for linear solvers applied to (7). In particular for a relaxation parameter $r \in (0, 1)$, let us define iterates according to Richardson's method

$$\mathfrak{p}^{(n+1)} = \mathfrak{p}^{(n)} + r\Pi_\delta\mathrm{S}_\delta(\mathfrak{p}^{(n)}) + r\Pi_\delta(\tilde{\mathfrak{f}})$$

If $\mathfrak{p}^\infty$ refers to the solution to (7), then there exists $C > 0$ and $\tau \in (0, 1)$ such that $\|\mathfrak{p}^{(n)} - \mathfrak{p}^\infty\|_{\mathbb{H}_{\mathrm{N}}} \leq C\tau^n$.

References

[1] X. Claeys. A new variant of the Optimised Schwarz Method for arbitrary non-overlapping subdomain partitions. ArXiv preprint, 2019.

[2] F. Collino, S. Ghanemi, and P. Joly. Domain decomposition method for harmonic wave propagation: a general presentation. *Comput. Methods Appl. Mech. Engrg.*, 184(2-4):171–211, 2000.

[3] B. Després. *Méthodes de décomposition de domaine pour les problèmes de propagation d'ondes en régime harmonique. Le théorème de Borg pour l'équation de Hill vectorielle.* INRIA Rocquencourt, 1991. Thèse, Université de Paris IX (Dauphine), 1991.

Fast iterative BEM for high-frequency scattering problems in 3D elastodynamics

Marion Darbas

(joint work with S. Chaillat, F. Le Louër)

1. Introduction

The numerical solution of high-frequency scattering problems of time-harmonic elastic waves by a three-dimensional obstacle is a challenging task. The fast multipole method is an efficient technique to accelerate the solution of large scale 3D scattering problems with boundary integral equations. However, the fast multipole accelerated boundary element method (FM-BEM) is intrinsically based on an iterative solver. It has been shown that the number of iterations can significantly hinder the overall efficiency of the FM- BEM. The derivation of robust preconditioners for FM-BEM is inevitable to increase the size of the problems that can be considered. Analytic preconditioners offer a very interesting strategy by improving the spectral properties of the boundary integral equations ahead from the discretization. We propose to combine an approximate adjoint Dirichlet-to-Neumann (respectively Neumann-to-Dirichlet) map as an analytic preconditioner with a FM-BEM solver to treat Dirichlet (respectively Neumann) exterior scattering problems in 3D elasticity. We compare standard and preconditioned Combined Field Integral Equations (CFIEs).

2. The Navier exterior problem

We consider a bounded domain Ω^- in $\mathbb{R}^d$, $d = 2, 3$, with a closed smooth boundary $\Gamma := \partial\Omega^-$. Let Ω^+ denote the exterior domain $\mathbb{R}^d \backslash \overline{\Omega^-}$ and $\boldsymbol{n}$ the outer unit normal vector to the boundary Γ. The scattering problem is formulated as follows : Given an incident displacement wave $\boldsymbol{u}^{inc}$, find the solution $\boldsymbol{u}$ of the Navier exterior problem:

$$
\begin{array}{l}
\mu \boldsymbol{\Delta u} + (\lambda + \mu) \boldsymbol{\nabla} \operatorname{div} \boldsymbol{u} + \rho \omega^2 \boldsymbol{u} = 0, \text{ in } \Omega^+, \\
\boldsymbol{u} = -\boldsymbol{u}^{inc} \text{ or } \boldsymbol{t}_{|\Gamma} = -\boldsymbol{t}^{inc}_{|\Gamma}, \text{ on } \Gamma, \\
\lim\limits_{r\to\infty} r \left(\dfrac{\partial \boldsymbol{u}_p}{\partial r} - i\kappa_p \boldsymbol{u}_p \right) = 0, \quad \lim\limits_{r\to\infty} r \left(\dfrac{\partial \boldsymbol{u}_s}{\partial r} - i\kappa_s \boldsymbol{u}_s \right) = 0, r = |\mathbf{x}|.
\end{array} \tag{1}
$$

where $\omega > 0$ is the frequency, and the Lamé parameters μ, λ and the density ρ are positive constants. The field $\boldsymbol{u}$ is decomposed into a longitudinal field $\boldsymbol{u}_p$ with vanishing curl and a transverse divergence-free field $\boldsymbol{u}_s$ solutions to

$$\boldsymbol{\Delta} \boldsymbol{u}_p + \kappa_p^2 \boldsymbol{u}_p = 0, \mathbf{curl}\,\mathbf{curl}\,\boldsymbol{u}_s - \kappa_s^2 \boldsymbol{u}_s = 0,$$

with respective wavenumbers $\kappa_p^2 = \rho\omega^2(\lambda + 2\mu)^{-1}$ and $\kappa_s^2 = \rho\omega^2\mu^{-1}$. The Neumann trace, defined by $\boldsymbol{t}_{|\Gamma} := \boldsymbol{T}\boldsymbol{u}$, is given by the traction operator

$$\boldsymbol{T} = 2\mu \frac{\partial}{\partial \boldsymbol{n}} + \lambda \boldsymbol{n}\,\mathrm{div} + \mu\, \boldsymbol{n} \times \mathbf{curl}\,.$$

We have set $\boldsymbol{t}_{|\Gamma}^{inc} = \boldsymbol{T}\boldsymbol{u}^{inc}$.

3. Standard and preconditioned CFIEs

3.1. **Dirichlet boundary condition.** Integral equation method is based on the potential theory. The field $\boldsymbol{u}$ is uniquely determined by the knowledge of the Cauchy data $(\boldsymbol{u}_{|\Gamma}, \boldsymbol{t}_{|\Gamma})$. The standard CFIE consists in finding the physical unknown $\boldsymbol{\varphi} = -\big(\boldsymbol{t}_{|\Gamma} + \boldsymbol{t}_{|\Gamma}^{inc}\big) \in \boldsymbol{H}^{-\frac{1}{2}}(\Gamma)$ solution to

$$(\frac{\mathrm{I}}{2} + D^{'} + i\eta S)\boldsymbol{\varphi} = -\big(\boldsymbol{t}^{inc} + i\eta \boldsymbol{u}_{|\Gamma}^{inc}\big), \quad \text{on } \Gamma, \tag{2}$$

where η is a non-zero real constant and the single- and double-layer boundary integral operators S and D are defined by

$$S\boldsymbol{\varphi}(\boldsymbol{x}) = \int_\Gamma \Phi(\boldsymbol{x}, \boldsymbol{y})\boldsymbol{\varphi}(\boldsymbol{y})\, ds(\boldsymbol{y}), D\boldsymbol{\psi}(\boldsymbol{x}) = \int_\Gamma [\boldsymbol{T}_{\boldsymbol{y}}\Phi(\boldsymbol{x}, \boldsymbol{y})]^{\mathsf{T}} \boldsymbol{\psi}(\boldsymbol{y})\, ds(\boldsymbol{y}). \tag{3}$$

The standard CFIE is not suited for an iterative solution. To expect an eigenvalue clustering and hence a fast convergence of the iterative solver GMRES, we derive preconditioned CFIEs: Find $\boldsymbol{\varphi} = -\big(\boldsymbol{t}_{|\Gamma} + \boldsymbol{t}_{|\Gamma}^{inc}\big) \in \boldsymbol{H}^{-\frac{1}{2}}(\Gamma)$ solution to

$$(\frac{\mathrm{I}}{2} + D^{'} - \boldsymbol{\Lambda}' S)\boldsymbol{\varphi} = -\big(\boldsymbol{t}_{|\Gamma}^{inc} - \boldsymbol{\Lambda}' \boldsymbol{u}_{|\Gamma}^{inc}\big), \quad \text{on } \Gamma, \tag{4}$$

where $\boldsymbol{\Lambda}'$ is an approximation of the exact adjoint Dirichlet-to-Neumann (DtN) map

$$\boldsymbol{\Lambda}^{\mathrm{ex}} : \boldsymbol{u}_{|\Gamma} \in \boldsymbol{H}^{\frac{1}{2}}(\Gamma) \mapsto \boldsymbol{\Lambda}^{\mathrm{ex}} \boldsymbol{u}_{|\Gamma} := \boldsymbol{t}_{|\Gamma} \in \boldsymbol{H}^{-\frac{1}{2}}(\Gamma)\,.$$

The spectral properties of (4) depend on the choice of the approximation $\boldsymbol{\Lambda}'$. In [2], we have obtained new approximations of the DtN map in the spirit of OSRC methods. For any real-valued constant α, we introduce the modified Neumann trace $\boldsymbol{t}_\alpha \in \boldsymbol{H}^{-\frac{1}{2}}(\Gamma)$

$$\boldsymbol{t}_\alpha = \boldsymbol{t}_{|\Gamma} - \alpha \boldsymbol{\mathcal{M}} \boldsymbol{u}_{|\Gamma}$$

with $\boldsymbol{\mathcal{M}}$ the tangential Günter derivative. The idea is to consider the decomposition

$$\boldsymbol{\Lambda}^{\mathrm{ex}} = \boldsymbol{\Lambda}_\alpha^{\mathrm{ex}} + \alpha \boldsymbol{\mathcal{M}}$$

and to keep only the principal part of the operator $\boldsymbol{\Lambda}_\alpha^{\mathrm{ex}}$. We compare low- and high-order adjoint DtN approximations $\boldsymbol{\Lambda}'$, and the corresponding LO and HO

preconditioned CFIEs [1]. The high-order adjoint DtN approximations are expressed in terms of surface differential operators, square-root operators and their inverse. An artificial singularity of square-root operators appears in the zone from the propagating modes to the evanescent ones. To model the behavior in the transition zone of grazing modes, we use a regularization by adding a small local damping parameter to the wavenumbers. Furthermore, complex Padé rational approximants provide local and uniform representations of the square-root operators.

3.2. **Neumann boundary condition.** The standard CFIE consists in finding the physical unknown $\psi = \boldsymbol{u}_{|\Gamma} + \boldsymbol{u}^{inc}_{|\Gamma} \in \boldsymbol{H}^{\frac{1}{2}}(\Gamma)$ solution to

$$(\frac{\mathrm{I}}{2} - D - i\eta N)\psi = \boldsymbol{u}^{inc}_{|\Gamma} + i\eta \boldsymbol{t}^{inc}_{|\Gamma}, \quad \text{on } \Gamma, \tag{5}$$

with η a non-zero real constant. The integral equation (5) is well-posed for any frequency ω and any non-zero real parameter η [4, 3]. However, it involves the hypersingular boundary integral operator N which is a pseudodifferential operator of order 1. This boundary integral equation is of the first-kind and admits a countable set of eigenvalues that tends to infinity. We construct different local approximations $\boldsymbol{V'}$ of the exact adjoint Neumann-to-Dirichlet map and use them as analytical preconditioners in order to regularize the operator N.

Low-order approximation. We obtain the following adjoint NtD approximation

$$\boldsymbol{V}' := \boldsymbol{V}'_{\mathrm{LO}} = -i\Big(\frac{1}{(\lambda+2\mu)\kappa_p}\mathrm{I}_{\boldsymbol{n}} + \frac{1}{\mu\kappa_s}\mathrm{I}_{\boldsymbol{t}}\Big). \tag{6}$$

This low-order approximation is the equivalent in elasticity of the zeroth-order approximation $1/(i\kappa)$ of the acoustic NtD map where κ is the wavenumber. The associated preconditioned integral equation is given by

$$(\frac{\mathrm{I}}{2} - D + \boldsymbol{V}'_{\mathrm{LO}}N)\boldsymbol{\psi} = \boldsymbol{u}^{inc}_{|\Gamma} - \boldsymbol{V}'_{\mathrm{LO}}\boldsymbol{t}^{inc}_{|\Gamma}, \quad \text{on } \Gamma, \tag{7}$$

and is called *LO-preconditioned CFIE* (LO P-CFIE). This preconditioner is very easy to implement and this is a main advantage.

High-order approximations. Similarly to previous works [2, 1] realised for the Dirichlet boundary condition case, we propose to consider the two following high-order approximations of the adjoint NtD map

$$\boldsymbol{V}'_{\mathrm{HO}(1)} = -2P(S) \text{ or } \boldsymbol{V}'_{\mathrm{HO}(2)} = -P(S)\Big(\frac{\mathrm{I}}{2} - P(D)\Big)^{-1} \tag{8}$$

where $P(S)$ and $P(D)$ are the respective principal parts of the operators S and D.

4. Numerical results

The numerical efficiency of the different new preconditioned CFIEs is illustrated for several more or less complex geometries. An analytical study for the spherical case underlines an excellent eigenvalue clustering around the point (1, 0) for the preconditioned HO-CFIEs. This is not the case for the standard CFIE (see Figure 1). For the Dirichlet case, the number of GMRES iterations is drastically reduced

when the preconditioned CFIEs are considered, independently of the frequency. For the Neumann case, first 2D numerical results show that the HO-PCFIEs allow to get a convergence independent of the mesh refinement. The number of iterations still depend on the frequency, but is efficiently reduced compared to the standard CFIE. We fix $\eta = 1$ and $\kappa_s = \sqrt{3}\kappa_p$.

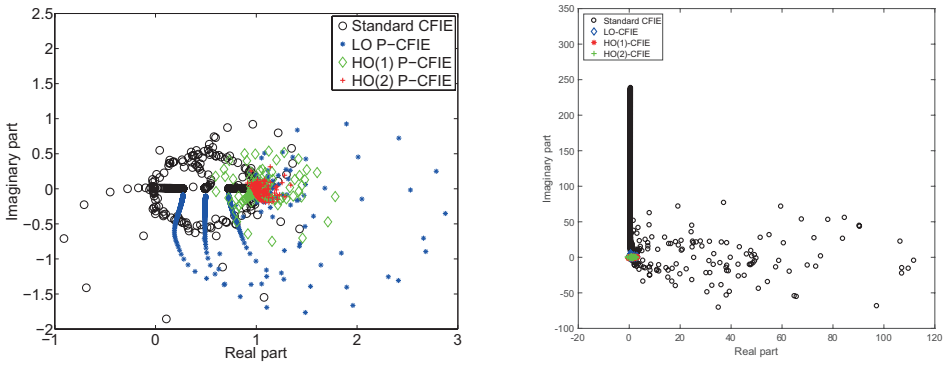

FIGURE 1. Unit sphere. Eigenvalue distribution of the standard and different P-CFIEs. Left: Dirichlet case ($\kappa_s = 16\pi$, $n_{\lambda_s} = 10$). Right: Neumann case ($\kappa_s = 50$, $n_{\lambda_s} = 12$).

#DOFs	ω	# iter CFIE	# iter LO P-CFIE	# iter HO(1) P-CFIE	# iter HO(2) P-CFIE
1 926	4	18	8	7	5 (11)
7 686	8.25	27	8	6	4 (11)
30 726	16.5	51	9	6	3 (13)
122 886	33	180	9	6	3 (13)
490 629	66.5	> 500	9	6	3 (14)

TABLE 2. Dirichlet. Diffraction of P-waves by the unit sphere. Number of GMRES iterations. Density of points $n_{\lambda_s} = 10$. Tolerance $\epsilon = 10^{-3}$ (inner $\epsilon = 10^{-4}$).

ω	# iter CFIE	# iter LO P-CFIE	# iter HO(1) P-CFIE	# iter HO(2) P-CFIE
2π	26	13	11	8(24)
4π	46	19	19	8(32)
6π	65	27	25	9(39)
8π	91	36	31	10(45)
16π	186	66	51	14(68)

TABLE 3. Neumann. Diffraction of S-waves by the unit disk. Number of GMRES iterations. Density of points $n_{\lambda_s} = 20$. Tolerance $\epsilon = 10^{-3}$ (inner $\epsilon = 10^{-5}$).

REFERENCES

[1] S. Chaillat, M. Darbas and F. Le Louër, *Fast iterative boundary element methods for high-frequency scattering problems in 3D elastodynamics*, JCP, **41** (2017), 429–446.

[2] M. Darbas and F. Le Louër, *Analytic preconditioners for the iterative solution of elasticity scattering problems*, M2AS, **38** (2015), 1705–1733.

[3] V. D. Kupradze, *Potential methods in the theory of elasticity*, Translated from the Russian by H. Gutfreund. Translation edited by I. Meroz, Israel Program for Scientific Translations, Jerusalem, 1965.
[4] G. C. Hsiao, W. L. Wendland, *Boundary integral equations*, **164** of Applied Mathematical Sciences, Springer-Verlag, Berlin, 2008.

Recent Advances of Isogeometric Boundary Element Methods for Electromagnetic Scattering Problems

Jürgen Dölz
(joint work with Stefan Kurz, Sebastian Schöps, Felix Wolf)

We consider the numerical solution of the electric field integral equation (EFIE) on a Lipschitz boundary Γ. In its variational form it seeks for a given $\mathbf{g} \in \mathbf{H}_\times^{-1/2}(\operatorname{div}_\Gamma, \Gamma)$ a surface current $\mathbf{j} \in \mathbf{H}_\times^{-1/2}(\operatorname{div}_\Gamma, \Gamma)$ such that

$$\int_\Gamma \int_\Gamma G_\kappa(\mathbf{x}-\mathbf{y}) \left(\mathbf{j}(\mathbf{x}) \cdot \mathbf{v}(\mathbf{y}) - \frac{1}{\kappa^2} \operatorname{div}_\Gamma \mathbf{j}(\mathbf{x}) \operatorname{div}_\Gamma \mathbf{v}(\mathbf{y}) \right) \mathrm{d}\sigma_{\mathbf{y}} \, \mathrm{d}\sigma_{\mathbf{x}} = \int_\Gamma \big(\mathbf{g}(\mathbf{x}) \times \mathbf{n}_{\mathbf{x}} \big) \cdot \mathbf{v}(\mathbf{x}) \, \mathrm{d}\sigma_{\mathbf{x}},$$

for all $\mathbf{v} \in \mathbf{H}_\times^{-1/2}(\operatorname{div}_\Gamma, \Gamma)$. We denote by $G_\kappa(\mathbf{x}) = \frac{e^{i\kappa\|\mathbf{x}\|}}{4\pi\|\mathbf{x}\|}$ the Helmholtz fundamental solution and by $\mathbf{H}_\times^{-1/2}(\operatorname{div}_\Gamma, \Gamma)$ the rotated tangential trace of $\mathbf{H}(\mathbf{curl})$. In the spirit of isogeometric analysis, we assume that Γ is given as a family of smooth, invertible geometry mappings

$$\mathbf{F}_j \colon \square \coloneqq [0,1]^2 \to \Gamma_j \subset \mathbb{R}^3,$$

where the intersections of the Γ_i are required to be empty, a vertex or an edge. In the case of an edge $\Gamma_i \cap \Gamma_j$, we assume that $\mathbf{F}_j(\cdot, 1) \equiv \mathbf{F}_i(\cdot, 0)$ holds up to rotation of $\square$.

For the discretization of the EFIE we consider B-spline based conforming finite element spaces. Therefore, the spline spaces $S^p(\Xi)$ of order p over a *p-open knot vector* Ξ on $[0,1]$ are defined as $\operatorname{span}(\{b_i^p\}_{i \le k})$, where the basis functions b_i^p are defined via the well known de Boor recursion fomula. B-spline bases on the unit square $\square$ are defined by a tensor product construction as $S_{p_1,p_2}(\Xi_1, \Xi_2)$, where the indices of polynomial degree and knot vector refer to the degrees and knot vectors used within each separate direction. Let $\mathbf{p} = (p_1, p_2)$ be a pair of polynomial degrees $p_1, p_2 > 0$ and Ξ_1, Ξ_2 be p_1- and p_2-open knot vectors on $[0,1]$. Let Ξ_1', Ξ_2' denote their truncation, i.e., the knot vector without its first and last element. We define the spline space $\mathbb{S}^1_{\mathbf{p},\boldsymbol{\Xi}}(\square)$ on $\square$ as $S^{p_1,p_2-1}(\Xi_1, \Xi_2') \times S^{p_1-1,p_2}(\Xi_1', \Xi_2)$. Mapping $\mathbb{S}^1_{\mathbf{p},\boldsymbol{\Xi}}(\square)$ onto each Γ_j with the Piola transformation ι_1 and enforcing normal continuity, one can define the boundary spline space

$$\mathbb{S}^1_{\mathbf{p},\boldsymbol{\Xi}}(\Gamma) = \big\{ \mathbf{f} \in \mathbf{H}_\times^{-1/2}(\operatorname{div}_\Gamma, \Gamma) \colon \iota_1^{-1}(\mathbf{F}_j)(\mathbf{f}|_{\Gamma_j}) \in \mathbb{S}^1_{\mathbf{p},\boldsymbol{\Xi}}(\square) \big\},$$

see also [4]. It can be shown that this space provides optimal approximation properties within $\mathbf{H}_\times^{-1/2}(\operatorname{div}_\Gamma, \Gamma)$, cf. [5].

To show existence and uniqueness of the solution of Galerkin discretizations of the EFIE using the spline space $\mathbb{S}^1_{\mathbf{p},\boldsymbol{\Xi}}(\Gamma)$, a discrete inf-sup condition has to be shown. Therefore, it is enough to construct continuous and discrete decompositions

$$\begin{aligned}\mathbf{H}_\times^{-1/2}(\mathrm{div}_\Gamma,\Gamma) &= \mathbf{W}\oplus\mathbf{V}\\ \mathbb{S}^1_{\mathbf{p},\boldsymbol{\Xi}}(\Gamma) &= \mathbf{W}_h\oplus\mathbf{V}_h\end{aligned}$$

such that

(1) the bilinear form is stable and coercive on $\mathbf{V}\times\mathbf{V}$ and $\mathbf{W}\times\mathbf{W}$, and compact on $\mathbf{V}\times\mathbf{W}$ and $\mathbf{W}\times\mathbf{V}$,
(2) $\mathbf{W}_h$ and $\mathbf{V}_h$ are closed subspaces of $\mathbf{H}_\times^{-1/2}(\mathrm{div}_\Gamma,\Gamma)$,
(3) $\mathbf{W}_h$ and $\mathbf{V}_h$ are stable under complex conjugation,
(4) it holds that $\mathbf{W}_h\subseteq\mathbf{W}$ and the *gap-property*

$$\sup_{\mathbf{v}_h\in\mathbf{V}_h}\inf_{\mathbf{v}\in\mathbf{V}}\frac{\|\mathbf{v}-\mathbf{v}_h\|_{\mathbf{H}_\times^{-1/2}(\mathrm{div}_\Gamma,\Gamma)}}{\|\mathbf{v}_h\|_{\mathbf{H}_\times^{-1/2}(\mathrm{div}_\Gamma,\Gamma)}}\xrightarrow{h\to 0}0,$$

see also [1, 3]. A common aproach to define these decompositions is to rely on a regularizing projection and to apply commuting quasi-interpolation operators into a finite element space. Unfortunately, the available quasi interpolation operators onto $\mathbb{S}^1_{\mathbf{p},\boldsymbol{\Xi}}(\Gamma)$ defined in [5] require more regularity than the standard regularizing projection from the literature provides. In [9], we show how this obstacle can be circumvented by introducing a modified regularizing projection for the construction of a discrete splitting which implies discrete inf-sup stability. Together with standard inf-sup theory, this yields optimal convergence rates of the isogeometric approach for the EFIE.

Besides these theoretical considerations, an efficient implementation is inevitable for practical use of the isogeometric approach. It is known since [10] that lowest order boundary element methods on parametric surfaces provide various algorithmic simplifications for the efficient compression of the arising dense system matrices within the $\mathcal{H}^2$-matrix format [2]. While traditional implementations of fast boundary element methods are based on a degree or freedom based clustering strategy, we propose to assemble and compress the discontinuous version of the system matrices and to use an element based clustering strategy. The continuity requirements of the B-splines are then enforced by transfer matrices which amounts to the "superspace" approach [6, 7].

A particular advantage of the described setting is that a black-box compression of the kernel function in admissible parts $\Gamma_{\boldsymbol{\lambda}}\times\Gamma_{\boldsymbol{\lambda}'}\subset\Gamma\times\Gamma$ can be directly performed on the unit square rather than on the boundary or in space. For the Helmholtz case, this yields an approximation of admissible matrix blocks of the kind

$$\begin{aligned}\big[\mathbf{A}_\kappa\big]_{i,j} &= \int_\Gamma \int_\Gamma G_\kappa(\mathbf{x}-\mathbf{y})\varphi_j(\mathbf{x})\varphi_i(\mathbf{y})\,\mathrm{d}\sigma_{\mathbf{y}}\,\mathrm{d}\sigma_{\mathbf{x}} \\ &= \int_\square \int_\square G_{\kappa,\boldsymbol{\lambda},\boldsymbol{\lambda}'}(\mathbf{s},\mathbf{t})\hat{\varphi}_j(\mathbf{s})\hat{\varphi}_i(\mathbf{t})\,\mathrm{d}\mathbf{t}\,\mathrm{d}\mathbf{s} \\ &\approx \sum_{\substack{\|\mathbf{m}\|_\infty \le q \\ \|\mathbf{m}'\|_\infty \le q}} G_{\kappa,\boldsymbol{\lambda},\boldsymbol{\lambda}'}(\mathbf{s}_\mathbf{m},\mathbf{t}_{\mathbf{m}'}) \int_\square \mathbf{L}_{\mathbf{m}'}(\mathbf{t})\widehat{\varphi}_i(\mathbf{t})\,\mathrm{d}\mathbf{t} \int_\square \mathbf{L}_\mathbf{m}(\mathbf{s})\widehat{\varphi}_j(\mathbf{s})\,\mathrm{d}\mathbf{s},\end{aligned}$$

with interpolation points $\mathbf{s}_\mathbf{m}$ and $\mathbf{t}_{\mathbf{m}'}$ and corresponding Lagrange polynomials $\mathbf{L}_\mathbf{m}$ and $\mathbf{L}_{\mathbf{m}'}$ on the unit square. The approximation reads

$$\big[\mathbf{A}_\kappa\big]_{i,j} = \big[\mathbf{M}_{|\boldsymbol{\lambda}|}\mathbf{K}_{\kappa,\boldsymbol{\lambda},\boldsymbol{\lambda}'}\mathbf{M}_{|\boldsymbol{\lambda}'|}^\intercal\big]_{i,j},$$

in matrix notation.

Unfortunately, the specific form of the electric single layer operator from the EFIE does not readily fit into this framework due to the involved surface differential operators. However, several small algorithmic modifications allow the neatless compression of the system matrix within the above framework. Summarizing, these modifications yield a matrix compression of the kind

$$\mathbf{A}_\kappa^{(\alpha,\beta)}\Big|_{\boldsymbol{\lambda},\boldsymbol{\lambda}'} \approx \begin{bmatrix}\mathbf{M}_{|\lambda|} & \mathbf{M}^\alpha_{|\lambda|}\end{bmatrix} \begin{bmatrix}\mathbf{K}^{(\alpha,\beta)}_{\kappa,\boldsymbol{\lambda},\boldsymbol{\lambda}',1} & \\ & \mathbf{K}^{(\alpha,\beta)}_{\kappa,\boldsymbol{\lambda},\boldsymbol{\lambda}',2}\end{bmatrix} \begin{bmatrix}\big(\mathbf{M}_{|\lambda|}\big)^\intercal \\ \big(\mathbf{M}^\beta_{|\lambda|}\big)^\intercal\end{bmatrix},$$

where we denote by $\alpha,\beta \in \{1,2\}$ the vector components of $\mathbb{S}^1_{\mathbf{p},\boldsymbol{\Xi}}(\Gamma)$ such that the system matrix of the EFIE reads

$$\mathbf{A}_\kappa = \begin{bmatrix}\mathbf{A}_\kappa^{(1,1)} & \mathbf{A}_\kappa^{(1,2)} \\ \mathbf{A}_\kappa^{(2,1)} & \mathbf{A}_\kappa^{(2,2)}\end{bmatrix}.$$

The corresponding algorithms are implemented and publicly available in our open source library Bembel [8] on `www.bembel.eu`.

References

[1] A. Bespalov, N. Heuer, R. Hiptmair, Convergence of the natural hp-BEM for the electric field integral equation on polyhedral surfaces, *SIAM Journal on Numerical Analysis*, 48, 1518–1529, 2010.

[2] S. Börm, Efficient Numerical Methods for Non-local Operators, European Mathematical Society (EMS), Zürich, 2010.

[3] A. Buffa, S. H. Christiansen, The Electric Field Integral Equation on Lipschitz Screens: Definitions and Numerical Approximation, *Numerische Mathematik*, 94(2):229–267, 2003.

[4] A. Buffa, J. Rivas, G. Sangalli, R. Vázquez, "Isogeometric discrete differential forms in three dimensions", *SIAM Journal on Numerical Analysis*, 49(2), 818–844, 2011.

[5] A. Buffa, J. Dölz, S. Kurz, S. Schöps, R. Vázquez, F. Wolf, "Multipatch approximation of the de Rham sequence and its traces in isogeometric analysis", *Numerische Mathematik*, 144, 201–236, 2020.

[6] J. Dölz, H. Harbrecht, M. Peters, An interpolation-based fast multipole method for higher-order boundary elements on parametric surfaces, *International Journal for Numerical Methods in Engineering*, 108(13), 1705–1728, 2016.

[7] J. Dölz, H. Harbrecht, S. Kurz, S. Schöps, F. Wolf, A Fast Isogeometric BEM for the Three Dimensional Laplace- and Helmholtz Problems, *Computer Methods in Applied Mechanics and Engineering*, 330(Supplement C), 83–101, 2018.
[8] J. Dölz, H. Harbrecht, S. Kurz, M. Multerer, S. Schöps, F. Wolf, Bembel: The fast isogeometric boundary element C++ library for Laplace, Helmholtz, and electric wave equation, *preprint: arXiv 1906.00785*, 2019.
[9] J. Dölz, S. Kurz, S. Schöps, F. Wolf, "Isogeometric boundary elements in electromagnetism: rigorous analysis, fast methods, and examples", *SIAM Journal on Scientific Computing*, 41 (5), B983–B1010, 2019.
[10] H. Harbrecht and M. Peters, Comparison of fast boundary element methods on para-metric surfaces, *Computer Methods in Applied Mechanics and Engineering*, 261–262:39–55, 2013.

`deltaBEM`: A rigorous theoretical analysis

Víctor Domínguez
(joint work with Tonatiuh Sánchez-Vizuet and Francisco-Javier Sayas)

`deltaBEM` is a compatible numerical discretization originally proposed for the four layer boundary operators, and potentials, for the Helmholtz equation in 2D smooth domains cf. [2] which was extended afterwards for the Elasticity and Elastodynamic case cf. [3]. The method provides the necessary tools for solving boundary integral equations for Dirichlet, Neumann, Robin and Transmission problems attaining a modest, but often sufficiently high, order 3. One of the strongest points is its computational simplicity: only evaluation of the fundamental solution and the parameterization of the curve and its first derivatives (the normal and tangent fields for the curve and normal derivative/stress tensor of the fundamental solution) are used—unlike other powerful schemes available in the literature.

The method was devised on the basis of rather formal arguments and some intuitive understanding of what might happen in the *backstage*. Hence, a mathematical analysis that provided a rigorous justification of what was observed in practice was missing. This work presents the first results leading to such analysis. In spite of its complexity—the theoretical framework comprises several technical results that require thoughtful attention—the analysis can be outlined in two main steps: (a) a consistency error expansion, and (b) stability as an inf-sup condition.

We sketch such analysis in section 3 of this abstract and leave for section 2 a fast presentation of the method.

1. deltaBEM METHOD

The boundary layer operators and equations, with a regular smooth 1−periodic parameterization of the boundary, are combinations of the identity operator, integral, and integro-differential operators as

$$(1a)\quad (\mathrm{H}\varphi)(\tau) = \mathrm{i\,p.v.}\int_0^1 \cot \pi(\tau - t)\varphi(t)\,\mathrm{d}\tau,$$

$$(1b)\quad (\mathrm{V}\varphi)(\tau) = \int_0^1 V(\tau,t)\varphi(t)\,\mathrm{d}t, \quad V(\tau,t) := A(\tau,t)\log\sin^2\pi(\tau-t),$$

$$(1c)\quad (\mathrm{K}\varphi)(\tau) = \int_0^1 K(\tau,t)\varphi(t)\,\mathrm{d}t,$$

$$(1d)\quad \mathrm{W} = -\mathrm{D}(\mathrm{V}_1 + \mathrm{K}_1)\mathrm{D} + \mathrm{V}_2 + \mathrm{K}_2, \quad \mathrm{D}\varphi := \varphi'$$

("p.v." stands for principal value in the Cauchy sense, functions A and K are smooth and 1–periodic and V_1, V_2 in (1c) are as in (1b)) which are usually referred to respectively as (periodic) Hilbert transform, logarithmic, smoothing and hypersingular operators. In the scale of 1–periodic Sobolev spaces $\{H^s\}_{s\in\mathbb{R}}$ they are known to be pseudo-differential operators of order 0, -1, $-\infty$ and 1 (see [6]).

Let A be a combination of such operators, of order $n \in \{-1, 0, 1\}$ and consider an operator equation stated in $H^{\pm 1/2}$

$$(2)\qquad \mathrm{A}\varphi = f \ \text{ or equivalently } \ (\psi, \mathrm{A}\varphi) = (\psi, f) \quad \forall \psi \in H^{\mp 1/2}.$$

Here $(\cdot,\cdot)$ denotes the $L^2(0,1)$ product extended to a sesquilinear form which provides the dual product $H^{\mp 1/2} \times H^{\pm 1/2}$ representation. Moreover, the unknown φ naturally lives either in $H^{\pm 1/2}$ (i.e. for single layer equations or double layer formulations for Neumann problems) or $H^{1/2}$ (i.e. hypersingular equations or double layer formulation in the Dirichlet case).

The `deltaBEM` algorithm starts from the sesquilinear form in (2). Hence, let N be a positive integer, set $h := 1/N$ and $t_\alpha = \alpha h$, and construct the main grid, $\{t_i\}_{i\in\mathbb{Z}}$ and the companion grids $\{t_{i\pm 1/6}\}_{i\in\mathbb{Z}}$. The trial spaces will be

$$(3)\qquad T_h := \{\delta_i \ : \ i = 1,\dots,N\}, \quad S_h := \{\chi_i \ : \ i = 1,\dots,N\}$$

where $\delta_\alpha = \delta(\cdot - \alpha h)$ and χ_c are, respectively, the 1–periodization of the Dirac delta at t_α and the characteristic function of the interval $(ch - h/2, ch + h/2)$. The spaces T_h and S_h are intended to replace $H^{-1/2}$ and $H^{1/2}$, respectively, in the continuous formulation. For the test spaces we proceed similarly with

$$(4)\quad T_h^\star = \{\delta_i^\star \ : \ i = 1,\dots,N\} \approx H^{-1/2}, \quad S_h^\star = \{\chi_i^\star \ : \ i = 1,\dots,N\} \approx H^{1/2}$$

where,

$$(5)\qquad \eta^\star := \alpha(\eta(\cdot - \tfrac{1}{6}h) + \eta(\cdot + \tfrac{1}{6}h)) + (1-\alpha)(\eta(\cdot - \tfrac{5}{6}h) + \eta(\cdot + \tfrac{1}{6}h)),$$

a weighted average of shiftings defined for any function/distribution η with weight $\alpha \in (1/2, 1]$. Let us point out that the necessity of working with such kind of grids, with this surprising $h/6$-shifting, was first noticed in [5] where a second-order quadrature method for logarithmic integral equations was devised.

Any integral appearing in what follows, either in the definition of the operator (H, V or K as in (1)) or when testing with elements in $S_h^\star$ is carried over intervals as $[x-h/2, x+h/2]$. These integrals will be approximated by the following third-order rule, which uses points outside the integration interval:

$$\int_{x-h/2}^{x+h/2} g(t)\,\mathrm{d}t \approx \tfrac{1}{24} h\left(g(x-h) + 22g(x) + g(x+h)\right). \tag{6}$$

Finally there are two cases whose discretization deserves special attention. First, the identity operator for which we have to consider the interaction between $\chi_i^\star$ and δ_j on one hand (equations posed in and with unknown in $H^{-1/2}$) and between $\delta_i^\star$ and χ_j on the other (equations in $H^{1/2}$ with unknowns in the same space). This will be done in the following non-intuitive fashion:

$$\{\chi_i^\star, \delta_j\}_h = \{\delta_i^\star, \chi_j\}_h = \begin{cases} 0 & |i-j| \neq 1 \mod N, \\ \frac{1}{18}(7-6a) & i = j, \\ \frac{2}{9}(1+3a) & |i-j| = 1 \mod N. \end{cases} \tag{7}$$

The analysis will eventually explain the rationale behind this definition. Secondly, the main part for the hypersingular operator:

$$\psi, \varphi \in H^{1/2} \; -(\psi, \mathrm{DVD}\varphi) = (\mathrm{D}\psi, \mathrm{VD}\varphi) \quad \rightsquigarrow \quad \psi_h \in T_h^\star, \varphi_h \in S_h^\star, \; (\mathrm{D}\psi_h, \mathrm{VD}\varphi_h).$$

Since $\mathrm{D}\chi_i^\circ = \delta_{i-1/2}^\circ - \delta_{i+1/2}^\circ$ for $\circ \in \{\emptyset, \star\}$ (trial and test), the sesquilinear form on $S_h^\star \times S_h$ involves just evaluations and averages of $V(t_{i+1/2\pm 1/6}, t_{j+1/2})$.

The `deltaBEM` scheme can be then summarized as follows:

$$\varphi_h \in R_h \quad \text{s.t.} \quad \{\psi_h^\star, \mathrm{A}_h\varphi_h\}_h = \{\psi_h^\star, f\}_h, \quad \forall \psi_h^\star \in R_h^\star \tag{8}$$

where the election of the test space $R_h \in \{S_h, T_h\}$, and trial space, $R_h^\star \in \{S_h^\star, T_h^\star\}$ is determined by the order of A and the space for which the continuous equation naturally holds. Finally, $\{\cdot,\cdot\}_h$ represents either the action of Dirac deltas or the quadrature rule (6) if piecewise constant functions are involved, taking into account (7).

The method can be then understood as a non-conforming Petrov-Galerkin method (the sesquilinear forms are well defined but are not continuos in the corresponding Sobolev norms since neither $S_h \notin H^{1/2}$ nor $T_h \in H^{-1/2}$) with possible quadrature for both test and operator. Note that the method requires only evaluating and averaging pointwise values of the kernel(s) of A at $(t_{i\pm 1/6}, t_j)$ and, if the hypersingular operator W is involved in the definition of A, $(t_{i\pm 1/6+1/2}, t_{j+1/2})$.

2. Convergence results and sketch of the analysis

Theorem 1. *Let φ be the solution of (2), $(\varphi_j)_{j=1}^n \subset \mathbb{C}$ so that is the discrete solution given by the scheme (8) is of the form*

$$\varphi_h = \sum_{j=1}^N \varphi_j \delta_j, \text{ if } R_h = T_h, \quad \text{or} \quad \varphi_h = \sum_{j=1}^N \varphi_j \chi_j, \text{ if } R_h = S_h.$$

Then, for φ sufficiently smooth, it holds

$$\max_j |\varphi(t_j) - \varphi_j^\bullet| \leq Ch^3 \|\varphi\|_{H^5}, \quad \textit{with} \quad \varphi_j^\bullet := \begin{cases} h^{-1}\varphi_j, & \textit{for } R_h = T_h, \\ \varphi_{j-1} + 22\varphi_j + \varphi_{j+1}, & \textit{for } R_h = S_h. \end{cases}$$

Let us discuss briefly the *pointwise* error estimate given above. For T_h, as the numerical solution is a linear combination of Dirac deltas, the term h^{-1} is consistent with the intuitive understanding of a delta as a unit mass *function* with support concentrated at one point. On the other hand, for piecewise constant functions in S_h, the linear combination for which third order convergence is obtained corresponds precisely to the weights appearing in the quadrature rule (6).

For the sake of brevity we just outline the analytical tools used in the proof and refer the reader to [4] for detailed proofs. Hence, we have

(a) A consistency error of the form

$$|\{\psi_h^\star, \mathrm{A}P_h\varphi\}_h - (\psi_h^\star, \mathrm{A}\eta)| \leq Ch^3 \|\varphi\|_{H^4} \|\psi_h\|_\diamond$$

In the expression above $\|\cdot\|_\diamond$ is either the L^2-norm (if applied to piecewise constant functions as that in $S_h^\star$ or S_h) or that of $H^{-1} = (H^1)'$ (for T_h and $T_h^\star$). On the other hand, P_h is a projection on the trial spaces defined by matching the Fourier central coefficient that is optimal in the following sense: It provides an $\mathcal{O}(h^r)$ approximation, for any r, which is attained by measuring the error in sufficiently weak Sobolev norms. This consistency error holds in fact for any choice of α in (5) with the sole—but important—constraint that we must take $\alpha = \frac{5}{6}$ if the Hilbert transform H is involved.

(b) An inf-sup condition, with $c > 0$ is independent of h:

$$\inf_{\varphi_h \in R_h} \sup_{\psi_h^\star \in R_h^\star} \frac{|\{\psi_h^\star, \mathrm{A}\varphi_h\}_h|}{\|\psi_h^\star\|_\diamond \|\varphi_h\|_\diamond} \geq c > 0.$$

The proof of this result is rather technical: it starts from the simplest cases for which A become convolution operators— hence diagonal in the complex exponential basis. The stability can be then reduced to showing the positivity of certain series functions, one for each canonical example, which is proven to hold provided that $\alpha \in (1/2, 1]$. Next, a perturbation argument can be devised to extend the inf-sup conditions for all practical cases.

Using the fact that the numerical and exact solutions are related by

$$\{\psi_h^\star, \mathrm{A}\varphi\}_h = (\psi_h^\star, \mathrm{A}\varphi),$$

(a) and (b) imply first

$$\|\varphi_h - \mathrm{P}_h\varphi\|_\diamond \sim \mathcal{O}(h^3)$$

and next, as consequence of the approximation properties of P_h,

$$\varphi_h - \varphi \sim \mathcal{O}(h^3).$$

These estimates, however, hold in rather weak—and not so useful—norms. This drawback is overcome using very well estabilished inverse inequalities in Sobolev

norms for S_h and T_h together with an enhanced consistency error estimate:

$$|\{\psi_h^\star, \mathrm{A}P_h\varphi\}_h - (\psi_h^\star, \mathrm{A}\eta) + h^3(\psi_h^\star, \mathrm{L_A}\eta)| \leq Ch^4\|\varphi\|_{H^5}\|\psi_h\|_\diamond \tag{9}$$

where $\mathrm{L_A}$ is a linear differential operator.

References

[1] `deltaBEM`, public repository in `https://team-pancho.github.io/deltaBEM/`

[2] V. Domínguez, S.L. Lu, F.J. Sayas, *A Nyström method for the two dimensional Helmholtz hypersingular equation*. Adv. Comput. Math. **40** (2014) 1121–157.

[3] V. Domínguez, T. Sánchez-Vizuet, F.J. Sayas, *A fully discrete Calderón calculus for the two-dimensional elastic wave equation*. Comput. Math. Appl. **69** (2015) 620–635.

[4] V. Domínguez, T. Sánchez-Vizuet, F.J. Sayas, *Theory and practice of* `deltaBEM`*: A simple toolkit for two-dimensional boundary integral equations*. In preparation.

[5] J. Saranen and L. Schroderu, *Quadrature methods for strongly elliptic equations of negative order on smooth closed curves*. SIAM J. Numer. Anal. **30** (1993) 1769–1795.

[6] J. Saranen and G. Vainikko. *Periodic Integral and Pseudodifferential Equations with Numerical Approximation*. Springer-Verlag, Berlin, 2002.

Progress on FEM-BEM frameworks for wave propagation in heterogeneous and unbounded media

Mahadevan Ganesh

(joint work with Víctor Domínguez)

Developing efficient mathematical and computational frameworks to understand propagation of acoustic and electromagnetic waves in bounded heterogeneous media, and also in the unbounded two- and three-dimensional free-space is fundamental for a large class of applications [2, 10, 13]. The inverse counterparts of the models facilitate understanding the heterogeneous media properties, by using measured far field data in the free-space [2]. The far field depends on the field scattered by the heterogeneous media, and the forward problem is governed by the mathematical models of the scattered field. For describing the scattered field, we start with a well known heterogenous media forward wave propagation problem.

Let the heterogeneous medium be $\Omega_0 \subset \mathbb{R}^d, d = 2, 3$, with its heterogeneity described by a spatially dependent refractive index n. The restriction of heterogeneity to Ω_0 can be defined by taking $n|_{\Omega_0^c} \equiv 1$, where $\Omega_0^c = \mathbb{R}^m \setminus \overline{\Omega}_0$ is the free-space complement of the Lipschitz configuration Ω_0 (that need not be connected). As shown in Figure 1, we consider the scenario of interaction of the heterogenous configuration and incident plane wave with wavenumber $\kappa = 2\pi/\lambda$, where λ is the wavelength. The interaction induces a scattered field u^s in Ω_0^c.

In case of acoustic and electromagnetic waves propagation in 2D ($d = 2$) or acoustic waves in 3D ($d = 3$), the total field ($u := u^s + u_{\mathrm{inc}}$) and scattered field can be mathematically modeled by the variable coefficient Helmholtz equation [2, 10, 13]

$$\Delta u(\boldsymbol{x}) + \kappa^2 n^2(\boldsymbol{x})u(\boldsymbol{x}) = 0, \qquad \boldsymbol{x} \in \mathbb{R}^d, \tag{1}$$

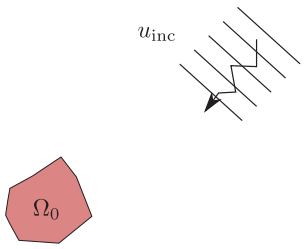

FIGURE 1. A model configuration with an input incident wave u_{inc} impinging on a heterogeneous medium Ω_0.

and the Sommerfeld radiation condition (SRC)

$$\lim_{|\boldsymbol{x}|\to\infty} |\boldsymbol{x}|^{(d-1)/2} \left(\frac{\partial u^s(\boldsymbol{x})}{\partial |\boldsymbol{x}|} - i\kappa u^s(\boldsymbol{x}) \right) = 0. \tag{2}$$

The limit in the SRC (2) holds uniformly in all directions $\widehat{\boldsymbol{x}} = \boldsymbol{x}/|\boldsymbol{x}| \in \mathbb{S}^{d-1}$. The scattered field u^s is a radiating field and, as a consequence of the SRC, its behavior at infinity is captured by the far field $u^\infty \in L^2(\mathbb{S}^{d-1})$, where

$$u^\infty(\widehat{\boldsymbol{x}}) = \lim_{|\boldsymbol{x}|\to\infty} |\boldsymbol{x}|^{(d-1)/2} e^{-i\kappa|\boldsymbol{x}|} u^s(\boldsymbol{x}), \qquad \widehat{\boldsymbol{x}} = \boldsymbol{x}/|\boldsymbol{x}| \in \mathbb{S}^{d-1}. \tag{3}$$

The mathematical and computational problem of our current interest is whether we can incorporate the SRC exactly in computational models, allow for general heterogeneity, and hence facilitate efficient simulation of the far field for the heterogeneous media problem. For a general Lipschitz heterogenous medium Ω_0, computational frameworks for solving the mathematical model (1)–(2) require tessellation of the wave propagation region with finitely many bounded sub-regions. Thus the progress, over several decades, for the above model wave propagation problem is based mainly on creating frameworks that use only bounded tessellation/approximation regions. Most of these frameworks solve the problem with substantial compromise on the SRC and/or the heterogeneity. Below we briefly describe progress in such frameworks, and conclude with our recently proposed and analyzed overlapped mathematical framework [4] that facilitates retaining both the SRC and heterogeneity and hence accurate simulations of the far field [4].

The key computational constraint is the restriction on frameworks that would require only finitely many unknowns on bounded regions. Hence heterogeneous media wave propagation computational frameworks have been based mainly on the idea of introducing an artificial truncation of the propagation region by considering a secondary domain, say, Ω_2 such that $\overline{\Omega_0} \subset \Omega_2$. Consequently, the widely studied computational frameworks are based on the approach of using, typically, a lower order approximation of the SRC in (2) to setup an appropriate (absorbing) condition on the boundary of Σ of Ω_2 and hence solving the Helmholtz equation in the restricted bounded domain Ω_2. It is important to note that Ω_2 should be sufficiently large to obtain accurate approximations to the far field u^∞ in (3).

Computational complexity in simulating the restricted bounded heterogeneous media model is dictated by the frequency κa of the problem, where a is the diameter of Ω_2. Simulation of the high-frequency heterogeneous media model is difficult

and it is still an active research area. In practice, the size of the artificially truncated region Ω_2 is taken to be small enough to accommodate the heterogeneous region Ω_0 so that κa is not large. Accordingly, accurate simulations of the far-field u^∞ in (3) is not possible through a bounded truncated framework only in Ω_2.

A widely used computational approach for simulating the Helmholtz model in Ω_2, with some boundary condition on Σ, is the finite element method (FEM) [10]. For the FEM, it is efficient to choose Σ to be a polygonal boundary to avoid complex isoparametric FEM in 3D. Even for polygonal regions a major difficulty, especially in 3D, is because of the sign-indefiniteness of the algebraic system arising from the lack of coercivity in the standard variational formulations of the Helmholtz PDE [10]. A coercive variational formulation for the heterogeneous Helmholtz model was developed recently in [6], and an associated preconditioned sign-definite high-order FEM was also developed, analyzed and implemented in [6].

While the standard FEM for the restricted Helmholtz model avoids the SRC but efficiently incorporates the heterogeneity, one may consider instead fully incorporating the SRC and avoid general heterogeneity. For example, since $n|_{\Omega_2^c} \equiv 1$, we may consider the problem (1)–(2) in the free-space Ω_2^c with the Helmholtz operator $(\Delta + \kappa^2 I)$. Since the fundamental solution of this operator is known, the unbounded region problem can be reformulated [2, 13] as an equivalent boundary integral equation (BIE). The BIE unknown density occurs only on the bounded boundary Σ, and the density yields the scattered field u^s in Ω_2^c through a chosen potential ansatz [2, 13]. Computational methods for simulating the BIE are known as boundary element methods (BEM). The survey articles [1, 11], with hundreds of references, describe many coercive and non-coercive BIE reformulations [2, 13] based BEM for simulating the exterior homogeneous Helmholtz model.

Assuming the major restriction of avoiding general heterogeneity in (1)–(2), the BEM on an artificial boundary and an associated BEM-ansatz for u^s will facilitate (i) the evaluation of anywhere in the unbounded region Ω_2^c; (ii) exactly satisfying the SRC; and (iii) hence provide a boundary integral formula for the far-field [2, 13]. Following FEM, it is standard to develop BEM to mainly use polygonal boundaries and avoid curved elements. However, since the user can choose any artificial boundary, in order to reduce the computational complexity it is efficient to use a smooth boundary based spectral BEM [2]. Hence the choice Σ can be replaced by a smooth boundary Γ, leading to instead the exterior region for homogeneous model to, say, Ω_1^c. The discussed choices Ω_1 and Ω_2, with respective boundaries Γ and Σ, for the Figure 1 based model problem is shown in Figure 2.

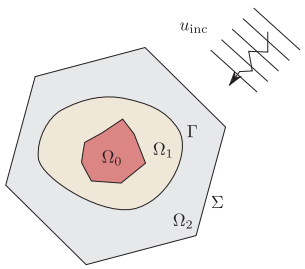

FIGURE 2. Two artificial boundaries in the model configuration.

The next natural approach is to consider coupling mathematical frameworks that can facilitate use of both FEM and BEM to simulate the model (1)–(2), and consequently incorporating the SRC exactly and also allow for general heterogeneous configurations. Such FEM-BEM friendly coupling mathematical frameworks have been developed and analyzed only by a few authors, but several researchers implemented the associated FEM-BEM computational frameworks. For example, see the review article [14] for the Johnson-Nédélec framework with coupling based on a single polygonal interface (such as only Σ in Figure 2). A framework with a single smooth boundary coupling interface in 2D (such as only Γ in Figure 2) was developed and analyzed by Kirsch and Monk [12]. Using two artificial interfaces (such as both Γ and Σ in Figure 2), a mathematical framework in 2D was developed over four decades ago by Jami and Lenoir in [9]; and recently (in 2D and 3D), a different overlapping mathematical framework (with Γ and Σ), for the wave propagation model (1)–(2), was developed by the authors of this article [4].

We are not aware of any 3D FEM-BEM implementation of the full model problem (1)–(2). However, 2D FEM-BEM implementations have been carried out by several authors: For the Johnson-Nédélec framework based implementations and numerical analysis, see [14] and references therein. For recent FEM-BEM implementations of the Kirsch-Monk framework for complex heterogeneity with a smooth artificial boundary see [5]; and with a rectangular boundary, see [7]. For the Jami-Lenoir framework implementations, see [3, 8]. In [4], we demonstrated the efficiency of our overlapped FEM-BEM framework in 2D. Our future work will include numerical analysis of the implementation in [4], and also overlapped FEM-BEM implementation and analysis for the 3D case using the framework in [4].

Acknowledgement. M. Ganesh was partially supported by the Simons Foundation and by the Mathematisches Forschungsinstitut Oberwolfach.

References

[1] S. N. Chandler-Wilde, I. G. Graham, S. Langdon, and E. A. Spence. Numerical-asymptotic boundary integral methods in high-frequency acoustic scattering. *Acta Numerica*, 21:89–305, 2012.

[2] D. Colton, R. Kress, Inverse Acoustic and Electromagnetic Scattering Theory, Springer, 2012.

[3] J. Coyle and P. Monk *Scattering of time-harmonic electromagnetic waves by anisotropic in homogeneous scatterers or impenetrable obstacles SIAM J. Numer. Anal.*, 37(5):1590–1617, 2004.

[4] V. Domínguez, M. Ganesh and F.-J. Sayas. An overlapping decomposition framework for wave propagation in heterogeneous and unbounded media: Formulation, analysis, algorithm, and simulation *J. Comput. Phys.*, 2020 (to appear, `https://doi.org/10.1016/j.jcp.2019.109052`).

[5] M. Ganesh and C. Morgenstern. High-order FEM-BEM computer models for wave propagation in unbounded and heterogeneous media: application to time-harmonic acoustic horn problem. *J. Comput. Appl. Math.*, 307:183–203, 2016.

[6] M. Ganesh and C. Morgenstern. A coercive heterogeneous media Helmholtz model: formulation, wavenumber-explicit analysis, and preconditioned high-order FEM. *Numerical Algorithms*, 2020 (to appear, 47 pages, `https://doi.org/10.1007/s11075-019-00732-8`).

[7] A. Gilman, A.H. Barnett, and P-G Martinsson A spectrally accurate direct solution technique for frequency-domain scattering problems with variable media BIT Numer. Math., 55:141–170, 2015.
[8] C. Hazard and M. Lenoir. On the solutions of time-harmonic scattering problems for Maxwell's equations. SIAM J. Math. Anal., 27:1597–1630, 1996.
[9] A. Jami and M. Lenoir, A variational formulation for exterior problems in linear hydrodynamics *Comput. Methods Appl. Mech. Engrg.*, 16:341–359, 1978.
[10] F. Ihlenburg. *Finite element analysis of acoustic scattering*, volume 132 of *Applied Mathematical Sciences*. Springer-Verlag, New York, 1998.
[11] S. Kirkup. The boundary element method in acoustics: A survey. *Applied Sciences*, 9:1642, 04 2019.
[12] A. Kirsch and P. Monk. Convergence analysis of a coupled finite element and spectral method in acoustic scattering. *IMA J. Numerical Analysis*, 9:425–447, 1990.
[13] J.-C. Nédélec. *Acoustic and Electromagnetic Equations*. Springer, 2001.
[14] F. J. Sayas. The validity of Johnson-Nédélec's BEM-FEM coupling on polygonal interfaces. *SIAM Review*, 55:131–146, 2013.

A fast direct solver for scattering problems in quasi-periodic layered media

Adrianna Gillman
(joint work with Yabin Zhang)

In this talk, we present a fast direct solver for quasi-periodic scattering problems in multilayered media. Scattering problems in $I+1$ layers are defined by

$$
\begin{aligned}
(\Delta+\omega_i^2)u_i(\boldsymbol{x}) &= 0 \qquad && \boldsymbol{x}\in\Omega_i \\
u_1-u_2 &= -u^{\text{inc}}(\boldsymbol{x}) && \boldsymbol{x}\in\Gamma_1 \\
\frac{\partial u_1}{\partial\nu}-\frac{\partial u_2}{\partial\nu} &= -\frac{\partial u^{\text{inc}}}{\partial\nu} && \boldsymbol{x}\in\Gamma_1 \\
u_i-u_{i+1} &= 0 && \boldsymbol{x}\in\Gamma_i,\ 1<i<I+1 \\
\frac{\partial u_i}{\partial\nu}-\frac{\partial u_{i+1}}{\partial\nu} &= 0 && \boldsymbol{x}\in\Gamma_i,\ 1<i<I+1
\end{aligned}
\tag{1}
$$

where u_i is the unknown solution in the region $\Omega_i\in\mathbb{R}^2$ and the wave number in Ω_i is given by ω_i for $i=1,\ldots,I+1$. The interface Γ_i for $i=1,\ldots,I$ between each layer is periodic with period d. The boundary conditions enforce continuity of the solution and its flux through the interfaces Γ_i. The incident wave u^{inc} is defined by $u^{\text{inc}}(\boldsymbol{x})=e^{\mathrm{i}\boldsymbol{k}\cdot\boldsymbol{x}}$ where the incident vector is $\boldsymbol{k}=(\omega_1\cos\theta^{\text{inc}},\omega_1\sin\theta^{\text{inc}})$ and the incident angle is $-\pi<\theta^{\text{inc}}<0$. Figure 1 illustrates a five layered periodic geometry. The incident wave u^{inc} is *quasi-periodic* up to a phase, i.e. $u^{\text{inc}}(x+d,y)=\alpha u^{\text{inc}}(x,y)$ for $(x,y)\in\mathbb{R}^2$, where α is the Bloch phase defined by

$$\alpha := e^{i\omega_1 d\cos\theta^{\text{inc}}}.$$

In the top and bottom layer, the solution satisifies a radition condition that is characterized by the uniform convergence of the Rayleigh-Bloch expansions [1].

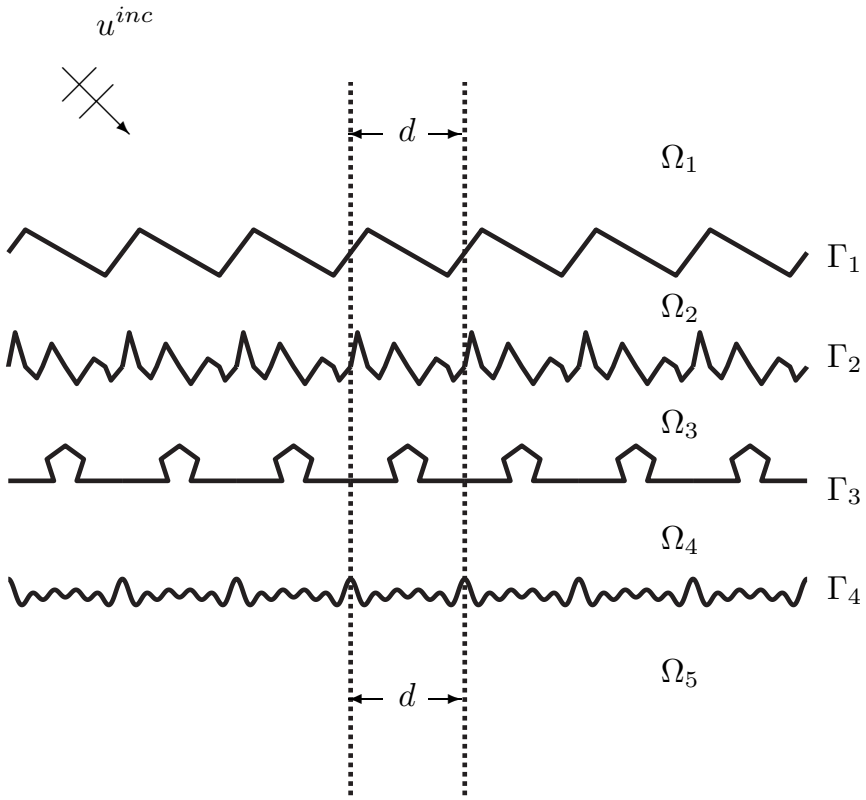

FIGURE 1. A five layered periodic geometry. 7 periods are shown.

Scattering problems involving multilayered media arise in applications such as material design and inverse scattering. In each of these applications, the scattering problem needs to be solved for hundreds of incident angles. Then the geometry is updated with either a change in the wave speed in a layer or a change in an interface. The presented fast direct solver is able to re-use the parts of the solver for the unchanged parts of the geometry.

The fast direct solver presented in this talk was constructed for the integral formulation proposed in [5]. This integral formulation represents the solution in a layer Ω_i via a combined field representation involving the free space Green's function and an additional term which enforces quasi-periodicity. For example, in the top layer, the solution to (1) is given by

$$u_1(\boldsymbol{x}) = (\tilde{\mathcal{S}}^{\omega_1}_{\Gamma_1}\sigma_1)(\boldsymbol{x}) + (\tilde{\mathcal{D}}^{\omega_1}_{\Gamma_1}\tau_1)(\boldsymbol{x}) + \sum_{j=1}^{P} c_j^1 \phi_j^{\omega_1}(\boldsymbol{x})$$

where

$$(\tilde{\mathcal{S}}^{\omega_1}_{\Gamma_1}\sigma_1)(\boldsymbol{x}) = \sum_{l=-1}^{1} \alpha^l \int_{\Gamma_1} G_{\omega_1}(\boldsymbol{x}, \boldsymbol{y} + l\boldsymbol{d})\sigma_1(\boldsymbol{y}) dl(\boldsymbol{y}),$$

$$(\tilde{\mathcal{D}}^{\omega_1}_{\Gamma_1}\tau_1)(\boldsymbol{x}) = \sum_{l=-1}^{1} \alpha^l \int_{\Gamma_1} \partial_{\nu_{\boldsymbol{y}}} G_{\omega_1}(\boldsymbol{x}, \boldsymbol{y} + l\boldsymbol{d})\tau_1(\boldsymbol{y}) dl(\boldsymbol{y}),$$

$G_{\omega_1}(\boldsymbol{x}, \boldsymbol{y})$ denotes the free space Green's function for Helmholtz equation, ϕ^{ω_1} are the functions used to enforce the quasi-periodicity of the solution, σ_1 and τ_1 are unknown boundary charge distributions, and $\{c_j^1\}_{j=1}^P$ are the unknown constants for enforcing quasi-periodicity. Each interface has it own set of unknown boundary charge distributions and each layer has its own set of periodizing constants. The integral formulation does not naturally satisfy the radiation condition. To enforce the radiation condition the integral representation is only used inside a unit cell containing all the interfaces. Outside the unit cell a truncated Rayleigh-Bloch expansion is used to enforce the radiation condition. The coefficients of the expansion are chosen so the two representations are continuous through the artificial unit cell interface.

Upon discretization, one has to solve the following linear system

$$\begin{bmatrix} \mathsf{A} & \mathsf{B} & \mathbf{0} \\ \mathsf{C} & \mathsf{Q} & \mathbf{0} \\ \mathsf{Z} & \mathsf{V} & \mathsf{W} \end{bmatrix} \begin{bmatrix} \hat{\boldsymbol{\sigma}} \\ \boldsymbol{c} \\ \boldsymbol{a} \end{bmatrix} = \begin{bmatrix} \boldsymbol{f} \\ \mathbf{0} \\ \mathbf{0} \end{bmatrix} \tag{2}$$

where all the matrices are sparse with block structure and the matrix A results from the discretization of the integral equations on each interface. The first row equation enforces the continuity of the scattered field and its flux through the interfaces. The second row equation enforces the quasi-periodicity of the solution and the flux. The last row equation enforces continuity of the integral representation and the Rayleigh-Bloch expansions.

When the interface geometries are complex, the cost solving (2) is dominated by the cost of inverting A. Fortunately, the matrix A is block tridiagonal and each of the blocks is amenable to fast linear algebra techniques. Specifically, the matrix A can be written as

$$\mathsf{A} = \underbrace{\begin{bmatrix} \mathsf{A}^s_{11} & 0 & 0 & 0 & 0 \\ 0 & \mathsf{A}^s_{22} & 0 & 0 & 0 \\ 0 & 0 & \ddots & 0 & 0 \\ 0 & 0 & 0 & \mathsf{A}^s_{(N-1)(N-1)} & 0 \\ 0 & 0 & 0 & 0 & \mathsf{A}^s_{NN} \end{bmatrix}}_{\mathsf{A}_0} + \underbrace{\begin{bmatrix} \mathsf{A}^{pm}_{11} & \mathsf{A}_{12} & 0 & 0 & 0 \\ \mathsf{A}_{21} & \mathsf{A}^{pm}_{22} & \mathsf{A}_{23} & 0 & 0 \\ 0 & 0 & \ddots & \ddots & 0 \\ 0 & 0 & \mathsf{A}_{(N-1),(N-2)} & \mathsf{A}^{pm}_{(N-1)(N-1)} & \mathsf{A}_{(N-1),N} \\ 0 & 0 & 0 & \mathsf{A}_{N,(N-1)} & \mathsf{A}^{pm}_{NN} \end{bmatrix}}_{\hat{\mathsf{A}}}$$

where A_{ii}^{s} corresponds to a discretized integral operator defined on Γ_i evaluated on Γ_i, A_{ii}^{pm} corresponds to a discretized integral operator defined on Γ_i evaluated on the left and right neighbor copied of Γ_i, and A_{ij} corresponds to an integral operator defined on Γ_i (and its left and right neighbor copies) evaluated on Γ_j. The matrices A_{ii}^{s} are amenable to fast inversion techniques such as *Hierarchically Block Separable (HBS)* methods [6, 8, 4], *Hierarchically Semi-Separable (HSS)* [12, 10, 11], the Hierarchical interpolative factorization [9], the $\mathcal{H}$ and $\mathcal{H}^2$-matrix methods [2, 3]. The matrices in $\hat{\mathsf{A}}$ correspond to interactions of "far" interfaces which means the matrices are low rank. Thus it is possible to apply the inverse of A in a manner that scales linearly with respect to the number of discretization points via a Woodbury formula [7]

$$\mathsf{A}^{-1} \approx (\mathsf{A}_0 + \mathsf{LR})^{-1} = \mathsf{A}_0^{-1} - \mathsf{A}_0^{-1}\mathsf{L}\left(\mathsf{I} + \mathsf{R}\mathsf{A}_0^{-1}\mathsf{L}\right)^{-1}\mathsf{R}\mathsf{A}_0^{-1}$$

where L and R are the low rank factors of $\hat{\mathsf{A}}$. The fast direct solver for A is built so that for each new Bloch phase the only new computation is the inverse of $\left(\mathsf{I} + \mathsf{R}\mathsf{A}_0^{-1}\mathsf{L}\right)^{-1}$ which is small (much smaller than A and block tridiagonal. Thus the application of the inverse can be constructed rapidly via a block version of the Thomas algorithm.

The talk highlights the important steps in constructing the fast direct solver and presents some numerical results. The details for constructing the fast direct solver and additional numerical results are presented [13].

References

[1] A-S. Bonnet-Bendhia and F. Starling. Guided waves by electromagnetic gratings and non-uniqueness examples for the diffraction problem. *Mathematical Methods in the Applied Sciences*, 17(5):305-338, 1994.

[2] S. Börm. *Efficient numerical methods for non-local operators*, volume 14 of *EMS Tracts in Mathematics*. European Mathematical Society (EMS), Zürich, 2010.

[3] S. Börm and W. Hackbusch. Approximation of boundary element operators by adaptive $\mathcal{H}^2$-matrices. In *Foundations of computational mathematics: Minneapolis, 2002*, volume 312 of *London Math. Soc. Lecture Note Ser.*, pages 58–75. Cambridge Univ. Press, Cambridge, 2004.

[4] J. Bremer, A. Gillman, and P. Martinsson. A high-order accurate accelerated direct solver for acoustic scattering from surfaces. *BIT Numerical Mathematics*, 55:141–170, 2015.

[5] M. Cho and A. Barnett. Robust fast direct integral equation solver for quasi-periodic scattering problems with a large number of layers. *Optics Express*, 23(2):1775–1799, 2015.

[6] A. Gillman, P. Young, and P. Martinsson. A direct solver $O(N)$ complexity for integral equations on one-dimensional domains. *Frontiers of Mathematics in China*, 7:217–247, 2012.

[7] G. H. Golub and C. F. Van Loan. *Matrix computations*. Johns Hopkins Studies in the Mathematical Sciences. Johns Hopkins University Press, Baltimore, MD, third edition, 1996.

[8] K. Ho and L. Greengard. A fast direct solver for structured linear systems by recursive skeletonization. *SIAM Journal of Scientific Computing*, 34(5):2507–2532, 2012.

[9] K. Ho and L. Ying. Hierarchical interpolative factorization for elliptic operators: Integral equations. *Communications on Pure and Applied Mathematics*, 69(7):1314–1353, 2015.

[10] Z. Sheng, P. Dewilde, and S. Chandrasekaran. Algorithms to solve hierarchically semi-separable systems. In *System theory, the Schur algorithm and multidimensional analysis*, volume 176 of *Operator Theory: Advances and Applications*, pages 255–294. Birkhäuser, Basel, 2007.

[11] J. Xia, S. Chandrasekaran, M. Gu, and X. Li. Fast algorithms for hierarchically semiseparable matrices. *Numerical Linear Algebra with Applications*, 17(6):953–976, 2010.
[12] J. Xia, S. Chandrasekaran, M. Gu, and X. S. Li. Superfast multifrontal method for large structured linear systems of equations. *SIAM Journal on Matrix Analysis and Applications*, 31(3):1382–1411, 2009.
[13] Y. Zhang and A. Gillman. A fast direct solver for two dimensional quasi-periodic multilayered media scattering problems. *In review.* Available at arXiv:1907.06223.

Pseudodifferential equations in polyhedral domains I: Regularity and singular expansions

Heiko Gimperlein
(joint work with R. Mazzeo, N. Louca, E. P. Stephan, J. Stocek, C. Urzua-Torres)

Solutions to elliptic boundary value problems in polyhedral domains exhibit singularities at edges and corners. Their asymptotic behavior has been studied for several decades, with seminal contributions, e.g. by Kondratiev, Dauge or Mazya. Explicit singular expansions give rise to h and hp discretizations with optimal convergence rates for finite [2] and boundary element methods [12].

This talk addressed corresponding questions for boundary problems involving nonlocal operators, such as the integral fractional Laplacian. We refer to the recent survey article [3] for motivation and recent advances.

Sharp results for the regularity of the solutions to such problems in smooth domains have been obtained by Grubb [11]. We here address a recent alternative approach given in [6], which we generalize to domains with corners. We obtain detailed asymptotic expansions for the solution at edges and vertices, which generalize classical results for mixed boundary problems for the standard Laplace equation. Applications to h and hp discretizations with optimal convergence rates are discussed in a second talk at this conference, by J. Stocek. In convex polygons, weighted Sobolev estimates were shown in [1], resulting in optimal convergence rates on graded meshes.

To be specific, we consider the integral fractional Laplacian, defined for a Schwartz function u on $\mathbb{R}^n$ by

$$(-\Delta)^s u(x) = c_{n,s}\, P.V. \int_{\mathbb{R}^n} \frac{u(x)-u(y)}{|x-y|^{n+2s}} dy, \qquad (s \in (0,1)).$$

Here *P.V.* denotes the Cauchy principal value and $c_{n,s} = \frac{2^{2s} s \Gamma\left(\frac{n+2s}{2}\right)}{\pi^{\frac{n}{2}}}$. The operator $(-\Delta)^s : \widetilde{H}^s(\mathbb{R}^n) \to H^{-s}(\mathbb{R}^n)$ is a pseudodifferential operator of order $2s$. For $s \to 1^-$ one recovers the Laplacian $-\Delta$.

The corresponding fractional Dirichlet problem in a domain $\Omega \subset \mathbb{R}^n$ is given by

$$\begin{aligned} (-\Delta)^s u &= f \text{ in } \Omega, \\ u &= 0 \text{ in } \Omega^C = \mathbb{R}^n \setminus \overline{\Omega}\ . \end{aligned} \tag{1}$$

For $f \in H^{-s}(\Omega)$ there exists a unique solution $u \in \widetilde{H}^s(\Omega)$, and the purpose of this talk is to discuss higher regularity of u for smoother f. Our first observation relates this problem to classical problems for boundary integral equations:

Theorem 1 ([10]). *a) For $s = \frac{1}{2}$, Problem (1) is equivalent to the hypersingular integral equation $2Wu = f$ on $\Omega \times \{0\} \subset \mathbb{R}^{n+1}$.*
b) Problem (1) admits an analytic extension to $s \in \mathbb{C}$. For $s = -\frac{1}{2}$, it is equivalent to the weakly singular integral equation $2Vu = f$ on $\Omega \times \{0\} \subset \mathbb{R}^{n+1}$.

An explicit solution to (1) when $\Omega = \mathcal{B}_1$ is the unit ball goes back to Boggio:

$$(2)\quad u(x) = \int_{\mathcal{B}_1} G_s(x,y) f(y)\, dy\,, G_s(x,y) = k_{n,s}|x-y|^{2s-n} \int_0^{r(x,y)} \frac{t^{s-1}}{(t+1)^{n/2}}\, dt\,,$$

where $r(x,y) = \dfrac{(1-|x|^2)_+(1-|y|^2)_+}{|x-y|^2}$ and $k_{n,s} = \dfrac{2^{1-2s}}{|\partial\mathcal{B}_1|\Gamma(s)^2}$. Similar exact solution formulas for V and W have been of recent interest [13, 14], with applications to preconditioning. They are recovered by Boggio's formula (2) and Theorem 1. The observation leads to a short proof for this line of results and generalizes them to arbitrary elliptic pseudodifferential boundary problems of order between -2 and 2, such as Problem (1).

Specifically, in [10] we consider conforming finite element discretizations of such problems by piecewise constant, resp. linear elements. Boggio's formula (2) defines an operator preconditioner C for the Galerkin matrix A of the boundary problem, which we show to be optimal:

Theorem 2 ([10]). *Under mild assumptions on the triangulation, the condition number of CA is independent of the mesh size.*

Boggio's formula also shows that when $\Omega = \mathcal{B}_1$ and f is smooth, the solution u admits an asymptotic expansion near $\partial\mathcal{B}_1$, with leading singular exponent $\nu = s$. This is a special case of the precise boundary behavior obtained in [11] near a smooth boundary $\partial\Omega$. We obtain asymptotic expansions for the solution u of (1) near the boundary and corners of a polygon Ω for all $s \in (0,1)$:

Theorem 3 ([6, 7]). *Let $\Omega \subset \mathbb{R}^2$ be a polygonal domain, $f \in C^\infty(\overline{\Omega})$. Then the solution u to (1) admits an asymptotic expansion near the boundary and the vertices. Near a smooth boundary point the leading singular exponent is given by s: $u(x) \sim \operatorname{dist}(x,\partial\Omega)^s$. At a vertex V the singular exponent λ, with $u(x) \sim \operatorname{dist}(x,V)^\lambda$, is the smallest eigenvalue of an elliptic differential operator of second order on S^2_+.*

Remark 4. This exponent λ is an increasing function of s and a decreasing function of the vertex angle. The upper and lower bounds $\lambda < 2s$, $\lambda > \max\{0, s - \frac{1}{2}\}$, are sharp and attained when the vertex angle tends to 2π. Our study of λ generalizes classical results for $s = \frac{1}{2}$, e.g. in [9].

The crucial idea in the proof of Theorem 3 is to reformulate (1) as a local, degenerate mixed boundary value problem in the upper half space $\mathbb{R}^3_+$ [6]. The

reformulation as a local differential equation allows to study the solution u using pseudodifferential techniques developed for boundary problems on singular spaces [4]. The idea to extend to $\mathbb{R}^3_+$ goes back to Caffarelli and Silvestre (2007), but its use for a precise regularity theory seems to be new.

References

[1] G. Acosta, J. P. Borthagaray, *A fractional Laplace equation: regularity of solutions and finite element approximations*, SIAM Journal on Numerical Analysis 55 (2017), 472–495.

[2] I. Babuška, *Finite element method for domains with corners*, Computing 6 (1970), 264–273.

[3] J. P. Borthagaray, W. Li, R. H. Nochetto, *Linear and Nonlinear Fractional Elliptic Problems*, arXiv:1906.04230.

[4] M. Dauge, *Elliptic boundary value problems in corner domains*, Lecture Notes in Mathematics 1341, Springer Verlag, 1988.

[5] G. Estrada-Rodriguez, H. Gimperlein and J. Stocek, *Nonlocal interface problems: Modelling, regularity, finite element approximation*, preprint (2020).

[6] H. Gimperlein, N. Louca, R. Mazzeo, in preparation.

[7] H. Gimperlein, E. P. Stephan and J. Stocek, *Corner Singularities for the Fractional Laplacian and Finite Element Approximation*, preprint (2020).

[8] H. Gimperlein, E. P. Stephan and J. Stocek, in preparation.

[9] J. A. Morrison, J. A. Lewis, *Charge Singularity at the Corner of a Flat Plate*, SIAM Journal on Applied Mathematics 31 (1976), 233-250.

[10] H. Gimperlein, J. Stocek and C. Urzua-Torres, *Optimal operator preconditioning for pseudodifferential boundary problems*, arxiv:1905.03846.

[11] G. Grubb, *Fractional Laplacians on domains, a development of Hörmander's theory of μ-transmission pseudodifferential operators*, Adv. Math. 268 (2015), 478-528.

[12] J. Gwinner, E. P. Stephan, *Advanced Boundary Element Methods – Treatment of Boundary Value, Transmission and Contact Problems*, Springer Series in Computational Mathematics 52, Springer, 2018.

[13] R. Hiptmair, C. Jerez-Hanckes, C. Urzua-Torres, *Closed-form inverses of the weakly singular and hypersingular operators on disks*, Integr. Equ. Oper. Theory 90 (2018), 14 pages.

[14] C. Jerez-Hanckes, J.-C. Nédélec, *Explicit variational forms for the inverses of integral logarithmic operators over an interval*, SIAM Journal on Mathematical Analysis 44 (2012), 2666–2694.

A wavelet-based approach for the optimal control of nonlocal operator equations

Helmut Harbrecht

(joint work with Stephan Dahlke and Thomas M. Surowiec)

1. Introduction

We are concerned with a wavelet-based approach for the optimal control of a class of nonlocal operator equations. Namely, we consider a quadratic cost functional where the state equation involves the fractional Laplace operator in integral form. When discretizing this nonlocal operator with standard finite element basis functions, one arrives at a densely populated system matrix. This imposes serious obstructions to the efficient numerical treatment of such problems. Therefore, we use a wavelet basis for discretizing the state equation and its adjoint and apply

wavelet matrix compression to arrive at a solver that has linear complexity. In particular, we show how to include box constraints to the optimal control.

2. Optimal control problem

We consider the following optimal control problem which is constrained by a nonlocal state equation:

$$\begin{aligned} &\inf \ \frac{1}{2}\|Cu - u_d\|_H^2 + \frac{\nu}{2}\|z\|_Z^2 \text{ over } (z,u) \in Z_{\mathrm{ad}} \times V \\ &\quad \text{such that} \quad \mathcal{L}u = Bz + f \quad \text{on } \Omega, \\ &\qquad\qquad\quad\ \ u = 0 \qquad\ \ \text{on } \Omega^c := \mathbb{R}^n \setminus \overline{\Omega}. \end{aligned} \tag{1}$$

Here, H and Z are a real Hilbert spaces, $Z_{\mathrm{ad}} \subset Z$ is a nonempty, closed, and convex set, $\nu > 0$, C is a bounded linear operator whose image represents the observation of the state u, and B is a bounded linear operator that maps the control z into the nonlocal equation. For $\Omega \subset \mathbb{R}^n$, $n \geq 1$, being an open and bounded domain, the fractional Laplacian $\mathcal{L} = (-\Delta)^s$, $0 < s < 1$, for some function $u : \Omega \to \mathbb{R}$ is given by

$$(\mathcal{L}u)(x) := 2 \int_{\mathbb{R}^n} \frac{u(y) - u(x)}{|x-y|^{n+2s}} \mathrm{d}y, \quad x \in \Omega.$$

The associated state space V is given by

$$V := \{v \in H^s(\mathbb{R}^n) : v = 0 \text{ on } \Omega^c\}.$$

In the present situation, it holds $V \cong H^s(\Omega)/\mathbb{R}$ for $0 < s < 1/2$ and $V \cong H_0^s(\Omega)$ for $1/2 < s < 1$. In the limit case $s = 1/2$, it holds $V \cong H_{00}^{1/2}(\Omega)$, where $H_{00}^{1/2}(\Omega)$ is obtained from interpolation between $L^2(\Omega)$ and $H_0^1(\Omega)$, compare [2].

The following theorem is a consequence of the standard theory for optimal control problems, see for example [3].

Theorem 1. *Under the standing assumptions, the optimal control problem* (1) *admits a unique solution* $z^\star \in Z_{\mathrm{ad}}$. *Furthermore, there exists an adjoint state* $\lambda^\star \in V$ *such that*

$$\mathcal{L}u^\star = B\mathfrak{P}\Big(-\frac{1}{\nu}B^\intercal \lambda^\star\Big), \tag{2a}$$

$$\mathcal{L}\lambda^\star = C^\intercal(u_d - Cu^\star). \tag{2b}$$

Here, $\mathfrak{P} : Z \to Z_{\mathrm{ad}}$ *is the usual metric projection onto the closed convex set* Z_{ad}.

Note that in case of $Z = L^2(\Omega)$ and $Z_{\mathrm{ad}} \subset Z$ resulting from the box constraints

$$z_{\min}(x) \leq z(x) \leq z_{\max}(x), \quad x \in \Omega, \tag{3}$$

the projection $\mathfrak{P}z$ is given by

$$\mathfrak{P}z(x) = \begin{cases} z_{\min}(x), & \text{if } z(x) < z_{\min}(x), \\ z(x), & \text{if } z_{\min}(x) \leq z(x) \leq z_{\max}(x), \\ z_{\max}(x), & \text{if } z(x) > z_{\max}(x). \end{cases}$$

3. Wavelet matrix compression

The fractional Laplacian is a *nonlocal operator*. Its discretization will thus amount to a *dense* system matrix, the assembly of which would require large amounts of time and computation capacities. Especially, as the fraction Laplacian is an operator of order $2s$, preconditioning becomes an issue.

We shall hence employ wavelet matrix compression. It employs that the wavelets' vanishing moments lead, in combination with the fact that the integral kernel becomes smoother when getting farther away from the diagonal, to a quasi-sparse system matrix. Moreover, by applying a diagonal scaling, the condition number stays uniformly bounded. Since the number of relevant entries in the system matrix for maintaining the convergence rate of the underlying Galerkin method scales only linearly, wavelet matrix compression leads to a numerical approach that has linear over-all complexity, compare [4] for the details.

4. Primal-dual active set strategy

In case of $H = Z = L^2(\Omega)$ and box constraints (3), we can rewrite the optimal control problem (2) as an equivalent KKT system of the following form:

$$\begin{aligned}
\mathcal{L}u^\star = Bz^\star \qquad & \mathcal{L}\lambda^\star = C^\intercal(u_d - Cu^\star) && \text{in } \Omega,\\
u^\star = 0 \qquad & \lambda^\star = 0 && \text{in } \Omega^c,\\
& \lambda^\star + \nu z^\star - \mu^\star_{\min} + \mu^\star_{\max} = 0 \quad \text{in } \Omega,\\
\mu^\star_{\min} \geq 0, \qquad & z_{\min} - z^\star \leq 0, \qquad \mu^\star_{\min}(z_{\min} - z^\star) = 0 && \text{in } \Omega,\\
\mu^\star_{\max} \geq 0, \qquad & z^\star - z_{\max} \leq 0, \qquad \mu^\star_{\max}(z^\star - z_{\max}) = 0 && \text{in } \Omega.
\end{aligned}$$

Here, $\mu_{\min}$ and $\mu_{\max}$ are Lagrange multipliers. In order to compute the solution to this KKT system, we apply the primal-dual active set strategy as introduced in [1]. The essential idea of this iterative solution strategy is to replace successively the inequality constraints by the related equality constraints for all the indices where the constraint becomes active. Since it can be reinterpreted as a semi-smooth Newton method, the primal-dual active set strategy converges superlinearly, see [5].

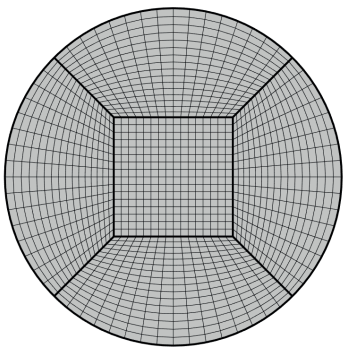

Figure 1. The domain Ω under consideration with mesh on level 4. The operator C is the projection onto the interior square.

Numerical results in case of Ω being the unit circle and $s = 1/4$ are given in Figure 2. Here, we computed the solution for about 80 000 piecewise constant ansatz functions each for the state and for the control (indeed, we use Haar wavelets for the discretization), where $z_{\min} = -0.1$, $z_{\max} = 0.1$, $\nu = 10^{-3}$, B is the identity, and C is the projection onto the square $(-\frac{1}{\sqrt{2}}, \frac{1}{\sqrt{2}})^2$, which is the interior patch seen in Figure 2.

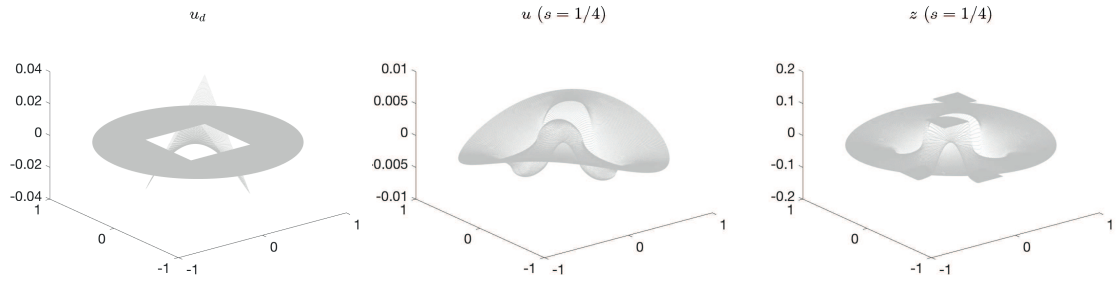

FIGURE 2. The desired state (left), the optimal state u (middle), and the optimal control z (right) in case of $s = 1/4$.

REFERENCES

[1] M. Bergounioux, K. Ito, and K. Kunisch. Primal-dual strategy for constrained optimal control problems. *SIAM J. Contr. Optim.*, 37:1176–1194, 1999.

[2] L. Caffarelli and L. Silvestre. An extension problem related to the fractional Laplacian. *Comm. Partial Differential Equations*, 32(7–9):1245–1260, 2007.

[3] J.L. Lions. *Optimal Control of Systems Governed by Partial Differential Equations*, volume 170 of *Grundlehren der mathematischen Wissenschaften*. Springer, Berlin–Heidelberg, 1971.

[4] H. Harbrecht and R. Schneider. Rapid solution of boundary integral equations by wavelet Galerkin schemes. In R. DeVore and A. Kunoth, editors, *Multiscale, Nonlinear and Adaptive Approximation*, pages 249–294. Springer, Berlin–Heidelberg, 2009.

[5] M. Hintermüller, K. Ito, and K. Kunisch. The primal-dual active set strategy as a semismooth Newton method. *SIAM J. Optim.*, 13:865–888, 2003.

Electromagnetic Force Computation in the Boundary Element Method

RALF HIPTMAIR
(joint work with Piyush Panchal)

Electrostatic boundary value problem. As a simple model problem we consider a conducting body in the interior of a metallic box. A fixed voltage drop U_0 between both is imposed so that the electrostatic potential u in the space Ω between both objects can be recovered as the solution of the Dirichlet boundary value problem

$$\Delta u = 0 \quad \text{in } \Omega\,, \quad u = g \quad \text{on } \partial\Omega\,, \quad g := \begin{cases} U_0 & \text{on conductor}\,, \\ 0 & \text{on box.} \end{cases} \tag{1}$$

The unknown Neumann trace $\psi := \nabla u \cdot \boldsymbol{n} \in H^{-\frac{1}{2}}(\Gamma)$, $\Gamma := \partial\Omega$, $\boldsymbol{n}$ the exterior unit normal vector field on Γ, can be obtained as the solution of a direct first-kind boundary integral equation (BIE) in weak form [10, Sect. 3.4.2.1]: Seek $\psi \in H^{-\frac{1}{2}}(\Gamma)$ such that

$$(2)\quad a_V(\psi,\varphi) := \int_\Gamma \int_\Gamma G(\boldsymbol{x},\boldsymbol{y})\psi(\boldsymbol{y})\varphi(\boldsymbol{x})\,\mathrm{d}S(\boldsymbol{x},\boldsymbol{y}) = \ell(\varphi)$$
$$:= \tfrac{1}{2}\int_\Gamma g(\boldsymbol{x})\varphi(\boldsymbol{x})\,\mathrm{d}S(\boldsymbol{x}) + \int_\Gamma \int_\Gamma \nabla_{\boldsymbol{y}} G(\boldsymbol{x},\boldsymbol{y})\cdot\boldsymbol{n}(\boldsymbol{y})g(\boldsymbol{y})\varphi(\boldsymbol{x})\mathrm{d}S(\boldsymbol{x},\boldsymbol{y})$$

for all $\varphi \in H^{-\frac{1}{2}}(\Gamma)$, with G the fundamental solution for $-\Delta$. The simplest boundary element Ritz-Galerkin discretization of (2) employs trial and test spaces of piecewise constant functions on a surface mesh of Γ.

Computing electrostatic surface forces. Starting from the Maxwell stress tensor we arrive at the formula $f(u) := \frac{1}{2}|\nabla u \cdot \boldsymbol{n}|^2$ for the *normal force density* on surfaces of conductors, see [8, Sect. 6.7]. Yet, the resulting expressions $\mathbf{F}(u) := \int_{\Gamma_0} f(u)\,\boldsymbol{n}\mathrm{d}S$ for the total force on a part $\Gamma_0 \subset \Gamma$ of the boundary are *not continuous* on the energy trace space $H^{-\frac{1}{2}}(\Gamma)$, because that space is not continuously embedded in $L^2(\Gamma)$.

This lack of continuity denies us the benefit of superconvergence, usually enjoyed by approximations of continuous (on the trial space) functionals in a Galerkin setting [1, Sect. 3]. In the context of finite element discretization based on the volume variational formulation of (1) an equivalent volume expression for the force offers a remedy,

$$(3)\qquad \mathbf{F}(u) = \int_\Omega \mathbf{T}(u)\cdot\mathbf{grad}\,\Psi\,\mathrm{d}\boldsymbol{x}\,,\quad \mathbf{T}(u) = \nabla u\cdot\nabla u^\top - \tfrac{1}{2}(\nabla u^\top \nabla u)\,\mathbf{I}\,,$$

where $\Psi \in H^1(\Omega)$ is a suitable cut-off function. This is the foundation of the so-called eggshell method [2, 3]. Yet, volume expressions are not an option for computations using the boundary element method (BEM).

Virtual work principle. Force is the *shape gradient* of the total field energy [4], which, for the linear electrostatic setting of (1), is given by

$$(4)\qquad \mathcal{E}(\Omega) := \frac{1}{2}\int_\Omega \|\nabla u(\boldsymbol{x})\|^2\,\mathrm{d}\boldsymbol{x} = \frac{1}{2}\int_{\partial\Omega} g(\boldsymbol{x})\nabla u(\boldsymbol{x})\cdot\boldsymbol{n}(\boldsymbol{x})\,\mathrm{d}S(\boldsymbol{x})\,.$$

Appealing to the velocity method of shape calculus, see [11, Sect. 2.11] or [5], we find for the force density (viewed as a distribution) the *boundary formula*

$$(5)\qquad \frac{d\mathcal{E}}{d\Omega}(\Omega;\boldsymbol{\mathcal{V}}) = \frac{1}{2}\int_{\partial\Omega}\big(((\nabla g - \nabla u)\cdot\boldsymbol{n})(\nabla u\cdot\boldsymbol{n}) + \nabla g\cdot\nabla u\big)(\boldsymbol{\mathcal{V}}\cdot\boldsymbol{n})\,\mathrm{d}S\,,$$

which generalizes the customary surface force formula. Here, $\boldsymbol{\mathcal{V}}$ is a continuously differentiable test vector field, defined on and compactly supported on the whole enclosing box.

Yet, as elaborated in [6], the Lagrangian pullback approach for PDE-constrained shape calculus yields an equivalent *volume formula* more suitable for use with

finite-element Galerkin discretization, see also [12, 14, 13]. This suggests that a similar *Lagrangian pullback approach* applied to the total energy functional (4) constrained by the BIE (2) may also provide a more stable boundary-based shape-gradient formula, which is better suited for the BEM.

On the technical level, the pullback approach relies on the flow map induced by $\boldsymbol{\mathcal{V}}$ to transform the integrals in (2) back to a fixed domain. Then, based on solution ψ of the state problem (2) and the solution ρ of the adjoint variational problem

$$\rho \in H^{-\frac{1}{2}}(\Gamma): \quad a_V(\varphi,\rho) = \tfrac{1}{2}\int_\Gamma g(\boldsymbol{x})\varphi(\boldsymbol{x})\,\mathrm{d}S(\boldsymbol{x}) \quad \forall \varphi \in H^{-\frac{1}{2}}(\Gamma)\,, \tag{6}$$

we arrive at an expression for the shape gradient that is entirely boundary-based [9, Thm. 2.1], [7]:

$$\begin{aligned}
\frac{d\mathcal{E}}{d\Omega}(\Omega;\boldsymbol{\mathcal{V}}) &= \tfrac{1}{2}\textstyle\int_\Gamma \psi(\widehat{\boldsymbol{x}})(\nabla g(\widehat{\boldsymbol{x}})\cdot\boldsymbol{\mathcal{V}}(\widehat{\boldsymbol{x}}))\mathrm{d}S(\widehat{\boldsymbol{x}}) \\
&+\textstyle\int_\Gamma\int_\Gamma \psi(\widehat{\boldsymbol{y}})\big\{\nabla_{\boldsymbol{x}}G(\widehat{\boldsymbol{x}},\widehat{\boldsymbol{y}})\cdot\boldsymbol{\mathcal{V}}(\widehat{\boldsymbol{x}})+\nabla_{\boldsymbol{y}}G(\widehat{\boldsymbol{x}},\widehat{\boldsymbol{y}})\cdot\boldsymbol{\mathcal{V}}(\widehat{\boldsymbol{y}})\big\}\rho(\widehat{\boldsymbol{x}})\mathrm{d}S(\widehat{\boldsymbol{x}})\mathrm{d}S(\widehat{\boldsymbol{y}}) \\
&-\textstyle\int_\Gamma\int_\Gamma\big\{\rho(\widehat{\boldsymbol{x}})g(\widehat{\boldsymbol{y}})\big(\nabla_{\boldsymbol{x}}\nabla_{\boldsymbol{y}}G(\widehat{\boldsymbol{x}},\widehat{\boldsymbol{y}})\cdot\boldsymbol{\mathcal{V}}(\widehat{\boldsymbol{x}})+ \\
&\qquad \nabla_{\boldsymbol{y}}\nabla_{\boldsymbol{y}}G(\widehat{\boldsymbol{x}},\widehat{\boldsymbol{y}})\cdot\boldsymbol{\mathcal{V}}(\widehat{\boldsymbol{y}})\big)\cdot\widehat{\boldsymbol{n}}(\widehat{\boldsymbol{y}})\big\}\quad \mathrm{d}S(\widehat{\boldsymbol{x}})\mathrm{d}S(\widehat{\boldsymbol{y}}) \\
&+\textstyle\int_\Gamma\int_\Gamma \rho(\widehat{\boldsymbol{x}})\; g(\widehat{\boldsymbol{y}})\;\nabla_{\boldsymbol{y}}G(\widehat{\boldsymbol{x}},\widehat{\boldsymbol{y}})\cdot\Big(\nabla\boldsymbol{\mathcal{V}}(\widehat{\boldsymbol{y}})\widehat{\boldsymbol{n}}(\widehat{\boldsymbol{y}})\Big)\,\mathrm{d}S(\widehat{\boldsymbol{x}})\mathrm{d}S(\widehat{\boldsymbol{y}}) \\
&-\textstyle\int_\Gamma\int_\Gamma \rho(\widehat{\boldsymbol{x}})\;\big(\nabla_{\boldsymbol{y}}G(\widehat{\boldsymbol{x}},\widehat{\boldsymbol{y}})\cdot\widehat{\boldsymbol{n}}(\widehat{\boldsymbol{y}})\big)\nabla\cdot\big(g(\widehat{\boldsymbol{y}})\;\boldsymbol{\mathcal{V}}(\widehat{\boldsymbol{y}})\big)\,\mathrm{d}S(\widehat{\boldsymbol{x}})\mathrm{d}S(\widehat{\boldsymbol{y}}) \\
&-\tfrac{1}{2}\textstyle\int_\Gamma \rho(\widehat{\boldsymbol{x}})(\nabla g(\widehat{\boldsymbol{x}})\cdot\boldsymbol{\mathcal{V}}(\widehat{\boldsymbol{x}}))\mathrm{d}S(\widehat{\boldsymbol{x}})\,.
\end{aligned} \tag{7}$$

The pink terms are clearly well-defined for all $\rho,\psi \in H^{-\frac{1}{2}}(\Gamma)$, whereas the yellow terms, some of which feature strongly singular kernels, seem to be problematic. Yet, smart rephrasing of these integrals reveals that there is a fortunate cancellation of singularities, which allows to recast them as double integrals with $L^\infty(\Gamma\times\Gamma)$- kernels!

Theorem 1. *On Lipschitz boundaries Γ and for g and $\boldsymbol{\mathcal{V}}$ continuously differentiable in a neighborhood of Γ, the expression (7) is well-defined for all $(\psi,\rho)\in H^{-\frac{1}{2}}(\Gamma)\times H^{-\frac{1}{2}}(\Gamma)$.*

This result suggests that, approximations obtained by plugging boundary element Galerkin solutions for ψ and ρ into the new formula (7) after stabilizing rearrangement may yield more accurate surface force distributions than using the boundary formula (5). As of the beginning of 2020 a rigorous theoretical underpinning of this expectation is still work in progress.

Numerical results. We point out that the expression (7) entails knowledge of an extension of the Dirichlet data g into a neighborhood of Γ. Of course, for (1) extension by a constant value is the natural choice and was employed in the numerical experiment below.

In numerical tests we studied approximate dual norms of the BEM-discretized shape gradients and observed that

- both the boundary formula (5) and the new expression (7) provide comparable accuracy, if Γ is smooth,
- the formula (7) is vastly superior to (5) in case of non-smooth Γ provided that a smooth extension of g is used.

We illustrate this for the 2D setting of a square box containing a conductor with a square cross-section and $U_0 = 1$ [9, Sect. 5.2.1]. The plot of Figure 1 displays the error in approximate dual norm for the two shape gradient formulas.

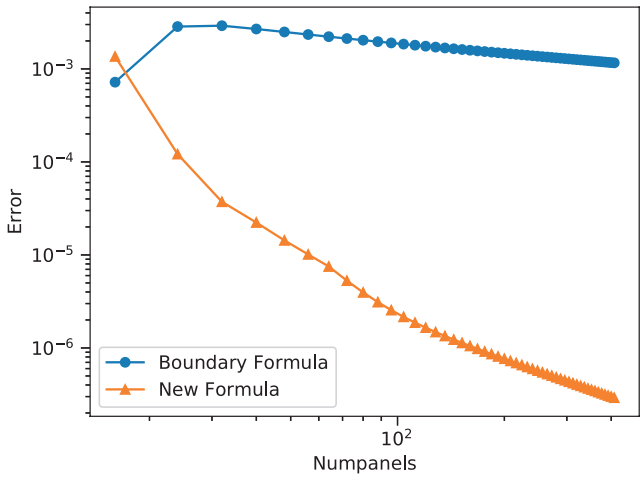

FIGURE 1. Dual norms of errors of shape gradient formulas with respect to a reference solution computed with BEM with 8000 panels.

REFERENCES

[1] M. GILES AND E. SÜLI, *Adjoint methods for PDEs: a posteriori error analysis and postporcessing by duality*, Acta Numerica, 11 (2002), pp. 145–236.
[2] F. HENROTTE, G. DELIEGE, AND K. HAMEYER, *The eggshell approach for the computation of electromagnetic forces in 2D and 3D*, COMPEL, 23 (2004), pp. 996–1005.
[3] F. HENROTTE AND K. HAMEYER, *Computation of electromagnetic force densities: Maxwell stress tensor vs. virtual work principle*, J. Comput. Appl. Math., 168 (2004), pp. 235–243.
[4] F. HENROTTE AND K. HAMEYER, *A theory for electromagnetic force formulas in continuous media*, IEEE Transactions on Magnetics, 43 (2007), pp. 1445–1448.
[5] R. HIPTMAIR AND J. LI, *Shape derivatives in differential forms I: An intrinsic perspective*, Ann. Mat. Pura Appl. (4), 192 (2013), pp. 1077–1098.
[6] R. HIPTMAIR, A. PAGANINI, AND S. SARGHEINI, *Comparison of approximate shape gradients*, BIT Numerical Mathematics, 55 (2014), pp. 459–485.
[7] R. HIPTMAIR AND P. PANCHAL, *BEM for electrostatic forces: Shape-gradient approach*, SAM Report 2020-XX, SAM, ETH Zurich, Switzerland, 2020. In preparation.
[8] J. JACKSON, *Classical Electrodynamics*, John Wiley, 3rd ed., 1998.
[9] P. PANCHAL, *Electrostatic force computation using shape calculus*, MSc thesis, SAM, D-MATH, ETH Zurich, 2020. URL.

[10] S. Sauter and C. Schwab, *Boundary Element Methods*, vol. 39 of Springer Series in Computational Mathematics, Springer, Heidelberg, 2010.
[11] J. Sokolowski and J.-P. Zolesio, *Introduction to Shape Optimization*, vol. 16 of Springer Series in Computational Mathematics, Springer, Berlin, 1992.
[12] S. Zhu, *Effective shape optimization of Laplace eigenvalue problems using domain expressions of Eulerian derivatives*, J. Optim. Theory Appl., 176 (2018), pp. 17–34.
[13] S. Zhu and Z. Gao, *Convergence analysis of mixed finite element approximations to shape gradients in the Stokes equation*, Comput. Methods Appl. Mech. Engrg., 343 (2019), pp. 127–150.
[14] S. Zhu, X. Hu, and Q. Wu, *On accuracy of approximate boundary and distributed H^1 shape gradient flows for eigenvalue optimization*, J. Comput. Appl. Math., 365 (2020), pp. 112374, 15.

Spectral Non-Conforming BEM for (local) Multiple Trace Formulations

Carlos Jerez-Hanckes
(joint work with José Pinto, Ignacio Labarca)

We are interested in solving time-domain and time-harmonic acoustic wave transmission problems arising by incident waves propagating through a composite object. More precisely, we consider a bounded Lipschitz domain $\Omega \in \mathbb{R}^d$, $d = 2, 3$, composed of M non-overlapping subdomains $\Omega_i, i = 1, \dots, M$, such that

$$\overline{\Omega} = \bigcup_{i=1}^{M} \overline{\Omega}_i,$$

where $\Omega_i \cap \Omega_j = \emptyset$ for $i \neq j$. We call $\Gamma_{ij} := \partial\Omega_i \cap \partial\Omega_j$ the interface between domains Ω_i and Ω_j. We also denote by $\Omega_0 := \mathbb{R}^d \setminus \overline{\Omega}$ the unbounded exterior domain. Notice that one can write

$$\partial\Omega_i = \bigcup_{j \in \Lambda_i} \Gamma_{ij},$$

where Λ_i corresponds to an index set defined by

$$\Lambda_i := \{j \in \{0, \dots, M\} : \quad j \neq i \text{ and } \Gamma_{ij} \neq \emptyset\}.$$

The above materials are characterized by piecewise-constant properties, $c_i > 0$ corresponding to domain wavespeeds (resp. wavenumbers κ_i) in each Ω_i, $i = 0, \dots, M$. Assuming some impinging wave, we denote by $u_i = u|_{\Omega_i}$ the total wave inside Ω_i and by $u_0 = u|_{\Omega_0}$ the scattered wave in the exterior domain. With this, for all $i = 0, \dots, M$, we seek to solve either time-domain or -harmonic acoustic transmission problems:

$$-\Delta u_i + \frac{1}{c_i^2}\frac{\partial^2 u_i}{\partial t^2} = 0 \text{ in } \Omega_i \times (0, \infty] \tag{1}$$

$$-\Delta u_i - \kappa_i^2 u_i = 0 \text{ in } \Omega_i. \tag{2}$$

Suitable transmission (and initial) conditions are imposed. We will attempt to solve the above problem by conveniently combining the following ingredients

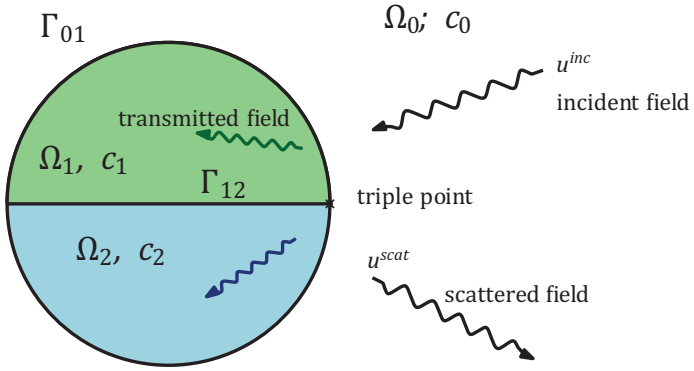

FIGURE 1. Example of scatterer with two homogenous subdomains.

(i) Boundary integral equations (BIEs) in the form of the local multiple traces formulation (MTF) following [1] (along with the notation therein);
(ii) Spectral Galerkin with Chebyshev polynomials for spatial discretization [2, 3]; and,
(iii) Convolution quadrature (CQ) for the time-domain case [4].

Problem 1 (Multiple traces formulation)**.** We seek $\boldsymbol{\lambda} \in \mathbb{V}_M := \mathbf{V}_0 \times \ldots \times \mathbf{V}_M$ such that the variational form:

$$\langle \mathsf{F}(s)\boldsymbol{\lambda}, \boldsymbol{\varphi} \rangle_\times = \langle \boldsymbol{g}, \boldsymbol{\varphi} \rangle_\times , \quad \text{for all } \boldsymbol{\varphi} \in \widetilde{\widetilde{\mathbb{V}}}_M, \tag{3}$$

is satisfied for $\boldsymbol{g} = (g_0, g_1, \ldots, g_M) \in \mathbb{V}_M$ with

$$\mathsf{F}(s) := \begin{pmatrix} \mathsf{A}_0(s) & -\frac{1}{2}\widetilde{\mathsf{X}}_{01} & \ldots & -\frac{1}{2}\widetilde{\mathsf{X}}_{0N} \\ -\frac{1}{2}\widetilde{\mathsf{X}}_{10} & \mathsf{A}_1(s) & \ldots & -\frac{1}{2}\widetilde{\mathsf{X}}_{1N} \\ \vdots & \vdots & \ddots & \vdots \\ -\frac{1}{2}\widetilde{\mathsf{X}}_{N0} & -\frac{1}{2}\widetilde{\mathsf{X}}_{N1} & \ldots & \mathsf{A}_M(s) \end{pmatrix} : \mathbb{V}_M \to \mathbb{V}_{\mathrm{pw},M}. \tag{4}$$

with the block operator composed of the standard boundary integral operators over $\partial\Omega_i$ with (complex)-wavenumber s:

$$\mathsf{A}(s) := \begin{pmatrix} -\mathsf{K}_\ell(s) & \mathsf{V}_\ell(s) \\ \mathsf{W}_\ell(s) & \mathsf{K}'_\ell(s) \end{pmatrix} : \mathbf{V}_\ell \to \mathbf{V}_\ell. \tag{5}$$

We consider spectral elements to discretize the spatial densities in the MTF. We assume that for each interface $\Gamma_{j\ell}$ there exists a C^1-parametrization $h_{j\ell}$ that maps the nominal segment $\widehat{\Gamma} := [-1, 1]$ into $\Gamma_{j\ell}$. We achieve a non-conforming Petrov-Galerkin discretization of problem (3) by using second kind Chebyshev polynomials:

$$U_n(t) := \frac{\sin(n+1)\theta}{\sin\theta}, \quad t = \cos\theta, \tag{6}$$

as trial functions and weighted second kind Chebyshev polynomials as test functions (see Table 4 for definition). Their density in spaces $\mathbf{V}_{pw,\ell}$ and $\widetilde{\widetilde{\mathbf{V}}}_\ell$ was given in [3]. We recall the orthogonality property:

$$\int_{-1}^{1} U_m(t)U_n(t)\sqrt{1-t^2}dt = \begin{cases} 0 & n \neq m, \\ \pi/2 & n = m, \end{cases} \tag{7}$$

which jointly with the relation between Fourier series and Chebyshev expansion lead us to a faster computation of the discretization matrix entries by means of the FFT. Basis and test functions are defined over a whole boundary $\partial\Omega_\ell$ as $\lambda_n^\ell := \sum_{j\in\Lambda_\ell} \lambda_n^{j\ell}\mathbf{1}_{\Gamma_{j\ell}}$ where $\mathbf{1}_{\Gamma_{j\ell}}$ is a characteristic function over the interface $\Gamma_{j\ell}$ and

$$\lambda_n^{j\ell} := \widehat{\lambda}_n \circ h_{j\ell}^{-1}, \quad \widehat{\lambda}_n(t) := (U_n(t), U_n(t)), \quad t \in \widehat{\Gamma}. \tag{8}$$

Similarly, test functions are defined as $\varphi_n^\ell := \sum_{j\in\Lambda_\ell} \varphi_n^{j\ell}\mathbf{1}_{\Gamma_{j\ell}}$ with

$$\varphi_n^{j\ell} := \widehat{\varphi}_n \circ h_{j\ell}^{-1}, \quad \widehat{\varphi}_n(t) := (U_n(t)\sqrt{1-t^2}, U_n(t)\sqrt{1-t^2}), \quad t \in \widehat{\Gamma}. \tag{9}$$

Letting $X_L^\ell := \operatorname{span}\{\lambda_n^\ell\}_{l=0}^L \subseteq \mathbf{V}_{pw,\ell}$ and $Y_L^\ell := \operatorname{span}\{\varphi_n^\ell\}_{l=0}^L \subseteq \widetilde{\widetilde{\mathbf{V}}}_\ell$ for $L \in \mathbb{N}$, we define the discrete version of Problem 1:

Problem 2 (Spectral non-conforming Petrov-Galerkin MTF)**.** We seek $\boldsymbol{\lambda} \in \mathbb{X}_L := X_L^0 \times \ldots X_L^M$ such that the variational form:

$$(\mathsf{F}(s)\boldsymbol{\lambda}, \boldsymbol{\varphi})_\times = (\boldsymbol{g}, \boldsymbol{\varphi}), \quad \text{for all } \boldsymbol{\varphi} \in \mathbb{Y}_L := Y_L^0 \times \ldots \times Y_L^M, \tag{10}$$

is satisfied for $\boldsymbol{g} = (g_0, g_1, \ldots, g_M) \in \mathbb{V}_M$.

Existence and uniqueness of solutions for Problem 2 depends on the existence of an inf-sup condition. This result remains elusive by now, but various numerical experiments show the good behaviour of the proposed discretization scheme [2, 3]. We will assume there exists a unique solution for Problem 2.

Notice that the discrete problem consists in finding a solution in the space $\mathbb{V}_{pw,M}$ instead of $\mathbb{V}_M$, which was the case for Problem 1. Existence and uniqueness for the continuous problem remains valid in $\mathbb{V}_{pw,M}$, as mentioned in [3], due to the equivalence of the duality product between $\mathbb{V}_M$ and $\mathbb{V}_{pw,M}$ when test functions are elements of $\widetilde{\widetilde{\mathbb{V}}}_M$.

Multistep-based and multistage CQ were introduced by Lubich in [5, 6] and in [7], respectively. Both methods will be explained in the following sections, with their assumptions and limitations, following the presentation given in [8].

References

[1] R. Hiptmair, C. Jerez-Hanckes, *Multiple Traces Boundary Integral Formulation for Helmholtz Transmission Problems*, Adv. Comp. Math., **37** (2012), 39–91.

[2] C. Jerez-Hanckes, J. Pinto, S. Tournier, *Local Multiple Traces Formulation for High-Frequency Scattering Problems*, Journal of Computational and Applied Mathematics, **289** (2015), 306–321.

Trial functions		Test functions	
$H^{1/2}(\widehat{\Gamma})$	$U_n(t)$	$\widetilde{H}^{-1/2}(\widehat{\Gamma})$	$U_n(t)\sqrt{1-t^2}$
$H^{-1/2}(\widehat{\Gamma})$	$U_n(t)$	$\widetilde{H}^{1/2}(\widehat{\Gamma})$	$U_n(t)\sqrt{1-t^2}$

TABLE 4. Functions used for the spectral elements discretization over $\widehat{\Gamma} = [-1, 1]$.

[3] C. Jerez-Hanckes, J. Pinto, S. Tournier, *Local Multiple Traces Formulation for High-Frequency Scattering Problems by Spectral Elements*, A. Bartel et al. (eds.), Scientific Computing in Electrical Engineering, Mathematics in Industry **23**, Springer (2016), 73–82.
[4] C. Jerez-Hanckes, I. Labarca, *Time-Domain Multiple Traces Boundary Integral Formulation for Acoustic Wave Scattering*, submitted to SN Partial Differential Equations and Application.
[5] C. Lubich, *Convolution Quadrature and Discretized Operational Calculus. I.* Numerische Mathematik, **52** (1988), 129–145.
[6] C. Lubich, *Convolution Quadrature and Discretized Operational Calculus. II.* Numerische Mathematik, **52** (1998), 413–425.
[7] C. Lubich, A. Ostermann, *Runge-Kutta Methods for Parabolic Equations and Convolution Quadrature.*, Mathematics of Computation, **60** (1993), 105–131.
[8] M. Hassell, F. J. Sayas, *Convolution Quadrature for Wave simulations*, Numerical simulation in physics and engineering, Springer (2016), 71–159.

3D Hybrid imaging method based on converging Gauss-Newton iterations

FRÉDÉRIQUE LE LOUËR
(joint work with Olha Ivanyshyn Yaman, Maria-Luisa Rapún)

1. INTRODUCTION

We are concerned with accurate full imaging methods of three-dimensional particles when a reduced amount of monochromatic data are available. While there exists a variety of instantaneous shape detection methods using multiple incident lights in multifrequency regime, one has to turn to iterative optimization methods when only limited aperture measurements are available from a single light scattering at a single frequency.

To solve this inverse shape problem, we shall distinguish global methods, such as topological imaging methods, from local methods, namely shape optimization methods. On the one hand, the inverse problem is commonly reformulated as the minimization problem of the least-squares functional, which accounts for the difference between the measured and reconstructed data. The topological gradient of this misfit functional measures the variations of such functional in the presence of an infinitesimal scatterer at each point of the region of interest. This indicator function localizes accurately inhomogeneities without a priori information on the

unknown particles. On the other hand, shape optimization of initial guesses can be performed through parametric boundary optimization and enables to recover the shape of the detected unknown particles.

Combination of topological [8, 9] and shape optimization [7] tools by means of converging Gauss-Newton iterations [4] generates full automatic algorithms for solving imaging problems, namely location and shape detection of a few particles. In a first part, we present the ingredients of this hybrid adaptive algorithm that was recently applied to 3D holographic imaging [1]. Ongoing works will be dedicated to an alternative approach by replacing shape derivatives with material derivatives of boundary integral operators. The resulting algorithm [10] initially introduced in [6] has the interesting feature to avoid the numerous numerical solution of boundary value problems at each regularized Gauss-Newton iteration step, that are replaced by simple matrix vector products.
Both theoretical and numerical aspects of the work may provide an overview of the applications of boundary integral equation methods in the shape and topological sensitivity analysis of linear waves problems.

2. Full automatic imaging algorithm based on Gauss-Newton iterations

Let Ω represent a finite number of disjoint bounded particles in the free space $\mathbb{R}^3$. We consider the perfect conductor problem at a single frequency $\kappa > 0$.

$$\begin{cases} \mathbf{curl}\,\mathbf{curl}\,\boldsymbol{E}^s - \kappa^2 \boldsymbol{E}^s = 0 & \text{in } \mathbb{R}^3 \backslash \overline{\Omega} \\ \boldsymbol{n} \times (\boldsymbol{E}^s + \boldsymbol{E}^{inc}) = 0 & \text{on } \partial\Omega \\ \lim\limits_{|\mathbf{x}|\to\infty} (\mathbf{curl}\,\boldsymbol{E}^s \times \mathbf{x} - i\kappa|\mathbf{x}|\boldsymbol{E}^s) = 0 & \end{cases}$$

where $\boldsymbol{E}^{inc}$ is an incident electromagnetic wave. Let Γ_{meas} be a discrete subset of nearfield observation points. We define the boundary to data map $\boldsymbol{F}(\partial\Omega) = \boldsymbol{E}^s_{|\Gamma_{\text{meas}}}$. Given noisy measured nearfield data $\boldsymbol{E}^*_\delta$ collected on Γ_{meas}, we want to solve the inverse problem equation $\boldsymbol{F}(\partial\Omega) = \boldsymbol{E}^*_\delta$. This can be performed by repeating a two-step algorithm: Let $\mathcal{R}$ be the investigated sampling area and $\Omega_{-1} = \varnothing$. For $k \geq -1$:

1. At iteration k, if $k = -1$ or the IRGN algorithm stagnates , compute new topological derivatives (TD) for all $\mathbf{z} \in \mathcal{R}$, denoted by $\mathcal{D}^k_T(\mathbf{z})$ [8, 9]. Then we consider the next updated shape $\Omega_{k+1} = \Omega_k \cup \{\mathbf{z} \in \mathcal{R}\backslash\overline{\Omega_k}\,;\ \mathcal{D}^k_T(\mathbf{z}) < (1 - C_k) \min\limits_{\mathbf{y}\in\mathcal{R}} \mathcal{D}^k_T(\mathbf{y})\}$, where $C_k > 0$ is arbitrarily chosen.
2. Or else, while a given stopping rule given by Morozov's principle is not reached and the IRGN does not stagnate, we solve the inverse problem equation using the converging IRGN method through first order linearization with respect to boundary parametrizations $\boldsymbol{q}$ of class $\mathscr{C}^1$ at least. Assuming $\partial\Omega_k = \boldsymbol{q}_k(\partial\Omega_{\text{ref}})$, we compute the next iterate $\boldsymbol{q}_{k+1}$ by solving

$$!\,\text{argmin}_{\boldsymbol{q}} \left[\|\boldsymbol{F}(\partial\Omega_k) + \partial_{\boldsymbol{q}}\boldsymbol{F}[\partial\Omega_k](\boldsymbol{q} - \boldsymbol{q}_k) - \boldsymbol{E}^*_\delta\|^2 + \alpha_k \|\boldsymbol{q} - \boldsymbol{q}_0\|^2 \right].$$

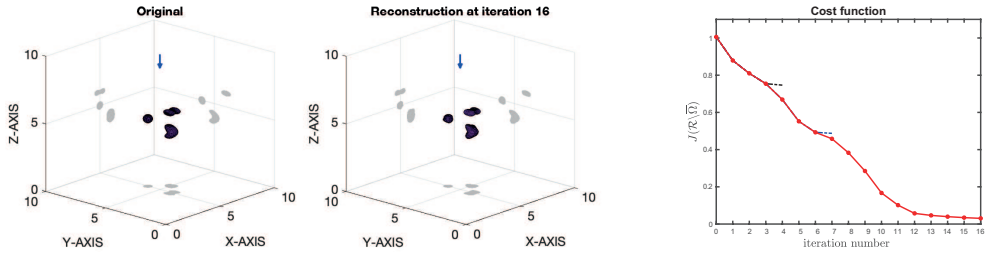

FIGURE 1. On the left, we present a full reconstruction of a few perfectly conducting particles using monochromatic data obtained from a single light scattering $\boldsymbol{E}^{inc} = (e^{-4ix_3}, 0, 0)$ with 2% noise level. On the right, we observe that subsets of original shapes are local minima, then the IRGN algorithm stagnates and new TDs are automaticcaly computed to recover new particles.

Remark 1. From a computational point of view, the indicator function and Fréchet derivatives formulæ [5, 8, 9] are relatively easy to implement with BEM solvers. However, Step 2 requires numerous solution of the direct problem to compute the Fréchet derivatives $\partial_{\boldsymbol{q}}\boldsymbol{F}[\partial\Omega_k]$ at each iteration step when using the conjugate gradient method to solve the regularized least squares problem. One may avoid this occurence using material derivatives of the integral representation of the boundary to data map $\boldsymbol{F}$.

3. Material derivatives of boundary integral operators

The potential theory allows to rewrite the inverse problem equation for the boundary to data map $\boldsymbol{F}$ as the following system of equations

$$\left\{ \begin{array}{rcl} \mathrm{I}_{op}[\boldsymbol{q}]\boldsymbol{\psi} & = & = \boldsymbol{f}[\boldsymbol{q}]\,, \\ \mathscr{P}[\boldsymbol{q}]_{|\Gamma_{\mathrm{meas}}}\boldsymbol{\psi} & = & \boldsymbol{E}^*_\delta{}_{|\Gamma_{\mathrm{meas}}}, \end{array} \right.$$

where $I_{op}[\boldsymbol{q}]$ is the boundary integral equation (BIE) operator posed on the surface $\boldsymbol{q}(\partial\Omega_{\mathrm{ref}})$ and $\mathscr{P}[\boldsymbol{q}]$ is the potential representation of the scattering field $\boldsymbol{E}^s$, and $\boldsymbol{f}[\boldsymbol{q}] = (-\boldsymbol{n}_{\boldsymbol{q}} \times \boldsymbol{E}^{inc})_{|\Gamma_{\boldsymbol{q}}}$.

Step 2. may be replaced by the application of the IRGN method to the first order linearization of this system [6, 10]. More precisely, at iteration k, both the BIE solution $\boldsymbol{\psi}$ and the parametrization $\boldsymbol{q}$ are updated simultaneously by solving

$$!\,\mathrm{argmin}_{\boldsymbol{\psi},\boldsymbol{q}} \left[\left\| A_k \begin{pmatrix} \boldsymbol{\psi} - \boldsymbol{\psi}_k \\ \boldsymbol{q} - \boldsymbol{q}_k \end{pmatrix} - B_k \right\|^2 + \alpha_k \left\| \begin{pmatrix} \boldsymbol{\psi} - \boldsymbol{\psi}_0 \\ \boldsymbol{q} - \boldsymbol{q}_0 \end{pmatrix} \right\|^2 \right],$$

where we have set

$$A_k = \begin{pmatrix} \mathrm{I}_{op}[\boldsymbol{q}_k] & \partial_{\boldsymbol{q}}(\mathrm{I}_{op}[\boldsymbol{q}_k]\boldsymbol{\psi}_k) - \partial_{\boldsymbol{q}}\boldsymbol{f}[\boldsymbol{q}_k] \\ \mathscr{P}[\boldsymbol{q}_k] & \partial_{\boldsymbol{q}}(\mathscr{P}[\boldsymbol{q}_k]\boldsymbol{\psi}_k) \end{pmatrix} \quad B_k = \begin{pmatrix} \boldsymbol{f}[\boldsymbol{q}_k] - \mathrm{I}_{op}[\boldsymbol{q}_k]\boldsymbol{\psi}_k \\ \boldsymbol{E}^*_\delta - \mathscr{P}[\boldsymbol{q}_k]\boldsymbol{\psi}_k \end{pmatrix}$$

The Fréchet differentiability analysis requires substantial trasformations of the involved operators. Many techniques have been proposed in the litterature [2, 3, 11] and the use of the Piola transform of $\boldsymbol{q}$ yields rather simple Fréchet derivative

formulæ [10]. The main result is that the Fréchet derivatives are obtained by differentiating their kernels with no loss of regularity, namely they are well defined in the standard energy spaces.

Ongoing works focus on the numerical comparison of these two algorithms. Conceptually, the underlying ideas presented in this short note can be extended to a wide class of linear waves problems provided that the Green's functions associated to the investigated media are available.

References

[1] A. Carpio, T. G. Dimiduk, F. Le Louër, M.L. Rapún, *When topological derivatives met regularized Gauss-Newton iterations in holographic 3D imaging*, J. Comput. Phys. **388** (2019), pages 534-560.

[2] M. Costabel, F. Le Louër *Shape derivatives of boundary integral operators in electromagnetic scattering. Part I: Shape differentiability of pseudo-homogeneous boundary integral operators*, Integral Equations and Operator Theory **72** (2012), pp. 509–535.

[3] M. Costabel, F. Le Louër *Shape derivatives of boundary integral operators in electromagnetic scattering. Part II: Application to scattering by a homogeneous dielectric obstacle*, Integral Equations and Operator Theory, **72** (2012), pp. 509–535.

[4] T. Hohage, *Iterative Methods in Inverse Obstacle Scattering: Regularization Theory of Linear and Nonlinear Exponentially Ill-Posed Problems*, PhD thesis, University of Linz, 1999.

[5] R. Kress. *Electromagnetic waves scattering : Scattering by obstacles*. Scattering (2001) 191–210. Pike, E. R. and Sabatier, P. C., eds., Academic Press, London.

[6] Rainer Kress and William Rundell, *Nonlinear integral equations and the iterative solution for an inverse boundary value problem*, Inverse Problems **21** (2005), pp. 1207–1223.

[7] F. Le Louër, *A spectrally accurate method for the direct and inverse scattering problems by multiple 3D dielectric obstacles*, ANZIAM e-Journal. **59** (2018), E1–E49.

[8] F. Le Louër, M.L. Rapún., *Topological sensitivity for solving inverse multiple scattering problems in three-dimensional electromagnetism. Part I: One step method*, SIAM J. Imaging Sci. **1**0 (2017), 1291-1321.

[9] F. Le Louër, M.L. Rapún., *Topological sensitivity for solving inverse multiple scattering problems in three-dimensional electromagnetism. Part II: Iterative method*, SIAM J. Imaging Sci. **11** (2018), 734–769.

[10] O. Ivanyshyn, F. Le Louër, *Material derivatives of boundary integral operators in electromagnetism and application to inverse scattering problems*, Inverse Problems **32** (2016),

[11] R. Potthast, *Domain derivatives in electromagnetic scattering*, Math. Methods Appl. Sci. **19** (1996), pp. 1157–1175.

The Wigner-Smith Time Delay Matrix in Computational Electromagnetics

Eric Michielssen

(joint work with Utkarsh R. Patel)

In 1960, Felix Smith published a seminal paper "Lifetime Matrix in Collision Theory", a description of procedures to characterize time delays that particles experience during quantum mechanical interactions [1]. Starting from the Schrödinger

equation, Smith showed that the matrix $\mathbf{Q}$ defined as

$$\mathbf{Q} = j\mathbf{S}^{\dagger}\frac{\partial \mathbf{S}}{\partial \omega} \tag{1}$$

where $\mathbf{S}$ is a potential well's scattering matrix and ω denotes angular frequency, fully characterizes the delays experienced by particles as they traverse the system. While the "WS time delay matrix" $\mathbf{Q}$ has found applications in the study of physical transport and chaos [2], few studies have focused on its use in (computational) electromagnetics.

This report discusses how the WS time delay theory can be extended to Maxwell's equations and explores its potential applications in electromagnetics. Starting from Maxwell's equations and their frequency derivative, closed-form expressions for the entries of the electromagnetic WS time delay matrix $\mathbf{Q}$ are developed for guiding (Fig. 1), scattering (Fig. 2), and radiating systems (Fig. 3) that are lossless and reciprocal.

For a guiding system with perfect electrically conducting walls that is terminated by homogeneous waveguides supporting M_g propagating modes, the (q,p)-th entry of the $M_g \times M_g$ Hermitian WS time delay matrix $\mathbf{Q}^g$ can be expressed as

$$\mathbf{Q}^g_{qp} = \widehat{\mathbf{Q}}_{qp} + \frac{j}{2}\mathbf{S}^{\dagger}_{qp}\frac{\partial}{\partial \omega}\left(\frac{1}{Z_p}\right)[n_p]^2 - \frac{j}{2}\mathbf{S}_{qp}\frac{\partial}{\partial \omega}\left(\frac{1}{Z_q}\right)[n_q]^2 \,. \tag{2}$$

Here, Z_p and n_p are waveguide impedance and power normalization constants and $\dagger$ represents adjoint. In (2), the (q,p)-th entry of $\widehat{\mathbf{Q}}$ is

$$\widehat{\mathbf{Q}}_{qp} = \frac{1}{2}\varepsilon\int_{\Omega}\mathbf{E}^*_q(\mathbf{r})\cdot\mathbf{E}_p(\mathbf{r})dV + \frac{1}{2}\mu\int_{\Omega}\mathbf{H}^*_q(\mathbf{r})\cdot\mathbf{H}_p(\mathbf{r})dV \,, \tag{3}$$

where the integration is performed over the volume of the guiding system Ω, ε and μ are permittivity and permeability of the material inside the guiding system, and $\mathbf{E}_{p/q}(\mathbf{r})$ and $\mathbf{H}_{p/q}(\mathbf{r})$ are electric and magnetic fields that arise upon excitation of the p-th and q-th ports. Note that the last two terms of the right-hand side of (2) are correction terms that are non-zero only when ports are excited by non-transverse electromagnetic modes.

For a scattering system with a scatterer circumscribed by a sphere of radius a and excited by a free-space port that is defined on a sphere of radius $R \gg a$ and that supports M_s propagating modes(see Fig. 2), the (q,p)-th entry of the

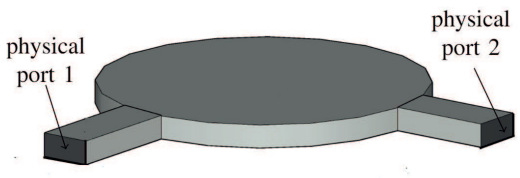

FIGURE 1. Guiding System. One or more propagating mode exist in each physical port.

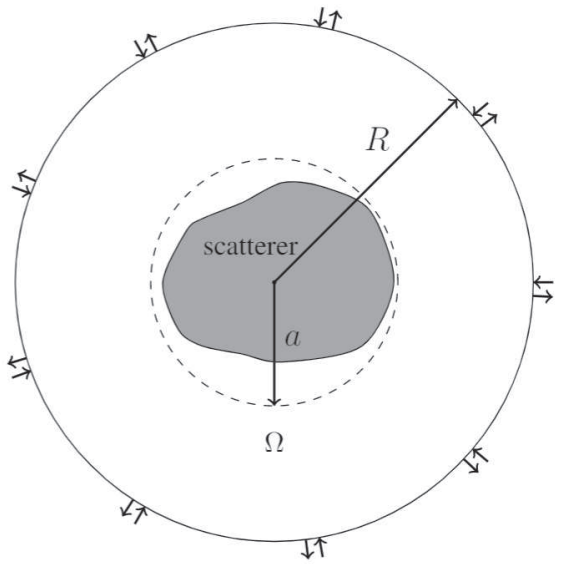

FIGURE 2. Scattering system excited through free-space port defined on a sphere of radius R.

$M_s \times M_s$ time delay matrix $\mathbf{Q}^s$ reads

$$\mathbf{Q}^s_{qp} = \frac{1}{2}\int_{R^3}\left[\varepsilon\mathbf{E}^*_q(\mathbf{r})\cdot\mathbf{E}_p(\mathbf{r}) - \mathbf{E}^*_{q,\|}(\mathbf{r})\cdot\mathbf{E}_{p,\|}(\mathbf{r})\right]dV + \frac{1}{2}\mu\int_{R^3}\left[\mathbf{H}^*_q(\mathbf{r})\cdot\mathbf{H}_p(\mathbf{r}) - \mathbf{H}^*_{q,\|}(\mathbf{r})\cdot\mathbf{H}_{p,\|}(\mathbf{r})\right]dV. \tag{4}$$

Here, the integration is performed over all of space, and $\mathbf{E}_{p,\|}(\mathbf{r})$ and $\mathbf{H}_{q,\|}(\mathbf{r})$ are the electric and magnetic fields computed with the far-field approximation. Note that compared to (3), (4) introduces a correction factor that is a function $\mathbf{E}_{p,\|}(\mathbf{r})$ and $\mathbf{H}_{p,\|}(\mathbf{r})$. This correction term extracts the time delay caused by the scattering process from the total time waves naturally dwell within Ω (which tend to infinity as $R \to \infty$).

Radiating systems are hybrids of the guiding and scattering systems. For a $M_r = M_g + M_s$-port radiating system composed of lossless antennas that are excited by PEC waveguides supporting M_g propagation modes and a free-space port supporting M_s modes, the $M_r \times M_r$ WS time delay matrix $\mathbf{Q}^r$ reads

$$\mathbf{Q}^r_{qp} = \widehat{\mathbf{Q}}^r_{qp} + \frac{j}{2}\mathbf{S}^\dagger_{qp}\frac{\partial}{\partial\omega}\left(\frac{1}{Z_p}\right)(n_p)^2\hat{\delta}_{p\le M_g} - \frac{j}{2}\mathbf{S}_{qp}\frac{\partial}{\partial\omega}\left(\frac{1}{Z_q}\right)(n_q)^2\hat{\delta}_{q\le M_g} \tag{5}$$

where $\widehat{\mathbf{Q}}^r_{qp}$ is also given by (4) and $\hat{\delta}_f = 1$ if f is true and is 0 otherwise.

Applications of the electromagnetic WS time delay matrix abound. Diagonalization of $\mathbf{Q}$ yields a set of modes that experience a well-defined time delay upon interacting with a system. Modes characterized by large time delays oftentimes are quasi-resonant in nature, whereas those with small delays behave in a ray-like manner. WS theory therefore allows for a classification of fields interacting with

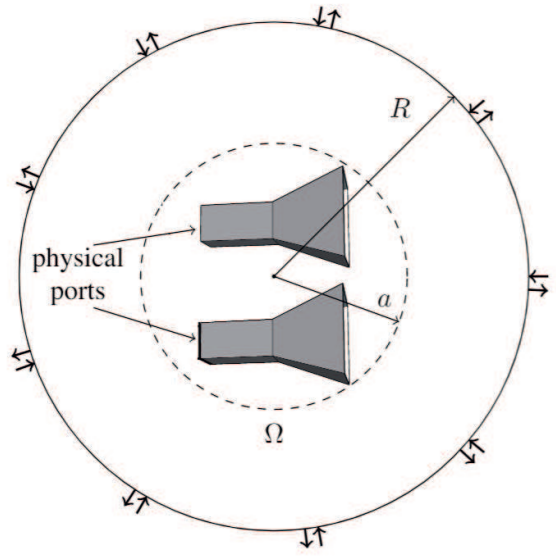

FIGURE 3. Radiating system excited through free-space and waveguide ports.

waveguides, scatterers, and antennas that naturally connects the wave and asymptotic ray regimes. WS theory also allows for a broadband characterization of the impedances of multiport systems.

REFERENCES

[1] F. T. Smith, "Lifetime Matrix in Collision Theory", Physical Review, vol. 118, no. 1, April. 1960.
[2] C. Texier, "Wigner time delay and related concepts: Application to transport in coherent conductors", Physica E, vol. 82, 2016

Functional a-posteriori error estimates for BEM

DIRK PRAETORIUS
(joint work with Stefan Kurz, Dirk Pauly, Sergey Repin, and Daniel Sebastian)

Introduction. We consider the Poisson model problem

(1) $\Delta u = 0$ in Ω subject to Dirichlet boundary conditions $u = g$ on $\Gamma := \partial\Omega$,

where $\Omega \subset \mathbb{R}^d$ is a Lipschitz domain with compact boundary, and (1) is supplemented by a natural radiation condition if Ω is unbounded.

For the ease of presenting the idea of [16], we consider an indirect BEM ansatz

(2) $$u = \widetilde{V}\phi \text{ in } \Omega \quad \text{with unknown density } \phi \in H^{-1/2}(\Gamma),$$

where $\widetilde{V}\colon H^{-1/2}(\Gamma) \to H^1_{\ell oc}(\mathbb{R}^d)$ is the single-layer potential operator defined by

$$(3)\quad \widetilde{V}\phi(x) := \int_\Gamma G(x-y)\phi(y)\,\mathrm{d}\Gamma(y) \quad \text{with} \quad G(z) = \begin{cases} -\frac{1}{2\pi}\log|z|, & \text{for } d=2,\\ +\frac{1}{4\pi}|z|^{-1}, & \text{for } d=3. \end{cases}$$

Taking the trace of (2), we obtain the weakly-singular integral equation

$$(4)\qquad g = V\phi \text{ on } \Gamma \text{ with unknown density } \phi \in H^{-1/2}(\Gamma),$$

where the integral representation of the weakly-singular boundary integral operator $V = (\widetilde{V}\cdot)|_\Gamma\colon H^{-1/2}(\Gamma) \to H^{1/2}(\Gamma)$ formally coincides with that of the single-layer potential (3). Since V is continuous and elliptic, the Lax–Milgram lemma proves that (4) admits a unique solution $\phi \in H^{-1/2}(\Gamma)$.

While the exact solution ϕ (as well as the corresponding potential $u = \widetilde{V}\phi$) can hardly be computed in practice, we suppose that $\phi_h \in H^{-1/2}(\Gamma)$ is a computed (but essentially arbitrary) approximation $\phi_h \approx \phi$. Owing to the mapping properties of the single-layer potential, it then holds that

$$(5)\quad \Delta u_h = 0 \text{ in } \Omega \text{ for the induced approximate potential } u_h := \widetilde{V}\phi_h \in H^1(\Omega)$$

We stress that, for the indirect BEM ansatz, the potential u has a physical meaning, while the integral density ϕ has not. In our recent work [16], we derive computable a-posteriori error estimators μ_h and η_h for the potential error

$$(6)\qquad \mu_h \le \|\nabla(u-u_h)\|_{L^2(\Omega)} \le \eta_h \quad (+ \text{ data oscillations})$$

with a particular emphasis on constant-free estimates. Clearly, the computation of u_h in Ω is computationally expensive and thus shall be avoided, until a prescribed accuracy $\eta_h \le \mathsf{tol}$ can be guaranteed. As a matter of fact, the advertised approach applies to *any* approximation $\phi_h \approx \phi$ and hence covers Galerkin BEM and collocation BEM as well as inexact computations based on iterative solvers.

State of the art. Earlier works provide a-posteriori estimates for the density error $\|\phi - \phi_h\|_{H^{-1/2}(\Gamma)}$ (mainly exploiting that ϕ_h is a Galerkin approximation of ϕ by piecewise polynomials). See, e.g., [6, 7, 2, 3] for weighted-residual error estimators, [17, 18, 15, 14] for two-level estimators, [20] for estimators exploiting the Calderón projector, [9, 10, 4] for estimators based on the localization of the $H^{1/2}$-residual norm, and [5, 13, 8] for averaging and $(h-h/2)$-type error estimators. Moreover, we refer to the recent review [11]. Clearly, a-posteriori error control of the density also provides a bound for the potential error: From boundedness of the single-layer potential operator $\widetilde{V}$, it follows that

$$(7)\qquad \|\nabla(u-u_h)\|_{L^2(\Omega)} \le C\,\|\phi-\phi_h\|_{H^{-1/2}(\Gamma)},$$

where, however, the constant $C > 0$ is generic, depends on Ω, and is hardly accessible. Finally, one particular advantage of BEM is its potentially high convergence order for point errors of the potential, i.e., $|u(x) - u_h(x)|$ for some fixed $x \in \Omega$, where we refer to [12, 1] for a-posteriori error control and adaptive algorithms.

Functional a-posteriori error estimate. We employ the so-called hypercircle method (see, e.g., [19]), which even simplifies because of $\Delta u = 0 = \Delta u_h$.

Theorem 1 (Functional error identity)**.** *Exploiting* (1) *and* (5)*, it holds that*

$$\max_{\substack{\boldsymbol{\tau}\in L^2(\Omega)\\ \nabla\cdot\boldsymbol{\tau}=0}} \underline{\mathfrak{M}}(\boldsymbol{\tau}; g-u_h|_\Gamma) = \|\nabla(u-u_h)\|^2_{L^2(\Omega)} = \min_{\substack{w\in H^1(\Omega)\\ w|_\Gamma = g-u_h|_\Gamma}} \overline{\mathfrak{M}}(\nabla w), \tag{8}$$

where $\underline{\mathfrak{M}}(\boldsymbol{\tau}; f) = 2\,\langle f\,,\,\boldsymbol{\tau}|_\Gamma\cdot\boldsymbol{n}\rangle_{L^2(\Gamma)} - \|\boldsymbol{\tau}\|^2_{L^2(\Omega)}$ *and* $\overline{\mathfrak{M}}(\nabla w) = \|\nabla w\|^2_{L^2(\Omega)}$*. Moreover, the unique maximizer (resp. minimizer) is* $w = u-u_h$ *(resp.* $\boldsymbol{\tau} = \nabla(u-u_h)$*).*

With Theorem 1, each $\boldsymbol{\tau}\in L^2(\Omega)$ with $\nabla\cdot\boldsymbol{\tau}=0$ provides a lower bound for the potential error $\|\nabla(u-u_h)\|_{L^2(\Omega)}$, while each $w\in H^1(\Omega)$ with $w|_\Gamma = g-u_h|_\Gamma$ provides an upper bound. To compute such functions, we employ the FEM. To lower the computational costs, we fix a *bounded* boundary layer domain $\omega\subseteq\Omega$ with $\Gamma\subset\partial\omega$ and $\operatorname{dist}(\Gamma,\partial\omega\backslash\Gamma)$ and let $\mathcal{T}_h$ be a conforming triangulation of ω.

To motivate the following corollaries, consider for $\omega=\Omega$ the problem

$$\Delta(u-u_h) = 0 \text{ in } \Omega \quad \text{subject to} \quad (u-u_h)|_\Gamma = g-u_h|_\Gamma, \tag{9}$$

Then, (10) is the mixed FEM formulation of (9) with $\boldsymbol{\tau}_h \approx \boldsymbol{\tau} = \nabla(u-u_h)$, while (13) is the primal FEM formulation of (9) with $w_h\approx u-u_h$. In either case, the zero boundary conditions on $\partial\omega\backslash\Gamma$ are motivated by the fact that, first, they are clearly exact if $g-u_h|_\Gamma=0$ and, second, they allow for a trivial extension of the computed functions from ω to Ω (which is needed to apply Theorem 1).

Corollary 2 (Computable lower bound)**.** *Let* $P^q(\mathcal{T}_h)$ *be the space of* $\mathcal{T}_h$*-piecewise polynomials of degree* q*. Let* $RT^q(\mathcal{T}_h)\subset P^{q+1}(\mathcal{T}_h)$ *be the corresponding Raviart–Thomas space on* ω *and* $RT^q_0(\mathcal{T}_h) := \{\boldsymbol{\tau}_h\in RT^q(\mathcal{T}_h) : \boldsymbol{\tau}_h|_{\partial\omega\backslash\Gamma}\cdot\boldsymbol{n}=0\}$*. Then, there exists a unique pair of* $\boldsymbol{\tau}_h\in RT^q_0(\mathcal{T}_h)$ *and* $p_h\in P^q(\mathcal{T}_h)$ *such that*

$$\left\{\begin{array}{rcl} \langle\boldsymbol{\tau}_h\,,\,\boldsymbol{\sigma}_h\rangle_{L^2(\omega)} + \langle\nabla\cdot\boldsymbol{\sigma}_h\,,\,p_h\rangle_{L^2(\omega)} &=& \langle g-u_h|_\Gamma\,,\,\boldsymbol{\sigma}_h|_\Gamma\cdot\boldsymbol{n}\rangle_{L^2(\Gamma)},\\ \langle\nabla\cdot\boldsymbol{\tau}_h\,,\,q_h\rangle_{L^2(\omega)} &=& 0, \end{array}\right. \tag{10}$$

for all $\boldsymbol{\sigma}_h\in RT^q_0(\mathcal{T}_h)$ *and all* $q_h\in P^q(\mathcal{T}_h)$*. Extending* $\boldsymbol{\tau}_h$ *by zero to* $\Omega\backslash\omega$*, it holds that* $\boldsymbol{\tau}_h\in L^2(\Omega)$ *with* $\nabla\cdot\boldsymbol{\tau}_h=0$*. In particular, we obtain that*

$$2\,\langle g-u_h|_\Gamma\,,\,\boldsymbol{\tau}_h|_\Gamma\cdot\boldsymbol{n}\rangle_{L^2(\Gamma)} - \|\boldsymbol{\tau}_h\|^2_{L^2(\omega)} \le \|\nabla(u-u_h)\|^2_{L^2(\Omega)}. \tag{11}$$

For the upper bound, we proceed analogously. However, since discrete FEM functions cannot satisfy continuous Dirichlet conditions, we must discretize the Dirichlet conditions of (9). Therefore, the upper bounds additionally involves certain data oscillation terms.

Corollary 3 (Computable upper bound)**.** *Let* $S^q(\mathcal{T}_h) := P^q(\mathcal{T}_h)\cap H^1(\omega)$ *be the standard Courant FEM space and* $S^q_0(\mathcal{T}_h) := \{v_h\in S^q(\mathcal{T}_h) : v_h|_{\partial\omega\backslash\Gamma}=0\}$*. Suppose that* $J_h : H^{1/2}(\Gamma)\to\{v_h|_\Gamma : v_h\in S^q(\mathcal{T}_h)\}$ *is, e.g., the* $L^2(\Gamma)$*-orthogonal projection. Then, there exists a unique* $w_h\in S^q_0(\mathcal{T}_h)$ *such that*

$$w_h|_\Gamma = J_h(g-u_h|_\Gamma) \quad \textit{and} \quad \langle\nabla w_h\,,\,\nabla v_h\rangle_{L^2(\omega)} = 0 \quad \textit{for all} \quad v_h\in S^q_0(\mathcal{T}_h). \tag{12}$$

Extend w_h by zero to $\Omega\backslash\omega$ to get $w_h \in H^1(\Omega)$, and the triangle inequality leads to

$$\|\nabla(u-u_h)\|_{L^2(\Omega)} \le \|\nabla w_h\|_{L^2(\omega)} + C\,\|(1-J_h)(g-u_h|_\Gamma)\|_{H^{1/2}(\Gamma)}, \tag{13}$$

where $C > 0$ depends only on the definition of the $H^{1/2}$-norm and $C = 1$ if the latter is defined by harmonic extension.

Adaptive algorithm. The discrete majorant $\|\nabla w_h\|_{L^2(\omega)}$ from Corollary 3 can be used to drive an adaptive mesh-refining algorithm.

In the initial step, let $\mathcal{T}_h^\Gamma$ be a (boundary) triangulation of Γ, which is extended to some (volume) triangulation $\mathcal{T}_h$ of some boundary layer $\omega \subseteq \Omega$.

In the successive steps of the adaptive loop, we proceed as follows: Given the triangulation $\mathcal{T}_h$ of ω, we extract the triangulation $\mathcal{T}_h^\Gamma$, compute the BEM solution ϕ_h and the FEM majorant w_h, use $\|\nabla w_h\|_{L^2(T)}$ to mark elements $T \in \mathcal{T}_h$, and refine the marked elements. By this procedure, we obtain a refined triangulation $\mathcal{T}_h$ of ω. We then use the latter to shrink the FEM domain ω (e.g., as a fixed-order patch of the new boundary mesh $\mathcal{T}_h^\Gamma$), restrict $\mathcal{T}_h$ to the shrunken ω, and continue with the next step of the adaptive loop.

Note that by shrinking ω, we practically ensure that the dimension of the BEM space stays proportional to the dimension of the auxiliary FEM space. Of course, it is important that Corollary 2–3 are independent of ω.

Conclusions. The proofs of Theorem 1 and Corollary 2–3 are independent of the approximation $\phi_h \approx \phi$ and avoid, in particular, the use of any Galerkin-type orthogonality. This makes the proposed approach interesting in engineering, where primarily collocation BEM is used. Moreover, the analysis applies to indirect BEM (as presented here) as well as direct BEM for both interior and exterior problems. Finally, the mathematical concepts go beyond the Poisson model problem.

In first experiments with lowest-order BEM for the 2D Poisson problem (1), our empirical observations are as follows [16]: For lowest-order BEM, first-order FEM elements are sufficient (i.e., $q = 1$ in Corollary 2–3). After a few adaptive steps, the oscillation term $\|(1-J_h)(g-u_h|_\Gamma)\|_{H^{1/2}(\Gamma)}$ becomes negligible and there even holds $\|\nabla(u-u_h)\|_{L^2(\Omega)} \le \|\nabla w_h\|_{L^2(\omega)}$ with $\|\nabla w_h\|_{L^2(\omega)}/\|\nabla(u-u_h)\|_{L^2(\Omega)} \approx 1.2$. Mathematically, it remains to prove that upper and lower bound in (6) are equivalent (at least up to oscillations terms) and that the proposed adaptive strategy leads to optimal convergence. Both is observed experimentally. We are currently working on a 3D implementation, where the overall goal will be to deal with 3D Maxwell.

An obvious drawback of the approach is that it requires a FEM mesh on a boundary layer $\omega \subseteq \Omega$ along Γ. However, we stress that the generation of such a FEM mesh is a standard problem for FEM computations, where the geometry is usually given in terms of a CAD representation.

References

[1] M. Bakry: *A goal-oriented a posteriori error estimate for the oscillating single layer integral equation*, Appl. Math. Lett. 69 (2017), 133–137.

[2] C. Carstensen: *An a-posteriori error estimate for a first-kind integral equation*, Math. Comp. **66** (1997), 139–155.

[3] C. Carstensen, M. Maischak, E.P. Stephan: *A posteriori error estimate and h-adaptive algorithm on surfaces for Symm's integral equation*, Numer. Math. **90** (2001), 197–213.

[4] C. Carstensen, D. Praetorius: *A posteriori error control in adaptive qualocation boundary element analysis for a logarithmic-kernel integral equation of the first kind*, SIAM J. Sci. Comp. **25** (2003), 259–283.

[5] C. Carstensen, D. Praetorius: *Averaging techniques for the effective numerical solution of Symm's integral equation of the first kind*, SIAM J. Sci. Comp. **27** (2006), 1226–1260.

[6] C. Carstensen, E.P. Stephan: *A posteriori error estimates for boundary element methods*, Math. Comp. **64** (1995), 483–500.

[7] C. Carstensen, E.P. Stephan: *Adaptive boundary element methods for some first kind integral equations*, SIAM J. Numer. Anal. **33** (1996), 2166–2183.

[8] C. Erath, S. Ferraz-Leite, S.A. Funken, D. Praetorius: *Energy norm based a posteriori error estimation for boundary element methods in two dimensions*, Appl. Numer. Math. **59** (2009), 2713–2734.

[9] B. Faermann: *Localization of the Aronszajn-Slobodeckij norm and application to adaptive boundary element methods. Part I: The two-dimensional case*, IMA J. Numer. Anal. **20** (2000), 203–234.

[10] B. Faermann: *Localization of the Aronszajn-Slobodeckij norm and application to adaptive boundary element methods. Part II: The three-dimensional case*, Numer. Math. **92** (2002), 467–499.

[11] M. Feischl, T. Führer, N. Heuer, M. Karkulik, D. Praetorius: *Adaptive boundary element methods*, Arch. Comput. Methods Eng. **22** (2015), 309–389.

[12] M. Feischl, T. Führer, G. Gantner, A. Haberl, D. Praetorius: *Adaptive boundary element methods for optimal convergence of point errors*, Numer. Math. 132 (2016), 541–567.

[13] S. Ferraz-Leite, D. Praetorius: *Simple a posteriori error estimates for the h-version of the boundary element method*, Computing **83** (2008), 135–162.

[14] N. Heuer, V.J. Ervin: *An adaptive boundary element method for the exterior Stokes problem in three dimensions*, IMA J. Numer. Anal. **26** (2006), 297–325.

[15] N. Heuer, M.E. Mellado, E.P. Stephan: *hp-adaptive two-level methods for boundary integral equations on curves*, Computing **67** (2001), 305–334.

[16] S. Kurz, D. Pauly, D. Praetorius, S. Repin, and D. Sebastian: *Functional a posteriori error estimates for boundary element methods*, Preprint `arXiv:1912.05789`, 2019.

[17] M. Maischak, P. Mund, E.P. Stephan: *Adaptive multilevel BEM for acoustic scattering*, Comput. Methods Appl. Mech. Engrg. **150** (1997), 351–367.

[18] P. Mund, E.P. Stephan, J. Weiße: *Two-level methods for the single layer potential in* $\mathbb{R}^3$, Computing **60** (1998), 243–266.

[19] S. Repin: *A posteriori estimates for partial differential equations*, de Gruyter, Berlin 2008.

[20] H. Schulz, O. Steinbach: *A new a posteriori error estimator in adaptive direct boundary element methods: the Dirichlet problem*, Calcolo **37** (2000), 79–96.

Asymptotically optimal BEM for the Vlasov-Poisson system

Sergej Rjasanow
(joint work with Torsten Keßler)

1. Introduction

In this talk, we consider a combination of the Boundary Element Methods (BEM) and of the particles method for numerical solution of the Vlasov–Poisson system. This system describes the time, space and velocity distribution function for collisionless electron plasma. The numerical evaluation of the acceleration force involves the solution of the Poisson equation in the whole spatial domain. However, by the use of the BEM, a volume mesh can be avoided and only the a discretisation of the boundary is required. The fast BEM, based on hierarchical techniques allows to reduce the computational costs from quadratic to linear complexity. In particular, the Coulomb forces acting on the particles are computed in linear complexity. We validate our approach with the help of classical non-linear plasma phenomena and show that our method is able to simulate electron plasma in complex three-dimensional domains with mixed boundary conditions in almost linear complexity.

2. Vlasov-Poisson system

Let $\Omega \subseteq \mathbb{R}^3$ be a physical domain. The Vlasov equation for the particle density

$$f : \mathbb{R}_+ \times \Omega \times \mathbb{R}^3 \to \mathbb{R}_+$$

reads

$$f_t + v \cdot \operatorname{grad}_x f + \frac{q}{m} \boldsymbol{E} \cdot \operatorname{grad}_v f = 0 \tag{1}$$

for the time, space and velocity variables $(t, x, v) \in \mathbb{R}_+ \times \Omega \times \mathbb{R}^3$. Here, $q \in \mathbb{R}$ denotes the charge and $m \in \mathbb{R}_+$ the mass of the particle. The electric field,

$$\boldsymbol{E} : \mathbb{R}_+ \times \Omega \to \mathbb{R}^3$$

is obtained from

$$\begin{aligned} \boldsymbol{E} &= -\nabla \phi \,, \\ -\varepsilon_0 \Delta \phi &= \varrho \,, \end{aligned} \tag{2}$$

and connected to the Vlasov equation via the macroscopic charge density

$$\varrho = q \int_{\mathbb{R}^3} f \, \mathrm{d}v \,. \tag{3}$$

The parameter ε_0 is the electric permittivity constant. The Vlasov-Poisson system (1)-(2) is subjected to an initial condition

$$f(0, x, v) = f_0(x, v) \,, \tag{4}$$

for $x \in \Omega$ and $v \in \mathbb{R}^3$. If Ω is a bounded Lipschitz domain with boundary Γ, then the outward unit normal vector $\boldsymbol{n}_x \in S^2$ is defined for almost all $x \in \Gamma$. In

this case also a set of boundary conditions for the unknown functions f and ϕ are required. An appropriate boundary condition for f can be specular or diffuse reflection (see [2] for more details) or simple absorption

$$f(t,x,v) = 0\,, \quad t > 0\,,\ x \in \Gamma\,,\ v \in \mathbb{R}^3\,.$$

The most simple boundary condition on the boundary Γ for the potential ϕ is a Dirichlet boundary condition

$$\phi(x) = g_D(x)\,, \quad t > 0\,,\ x \in \Gamma\,. \tag{5}$$

3. Numerical solution

For the numerical solution of the Vlasov equation (1), we first generate N_p numerical particles

$$\Big(\frac{1}{N_p}, x_j(0), v_j(0)\Big)\,, \quad j = 1, \dots, N_p \tag{6}$$

from the initial condition f_0. They will approximate the distribution function f for $t > 0$, i.e.

$$f(t,x,v) \approx \frac{|\Omega|}{N_p} \sum_{j=1}^{N_p} \delta_{x_j(t)}\, \delta_{v_j(t)}, \quad t > 0\,, \tag{7}$$

where $|\Omega|$ is the volume of the physical domain. The corresponding approximation of the charge density (3) reads

$$\varrho(t,x) = q \int_{\mathbb{R}^3} f(t,x,v)\,\mathrm{d}v \approx q\,\frac{|\Omega|}{N_p} \sum_{j=1}^{N_p} \delta_{x_j(t)}\,, \tag{8}$$

The Vlasov equation for the approximation (7) is equivalent to the following system of ODEs,

$$\begin{aligned} \dot{x}_i &= v_i\,, \\ \dot{v}_i &= -\frac{q}{m} \nabla\phi(x_i)\,, \quad i = 1, \dots, N_p, \end{aligned} \tag{9}$$

where ϕ is the solution to the boundary value problem

$$\begin{aligned} -\varepsilon_0 \Delta\phi &= q\,\frac{|\Omega|}{N_p} \sum_{j=1}^{N_p} \delta_{x_j(t)} \quad \text{in } \Omega, \\ \phi &= g_D \qquad\qquad\qquad\quad \text{on } \Gamma = \partial\Omega\,. \end{aligned} \tag{10}$$

If we denote the fundamental solution of the Laplace equation by

$$u^*(x,y) = \frac{1}{4\,\pi}\,\frac{1}{|x-y|}\,, \quad x, y \in \mathbb{R}^3\,, x \neq y$$

then a possible particular solution of the Poisson equation (10) is

$$\phi_p(x) = \frac{q}{\varepsilon_0}\,\frac{|\Omega|}{N_p}\sum_{j=1}^{N_p} u^*(x, x_j(t)) \tag{11}$$

and the Poisson equation (10) can be reduced to the Laplace equation

$$\begin{aligned} -\Delta\phi_L &= 0 && \text{in } \Omega, \\ \phi_L &= g_D - \phi_p && \text{on } \Gamma = \partial\Omega\,. \end{aligned} \tag{12}$$

The problem (12) can be efficiently solved by the use of the fast BEM, see [5],[6],[1]. The solution of the Poisson equation is then $\phi = \phi_L + \phi_p$. The problem (12) has a unique solution which is given for by the representation formula

$$\phi_L(x) = \int_\Gamma u^*(x,y)\gamma_1\phi_L(y)\,\mathrm{d}s_y - \int_\Gamma \gamma_{1,y}u^*(x,y)\gamma_0\phi_L(y)\,\mathrm{d}s_y, \tag{13}$$

where $\gamma_0\phi_L$ denotes the Dirichlet and $\gamma_1\phi_L$ the Neumann trace of the unknown solution ϕ_L. By applying the interior trace operator γ_0 to the representation formula (13) and using the jump relations (see e.g. [4]) and the Dirichlet boundary condition, we obtain the boundary integral equation

$$\int_\Gamma u^*(x,y)t(y)\mathrm{d}s_y = \frac{1}{2}g(x) + \int_\Gamma \gamma_{1,y}u^*(x,y)g(y)\mathrm{d}s_y \quad \text{for } x \in \Gamma\,, \tag{14}$$

where the abbreviations $t = \gamma_1\phi_L$ and $g = g_D - \phi_p$ have been used. The boundary element discretisation starts with a mesh on the boundary Γ, i.e. by a conforming surface triangulation Γ_h with $N_{\mathtt{BEM}}$ plane triangles τ_ℓ and $M_{\mathtt{BEM}}$ nodes $\boldsymbol{x}_i$ The piece-wise constant functions

$$\Psi = \left(\psi_1, \ldots, \psi_{N_{\mathtt{BEM}}}\right),$$

where ψ_ℓ is 1 on triangle τ_ℓ and 0 outside τ_ℓ will be used as a basis and test functions for the discretised single layer potential. For the double layer potential the piece-wise linear basis functions, i.e.

$$\Phi = \left(\varphi_1, \ldots, \varphi_{M_{\mathtt{BEM}}}\right),$$

where $\varphi_j(\boldsymbol{x}_i) = \delta_{ij}$ and φ_j is linear on each τ_ℓ, and piece-wise constant test functions. The BEM Galerkin method for (14) leads to a system of linear equations

$$V_h\underline{t} = \Big(\frac{1}{2}M_h + K_h\Big)\underline{g}\,, \tag{15}$$

Summarising, the numerical procedure for the Vlasov-Poisson system is as follows:

(1) Preparation step
- Generate the surface discretisation Γ_h,
- Generate the BEM matrices V_h and K_h in $\mathcal{H}^2$-format,
- Generate the initial particle system (6).

(2) Time steps
- Evaluate the particular solution (11) at the boundary nodes $\boldsymbol{x}_i$,
- Compute the projection of the boundary condition $\underline{g}$,
- Solve the linear system (15),
- Compute the gradient of the representation formula (13) at the positions of the particles,
- Change the velocities of the particles corresponding to (9),
- Change the positions of the particles corresponding to (9). If a particle hits the boundary, apply the boundary conditions for f.

4. Numerical results

In this section, we show that the above numerical procedure can be realised in almost linear complexity with respect to the most important discretisation parameters, namely in number of particles and in number of the surface triangles. Figure 1 illustrates the linear scaling of the computational times with the number of particles in case of a sphere meshed with 1 280 triangles. Figure 2 demonstrates the linear scaling with respect to the number of surface triangles for a fixed number of 10 000 particles. We refer to [3] for more numerical results.

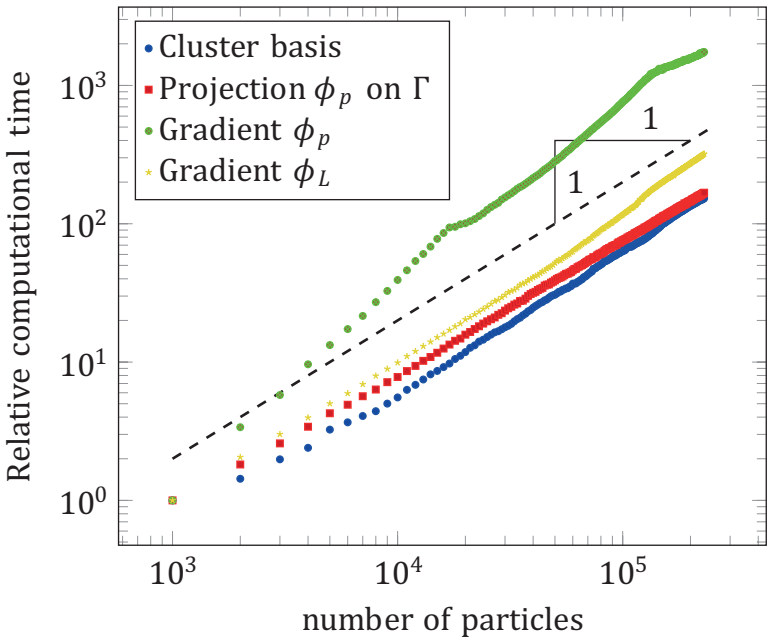

Figure 1. Double logarithmic plot of the computational times.

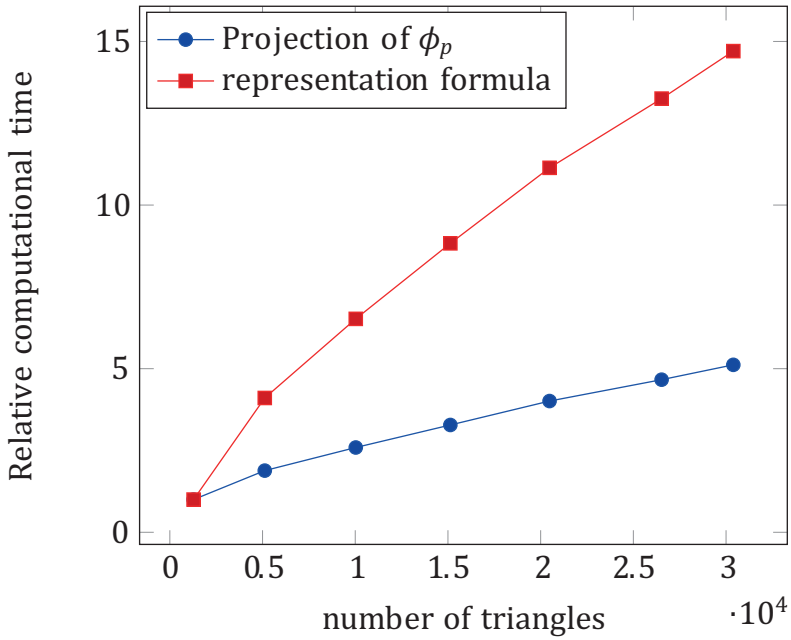

FIGURE 2. Computational times for a sequence of meshes of the sphere.

REFERENCES

[1] Börm, S., Christophersen, S.: Approximation of integral operators by Green quadrature and nested cross approximation. Numer. Math. **133**(3), 409–442 (2016)
[2] C. Cercignani.: The Boltzmann Equation and Its Applications. Springer, New York, 1988.
[3] Keßler, T., Rjasanow, S., Weißer, S.: Vlasov-Poisson system tackled by particle simulation utilizing boundary element methods. SIAM Journal on Scientific Computing, 42(1): B299–B326 (2020)
[4] McLean, W.: Strongly elliptic systems and boundary integral equations. Cambridge University Press, Cambridge (2000)
[5] Rjasanow, S., Steinbach, O.: The fast solution of boundary integral equations. Math. Anal. Tech. Appl. Eng. Springer, New York (2007)
[6] Steinbach, O.: Numerical approximation methods for elliptic boundary value problems. Springer, New York (2008)

Sparse Approximation of Integral Operators related to lossy Helmholtz Problems

STEFAN SAUTER
(joint work with Steffen Börm, Maria Lopez-Fernandez)

1. INTRODUCTION

In various applications (see, e.g., [1], [13], [22] for physical ones and [15], [16], [17], [18], [21], [24] for mathematical ones), the problem arises to discretize boundary integral operators related to the lossy Helmholtz operator $\mathcal{L}u = -\Delta u + \zeta^2 u$ for

complex frequencies ζ in $\mathbb{C}_{\geq 0} := \{\zeta \in \mathbb{C} \mid \operatorname{Re}\zeta \geq 0\}$. The boundary, typically, is the surface of a three-dimensional scatterer covering a bounded Lipschitz domain $\Omega \subset \mathbb{R}^3$ with $\Gamma := \partial\Omega$. In the most simple setting of the acoustic simple layer potential the arising boundary integral operator corresponds to the sesquilinear form

$$a_\zeta(\varphi,\psi) := (V(\zeta)\varphi,\psi) := \int_\Gamma \int_\Gamma G(\zeta, y-x)\,\varphi(y)\,\overline{\psi(x)}\,d\Gamma_y d\Gamma_x \quad \forall \varphi,\psi \in H^{-1/2}(\Gamma)$$

with the kernel function

$$G(\zeta,z) := \frac{\mathrm{e}^{-\zeta\|z\|}}{4\pi\|z\|}. \tag{1}$$

The Sobolev spaces $H^s(\Gamma)$ for $s \in \mathbb{R}$ are defined in the usual way (see, e.g., [19]). The norm is denoted by $\|\cdot\|_{H^s(\Gamma)}$. Here $(\cdot,\cdot)$ denotes the continuous extension of the $L^2(\Gamma)$ scalar product (with complex conjugation on the second argument) to the anti-dual pairing on $H^{1/2}(\Gamma) \times H^{-1/2}(\Gamma)$.

The Galerkin discretization of this sesquilinear form $a_\zeta(\cdot,\cdot)$ employs boundary element spaces which we briefly introduce. Let $\mathcal{G} = \left\{\tau_i : 1 \leq i \leq \tilde{M}\right\}$ denote a conforming triangulation of $\partial\Omega$, consisting of affine or possibly curved triangles. The finite-dimensional boundary element space of polynomial degree $p \in \mathbb{N}_0$ and smoothness degree $m \in \{-1, 0\}$ sub-ordinate to $\mathcal{G}$ is given by

$$S_{\mathcal{G}}^{p,m} := \left\{u \in L^1(\Gamma) \mid \forall \tau \in \mathcal{G} \quad u|_\tau \circ \chi_\tau \in \mathbb{P}_p\right\} \cap H^{m+1}(\Gamma).$$

If no confusion is possible, we write S short for $S_{\mathcal{G}}^{p,m}$. The standard Lagrange nodal basis is denoted by b_i, $i \in \mathcal{I} := \{1,\ldots,n\}$, and depends as well on p, m, $\mathcal{G}$. Finally we have

$$S_{\mathcal{G}}^{p,m} = \operatorname{span}\{b_i : 1 \leq i \leq n\} \subset H^{-1/2}(\Gamma). \tag{2}$$

The maximal mesh width is denoted by

$$h_{\mathcal{G}} := \max\{h_\tau : \tau \in \mathcal{G}\} \quad \text{with} \quad h_\tau := \operatorname{diam}\tau.$$

Another mesh parameter is

$$h_{\min} := \min\left\{\operatorname{dist}(\tau,\tau') : \forall \tau \in \mathcal{G} \quad \forall \tau' \in \mathcal{G} \text{ with } \tau \cap \tau' = \emptyset\right\}. \tag{3}$$

We say that a boundary element mesh is *quasi-uniform* if there exists a constant $0 < C_{\mathrm{qu}} = \mathcal{O}(1)$ such that

$$h_{\mathcal{G}} \leq C_{\mathrm{qu}} h_{\min}. \tag{4}$$

By using the basis b_i we obtain a representation of the sesquilinear form $a_\zeta(\cdot,\cdot)$ as an $n \times n$ matrix. Let $\mathbf{K}(\zeta) = (K_{i,j}(\zeta))_{i,j=1}^n \in \mathbb{C}^{n\times n}$ be defined by

$$K_{i,j}(\zeta) := (V(\zeta)\,b_j, b_i), \quad 1 \leq i,j \leq n. \tag{5}$$

Remark 1. The matrix $\mathbf{K}(\zeta)$ is fully populated containing, in general, n^2 non-zero entries. This is a major bottleneck in a numerical realization of the boundary element method.

The goal of this paper is to introduce a sparse approximation of the matrix $\mathbf{K}(\zeta)$ as a directional $\mathcal{H}^2$ matrix which enjoys exponential convergence with respect to its order. Since the mid 1980ies, the development of compression algorithms for densely populated matrices related to the numerical discretization of non-local operators has become an important topic in numerical analysis and scientific computing. We refer to [9] for a detailed literature review. We note that the existing literature on sparse representations of high frequency integral operators is mostly concerned with the "pure" Helmholtz problem, i.e., the operator $\mathcal{L}_\zeta u := -\Delta u + \zeta^2 u$ for purely imaginary frequency $\zeta \in \mathrm{i}\,\mathbb{R}$ (exceptions are the papers [3], [2], [14]). In our paper we consider more general frequencies $\zeta \in \mathbb{C}$ with $\operatorname{Re}\zeta \geq 0$.

2. Directional $\mathcal{H}^2$ Matrices for Helmholtz Equations with Decay

Directional $\mathcal{H}^2$ matrices have been introduced in [8], [10], [20], [4], [7], [5] for the high-frequency Helmholtz problems for purely imaginary frequency. The new point in this report is to introduce an *admissibility condition* which depends on the imaginary and real part of the complex frequency ζ to identify pairs of regions $\omega_t, \omega_s \subset \Gamma$, where the kernel function can be approximated by a *separable expansion* of the form:

$$G(\zeta, y-x) \approx \sum_{\nu=1}^{k}\sum_{\mu=1}^{k} \gamma_{\nu,\mu}(\zeta)\,\Phi_\nu^t(\zeta,x)\,\Psi_\mu^s(\zeta,y) \qquad \forall\,(x,y) \in \omega_t \times \omega_s,$$

i.e., an expansion where x and y appear only in a factorized way. The number k is the *rank* of the separable expansion.

To formulate the algorithm we first introduce some notation. For an indexed subset $\omega_t \subset \Gamma$, we denote by B_t the minimal axis-parallel *bounding box* B_t such that

$$\omega_t \subset B_t. \tag{6}$$

The *center* M_t of ω_t is defined as the barycenter of B_t..

Definition 2 (directional admissibility condition for complex frequencies)**.** For $\boldsymbol{\eta} = (\eta_i)_{i=1}^3 \in \mathbb{R}^3_{>0}$ a pair of regions ω_t, ω_s and a direction $c \in \mathbb{S}_2$ are $\boldsymbol{\eta}$*-admissible* with respect to a complex frequency $\zeta \in \mathbb{C}_{>0}$ if they satisfy the following three conditions:

$$|\operatorname{Im}\zeta| \left\| \frac{M_t - M_s}{\|M_t - M_s\|} - c \right\| \leq \frac{\eta_1}{\max\{\operatorname{diam}(B_t), \operatorname{diam}(B_s)\}}, \tag{7a}$$

$$\max\{\operatorname{diam}(B_t), \operatorname{diam}(B_s)\} \leq \eta_2 \operatorname{dist}(B_t, B_s), \tag{7b}$$

$$|\operatorname{Im}\zeta| \max\left\{\operatorname{diam}^2(B_t), \operatorname{diam}^2(B_s)\right\} \leq \max\{\eta_2, \eta_3(\operatorname{Re}\zeta)\operatorname{dist}(B_t, B_s)\} \operatorname{dist}(B_t, B_s). \tag{7c}$$

For the pure Helmholtz problem, i.e., $\operatorname{Re}\zeta = 0$, our conditions reduce to those in [10], [7, Sec. 3.3] which are very similar to those in the early paper [8]. Our

modification takes into account the exponential decay of the kernel function with increasing real part of the frequency ζ, reflected by the first factor in

$$G(\zeta, z) = \mathrm{e}^{-(\operatorname{Re}\zeta)\|z\|} \frac{\mathrm{e}^{-\mathrm{i}\operatorname{Im}(\zeta)\|z\|}}{4\pi\|z\|}$$

and provides a continuous transition of the elliptic to the hyperbolic case.

Based on this admissibility condition, it is nowadays standard to build a $\mathcal{H}^2$ matrix approximation of the sequilinear form $a_\zeta(\cdot,\cdot)$:

1) The index set $\mathcal{I}$ is organized as a *cluster tree*. Algorithms for building cluster trees from index sets $\mathcal{I}$ corresponding to boundary element basis functions can be found, e.g., in [25], [11].

2) A minimal partitioning of $\mathcal{I} \times \mathcal{I}$, consisting of admissible blocks and non-admissible pairs of (small) clusters, can be constructed by a simple divide and conquer algorithm [12].

3) For each admissible pair of clusters with admissible direction c, the kernel function is split according to

(8)

$$G(\zeta, z) = \mathrm{e}^{-\mathrm{i}(\operatorname{Im}\zeta)\langle z,c\rangle} G_c(\zeta, z) \quad \text{with} \quad G_c(\zeta, z) := \mathrm{e}^{-(\operatorname{Re}\zeta)\|z\|} \frac{\mathrm{e}^{-\mathrm{i}(\operatorname{Im}\zeta)(\|z\|-\langle z,c\rangle)}}{4\pi r}.$$

Then, the factor function $G_c(\zeta,\cdot)$ is approximation on the pair of clusters by a tensor polynomial Chebyshev expansion.

4) Finally, the polynomial expansion system is modified in order to satisfy a second functional hierarchy – this is the difference between $\mathcal{H}$-matrices and $\mathcal{H}^2$-matrices. The idea of a recursive definition of an approximate polynomial expansion system goes back to [23] and has been introduced for our application in [9].

3. Main Results

The $\mathcal{DH}^2$ sparse approximation of the Galerkin discretization of the boundary integral operator related to the acoustic single layer potential for the lossy Helmholtz problem satisfies:

(1) the compression algorithm presented here results in a sparse $\mathcal{DH}^2$-matrix approximation which converges exponentially with respect to the rank k of the expansion.

(2) The analysis in [9] shows how to choose the control parameters $(\boldsymbol{\eta},\ k)$ in order to satisfy a prescribed accuracy for this perturbation. However, numerical experiments indicate that the rank of this approximation may be larger than necessary. In [7], [6] a *recompression algorithm* is presented for the pure Helmholtz problem ($\zeta \in \mathrm{i}\,\mathbb{R}$) which further compresses an already sparse $\mathcal{DH}^2$-matrix. This recompression algorithm on top of our $\mathcal{DH}^2$-matrix approximation are employed numerical experiments which are presented in [9].

(3) The storage complexity of the algorithm is estimated in [9] for a quasi-uniform setting (cf. (4)) by

$$\mathcal{O}\left(\frac{n}{\eta_2^2} + \min\left\{(\log n)\left(\frac{|\operatorname{Im}\zeta|}{\eta_2}\right)^2, \frac{n}{\eta_3}\frac{|\operatorname{Im}\zeta|}{\operatorname{Re}\zeta}\right\}\right).$$

As long as $|\operatorname{Im}\zeta| \leq \mathcal{O}(\sqrt{n})$ or for the *sectorial case*, i.e., $|\operatorname{Im}\zeta| \leq \alpha \operatorname{Re}\zeta$, the complexity of the algorithm does not exceed $\mathcal{O}\left(n \log^2 n\right)$.

For the details and proofs we refer to [9].

References

[1] J. D. Achenbach. *Wave propagation in elastic solids*, volume 16 of *North-Holland Series in Applied Mathematics and Mechanics*. North-Holland Publishing Co., Amsterdam, first edition, 1976.

[2] L. Banjai and M. Kachanovska. Fast convolution quadrature for the wave equation in three dimensions. *J. Comput. Phys.*, 279:103–126, 2014.

[3] L. Banjai and M. Kachanovska. Sparsity of Runge-Kutta convolution weights for the three-dimensional wave equation. *BIT*, 54(4):901–936, 2014.

[4] M. Bebendorf, C. Kuske, and R. Venn. Wideband nested cross approximation for Helmholtz problems. *Numer. Math.*, 130(1):1–34, 2015.

[5] S. Börm. Directional $\mathcal{H}^2$-matrix compression for high-frequency problems. *Numer. Linear Algebra Appl.*, 24(6):e2112, 19, 2017.

[6] S. Börm and C. Börst. Hybrid matrix compression for high-frequency problems. *arXiv preprint arXiv:1809.04384*, 2018.

[7] S. Börm and J. M. Melenk. Approximation of the high-frequency Helmholtz kernel by nested directional interpolation: error analysis. *Numer. Math.*, 137(1):1–34, 2017.

[8] A. Brandt. Multilevel computations of integral transforms and particle interactions with oscillatory kernels. *Comput. Phys. Comm.*, 65(1-3):24–38, 1991.

[9] S. Börm, M. Lopez-Fernandez, and S. Sauter. Variable order, directional h2-matrices for helmholtz problems with complex frequency, 2019.

[10] B. Engquist and L. Ying. Fast directional multilevel algorithms for oscillatory kernels. *SIAM J. Sci. Comput.*, 29(4):1710–1737, 2007.

[11] W. Hackbusch. *Hierarchical matrices: algorithms and analysis*, volume 49. Springer, Heidelberg, 2015.

[12] W. Hackbusch and Z. Nowak. On the Fast Matrix Multiplication in the Boundary Element Method by Panel-Clustering. *Numerische Mathematik*, 54:463–491, 1989.

[13] J. D. Jackson. *Classical Electrodynamics*. John Wiley & Sons, New York, NY, 3 edition, 1998.

[14] M. Kachanovska. Hierarchical matrices and the high-frequency fast multipole method for the Helmholtz equation with decay. Technical report, MPI Leipzig, 3 2014.

[15] D. Lahaye, J. Tang, and K. Vuik, editors. *Modern solvers for Helmholtz problems*. Geosystems Mathematics. Birkhäuser/Springer, Cham, 2017.

[16] M. Lopez-Fernandez and S. Sauter. Generalized convolution quadrature with variable time stepping. *IMA J. Numer. Anal.*, 33(4):1156–1175, 2013.

[17] C. Lubich. Convolution Quadrature and Discretized Operational Calculus I. *Numerische Mathematik*, 52:129–145, 1988.

[18] C. Lubich. Convolution Quadrature and Discretized Operational Calculus II. *Numerische Mathematik*, 52:413–425, 1988.

[19] W. McLean. *Strongly Elliptic Systems and Boundary Integral Equations*. Cambridge, Univ. Press, 2000.

[20] M. Messner, M. Schanz, and E. Darve. Fast directional multilevel summation for oscillatory kernels based on Chebyshev interpolation. *J. Comput. Phys.*, 231(4):1175–1196, 2012.
[21] H.-M. Nguyen. Limiting absorption principle and well-posedness for the Helmholtz equation with sign changing coefficients. *J. Math. Pures Appl. (9)*, 106(2):342–374, 2016.
[22] E. G. Sauter. *Nonlinear Optics*, volume 44. John Wiley & Sons, 1996.
[23] S. Sauter. Variable order panel clustering. *Computing*, 64(3):223–261, 2000.
[24] S. Sauter and C. Schwab. *Boundary Element Methods*. Springer, Heidelberg, 2010.
[25] S. A. Sauter. Variable Order Panel Clustering. *Computing*, 64:223–261, 2000. Extended version: http://www.mis.mpg.de/preprints/1999/preprint1999_52.pdf.

Does the Galerkin method converge for the standard second-kind integral equations for the Laplacian on Lipschitz domains?

Euan A. Spence
(joint work with Simon N. Chandler-Wilde)

1. Formulation of the question

Given a bounded Lipschitz domain $\Omega \subset \mathbb{R}^d, d = 2, 3$, with boundary Γ, the interior and exterior Dirichlet and Neumann problems for Laplace's equation can be reformulated as boundary integral equations involving the operators

$$\frac{1}{2}I \pm D \quad \text{and} \quad \frac{1}{2}I \pm D' \tag{1}$$

where the *double-layer operator* D and the *adjoint double-layer operator* D' are defined by

$$D\phi(\mathbf{x}) = \int_\Gamma \frac{\partial \Phi(\mathbf{x},\mathbf{y})}{\partial n(\mathbf{y})}\phi(\mathbf{y})\,\mathrm{d}s(\mathbf{y}) \quad \text{and} \quad D'\phi(\mathbf{x}) = \int_\Gamma \frac{\partial \Phi(\mathbf{x},\mathbf{y})}{\partial n(\mathbf{x})}\phi(\mathbf{y})\,\mathrm{d}s(\mathbf{y}), \tag{2}$$

for $\mathbf{x} \in \Gamma$ and $\phi \in L^2(\Gamma)$, where $\Phi(\mathbf{x},\mathbf{y})$ is the fundamental solution for Laplace's equation:

$$\Phi(\mathbf{x},\mathbf{y}) := \frac{1}{2\pi}\log\left(\frac{a}{|\mathbf{x}-\mathbf{y}|}\right), \text{ for } d = 2, \quad \text{and } := \frac{1}{4\pi|\mathbf{x}-\mathbf{y}|}, \text{ for } d = 3, \tag{3}$$

with $a \in \mathbb{R}$. Integral equations involving the operators (1) can be posed in a variety of spaces. We work in the space $L^2(\Gamma)$, since this is the most natural space in which to seek approximations of the solutions of these equations via the Galerkin method. For simplicity of exposition, we restrict attention to $\frac{1}{2}I - D$, but highlight that analogues of our results below hold for all four of the operators in (1) (see [3]).

When Γ is Lipschitz, the integral in the definition of D is understood as a Cauchy principal value, D is bounded on $L^2(\Gamma)$ by [2], and $\frac{1}{2}I - D$ is invertible on $L^2(\Gamma)$ by [10].

A long-standing open question about the operator $\frac{1}{2}I - D$ posed on $L^2(\Gamma)$ is the following:

Q1. Can $\frac{1}{2}I - D$ be written as the sum of a coercive operator and a compact operator when Γ is Lipschitz ($d = 2$ or 3), in particular when Γ is Lipschitz polyhedral ($d = 3$)?

In this paper, we say that an operator $A : \mathcal{H} \to \mathcal{H}$, where $\mathcal{H}$ is a Hilbert space, is *coercive* if there exists an $\alpha > 0$ such that

$$\big|(A\phi, \phi)_{\mathcal{H}}\big| \geq \alpha \, \|\phi\|_{\mathcal{H}}^2 \quad \text{for all } \phi \in \mathcal{H}.$$

The main motivation for posing Q1 is to understand the behaviour of the Galerkin method applied to boundary integral equations involving $\frac{1}{2}I - D$.

Recall the definition of the *Galerkin method* for approximating solutions of the operator equation $A\phi = f$, where $\phi, f \in \mathcal{H}$, $A : \mathcal{H} \to \mathcal{H}$ is a bounded linear operator, and $\mathcal{H}$ is a Hilbert space: given a sequence $(\mathcal{H}_N)_{N=1}^{\infty}$ of nested finite-dimensional subspaces of $\mathcal{H}$ with $\dim(\mathcal{H}_N) \to \infty$ as $N \to \infty$,

$$\text{(4)} \qquad \text{find } \phi_N \in \mathcal{H}_N \text{ such that } \big(A\phi_N, \psi_N\big)_{\mathcal{H}} = \big(f, \psi_N\big)_{\mathcal{H}} \quad \text{for all } \psi_N \in \mathcal{H}_N.$$

We say that the *Galerkin method is convergent for the sequence* $(\mathcal{H}_N)_{N=1}^{\infty}$ if, for every $f \in \mathcal{H}$, the Galerkin equations (4) have a unique solution for all sufficiently large N and $\phi_N \to A^{-1}f$ as $N \to \infty$. We say that $(\mathcal{H}_N)_{N=1}^{\infty}$ *converges to* $\mathcal{H}$ if, for every $\phi \in \mathcal{H}$,

$$\inf_{\psi_N \in \mathcal{H}_N} \|\phi - \psi_N\| \to 0 \quad \text{as} \quad N \to \infty.$$

A necessary condition for the convergence of the Galerkin method is therefore that $(\mathcal{H}_N)_{N=1}^{\infty}$ converges to $\mathcal{H}$.

The significance of Q1 to the Galerkin method is given by the following theorem from [5, Chapter II, Lemma 5.1 and Theorem 5.1].

Theorem 1. *If A is invertible then the following are equivalent:*

- *The Galerkin method converges for every sequence $(\mathcal{H}_N)_{N=1}^{\infty}$ that converges to $\mathcal{H}$.*
- *$A = A_0 + K$ where A_0 is coercive and K is compact.*

Q1 can therefore be rephrased as

Q1′. Does the Galerkin method converge in $L^2(\Gamma)$ for the operator $\frac{1}{2}I - D$ for every sequence $(\mathcal{H}_N)_{N=1}^{\infty}$ that converges to $L^2(\Gamma)$ when Γ is Lipschitz ($d = 2$ or 3), in particular when Γ is Lipschitz polyhedral ($d = 3$)?

2. Previous work related to Q1.

It has been proved that $\frac{1}{2}I - D$ on $L^2(\Gamma)$ can be written as the sum of a coercive operator and a compact operator when:

- Γ is C^1, since here D is compact by [6].
- Γ is a 2d curvilinear polygon with each side $C^{1,\alpha}$ for some $0 < \alpha < 1$ and with each corner angle in the range $(0, 2\pi)$; in this case $\|D\|_{L^2(\Gamma),\text{ess}} < 1/2$, where $\|\cdot\|_{L^2(\Gamma)}$ is the *essential norm* on $L^2(\Gamma)$, defined by

$$\big\|D\big\|_{L^2(\Gamma),\text{ess}} := \inf_{K \text{ compact}} \big\|D - K\big\|_{L^2(\Gamma)}.$$

Therefore, if $\|D\|_{L^2(\Gamma),\mathrm{ess}} < 1/2$ then $D = D_0 + K$, where $\|D_0\|_{L^2(\Gamma)} < 1/2$ and K is compact. This result was given in [8, 9], and with the analogous result for polygons given independently in [1, §3 and Lemma 4].

Additionally, in the review article on the double-layer operator [11], Wendland highlights that $\frac{1}{2}I - D$ on $L^2(\Gamma)$ can be written as the sum of a coercive operator and a compact operator when Γ is Lipschitz with sufficiently small Lipschitz character due to the results of [7]. Indeed, the results in [7, Lemma 1, Page 392] concern the essential spectral radius but the arguments can be adapted to prove that $\|D\|_{L^2(\Gamma),\mathrm{ess}} < 1/2$ if the Lipschitz character of Γ is small enough (see [3]).

3. The answer

The paper [3] answers Q1 in the negative; i.e. [3] gives examples of 2-d Lipschitz domains and 3-d Lipschitz polyhedra for which $\frac{1}{2}I - D$ cannot be written as the sum of a coercive operator and a compact operator on $L^2(\Gamma)$. For brevity of exposition, we focus here on the 3-d Lipschitz polyhedral case.

The results in [3] are obtained by rephrasing Q1 in terms of the essential numerical range of the operator D. Recall that the *numerical range* and the *essential numerical range* of an operator $A : \mathcal{H} \to \mathcal{H}$ are defined by, respectively,

$$W(A) := \Big\{(A\psi,\psi)_{\mathcal{H}} \,:\, \|\psi\|_{\mathcal{H}} = 1\Big\}, \quad \text{and} \quad W_{\mathrm{ess}}(A) := \bigcap_{K \text{ compact}} \overline{W(A+K)}.$$

It is straightforward to show that (i) A is coercive iff $0 \notin \overline{W(A)}$, and (ii) A is the sum of a coercive operator plus a compact operator iff $0 \notin W_{\mathrm{ess}}(A)$. Q1 and Q1′ can therefore be rephrased as

Q1″. Are the points $\pm 1/2$ outside $W_{\mathrm{ess}}(D)$ on $L^2(\Gamma)$ when Γ is Lipschitz ($d = 2$ or 3), in particular when Γ is Lipschitz polyhedral ($d = 3$)?

Theorem 2 (Answer to Q1 when $d = 3$ and Γ is Lipschitz polyhedral)**.** *Let Ω be the "open book" polyhedron defined in* [3] *with opening angle θ and number of "pages" n (see Figure 1 for an example).*

(i) If $n = 2$ there exists θ_0 such that, for all $\theta \le \theta_0$, then $\pm 1/2 \in W_{\mathrm{ess}}(D)$.

(ii) For $n \ge 2$ there exists $\theta_1(n)$ such that, for all $\theta \le \theta_1$,

$$W_{\mathrm{ess}}(D) \supset \left\{z \in \mathbb{C} : |z| < \frac{1}{4}\sqrt{2n-1}\right\}$$

Since

$$W_{\mathrm{ess}}(D) \subset \big\{z \in \mathbb{C} : |z| \le \|D\|_{L^2(\Gamma),\mathrm{ess}}\big\},$$

Theorem 2 exhibits a class of Lipschitz polyhedra for which $\|D\|_{L^2(\Gamma),\mathrm{ess}}$ can be arbitrarily large. This is in contrast with the 2-d case where, as recalled above, $\|D\|_{L^2(\Gamma),\mathrm{ess}} < 1/2$ when Γ is a polygon by [8, 9, 1]. It is also in contrast to the result that the essential spectral radius of D on $L^2(\Gamma)$ is $< 1/2$ for every Lipschitz polyhedron [4, Theorem 4.1].

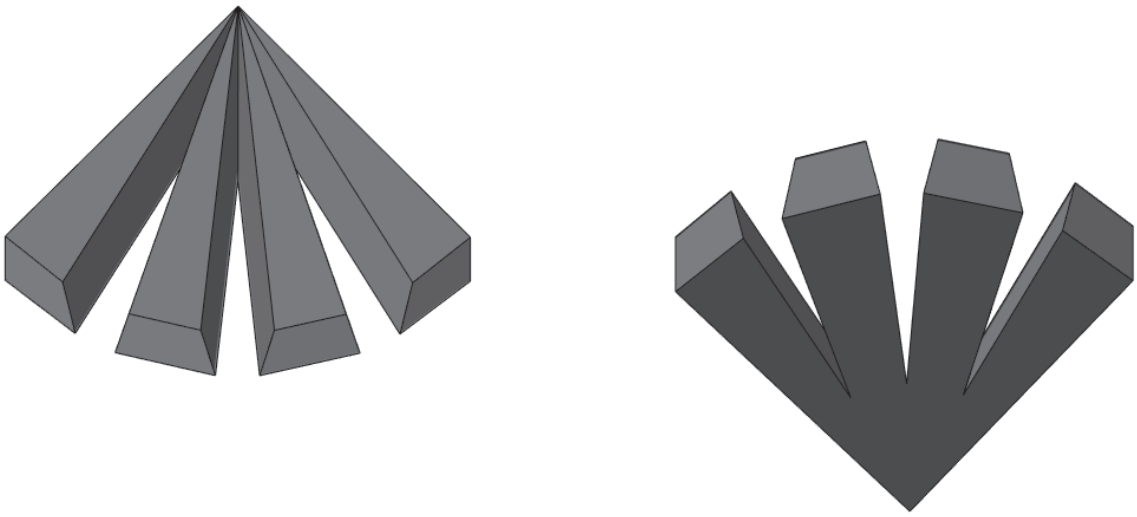

FIGURE 1. Views from above and below of the "open book" polyhedron Ω in the case that the number of "pages" $n = 4$ and the opening angle $\theta = \pi/2$.

REFERENCES

[1] G. A. Chandler. Galerkin's method for boundary integral equations on polygonal domains. *The ANZIAM Journal*, **26(1)** (1984), 1–13.

[2] R. R. Coifman, A. McIntosh, and Y. Meyer. L'intégrale de Cauchy définit un opérateur borné sur L^2 pour les courbes lipschitziennes. *Annals of Mathematics*, **116(2)** (1982), 361–387.

[3] S. N. Chandler-Wilde, E. A. Spence. *In preparation* (2020).

[4] J. Elschner. The double layer potential operator over polyhedral domains I: Solvability in weighted Sobolev spaces. *Applicable Analysis*, **45(1)** (1992), 117–134.

[5] I. Gohberg and I. A. Fel´dman. *Convolution equations and projection methods for their solution*, American Mathematical Society (1974).

[6] E. B. Fabes, M. Jodeit, and N. M. Riviere. Potential techniques for boundary value problems on C^1 domains. *Acta Mathematica*, **141(1)** (1978), 165–186.

[7] I. Mitrea. Spectral radius properties for layer potentials associated with the elastostatics and hydrostatics equations in nonsmooth domains. *Journal of Fourier Analysis and Applications*, **5(4)** (1999), 385–408.

[8] V. Y. Shelepov. On the index of an integral operator of potential type in the space L_p. *Soviet Math. Dokl.*, **10** (1969), 754–757.

[9] V. Y. Shelepov. On the index and spectrum of integral operators of potential type along radon curves. *Mathematics of the USSR-Sbornik*, **70(1)** (1991) 175–203.

[10] G. Verchota. Layer potentials and regularity for the Dirichlet problem for Laplace's equation in Lipschitz domains. *Journal of Functional Analysis*, **59(3)** (1984), 572–611.

[11] W. L. Wendland. On the Double Layer Potential. In A. Cialdea, P. E. Ricci, and F. Lanzara, editors, *Analysis, Partial Differential Equations and Applications*, **193** (2009), 319–334.

Space–time finite and boundary element methods for the heat equation

Olaf Steinbach

The numerical analysis of boundary integral equations and boundary element methods for the heat equation is well established, see, e.g., [1] and [2] for an overview. In fact, the heat single layer boundary integral operator V turns out to be elliptic in the anisotropic Sobolev space $H^{-1/2,-1/4}(\Sigma)$ with $\Sigma := \partial\Omega \times (0,T)$ being the lateral boundary of the space time domain $Q := \Omega \times (0,T)$. While in the case of the Laplace equation the ellipticity of the single layer boundary integral operator is related to the ellipticity of the interior and exterior Dirichlet forms, this relation with a domain variational formulation as used in finite element methods for the heat equation is not obvious. This is of particular interest when considering the non–symmetric coupling of finite and boundary element methods for the heat equation, see, e.g., [3, 4] for a free space transmission problem for the Poisson equation.

As first model problem we consider the Dirichlet problem for the heat equation,

$$\partial_t u - \Delta_x u = f \text{ in } Q, \quad u = 0 \text{ on } \Sigma, \quad u(0) = 0 \text{ in } \Omega. \tag{1}$$

The standard variational formulation of problem (1) in Bochner spaces reads to find $u \in X := \{w \in L^2(0,T;H^1_0(\Omega)), \partial_t w \in L^2(0,T;H^{-1}(\Omega)), w(0) = 0 \text{ in } \Omega\}$ such that

$$\int_0^T \int_\Omega \Big[\partial_t u\, v + \nabla_x u \cdot \nabla_x v\Big] dx\, dt = \int_0^T \int_\Omega f\, v\, dx\, dt \tag{2}$$

is satisfied for all $v \in Y := L^2(0,T;H^1_0(\Omega))$. Unique solvabilty of the variational formulation (2) and of related space–time finite element methods using conforming finite element spaces $Y_h = X_h \subset X$ is based on appropriate inf–sup stability conditions, e.g., [5]. Although in (2) we use the same finite element test and ansatz spaces $X_h = Y_h$, the underlying topology is different.

Instead we consider a different setting of the variational formulation (2) in anisotropic Sobolev spaces:

(3) Find $u \in H^{1,1/2}_{0;0,}(Q)$ such that (2) is satisfied for all $v \in H^{1,1/2}_{0;,0}(Q)$.

Note that the ansatz space $H^{1,1/2}_{0;0,}(Q)$ covers homogeneous Dirichlet boundary conditions and initial conditions, while the test space covers homogeneous Dirichlet boundary conditions and final conditions. The variational formulation (3) admits a unique solution $u \in H^{1,1/2}_{0;0,}(Q)$ for any given $f \in [H^{1,1/2}_{0;,0}(Q)]'$. In fact, using a modified Hilbert transformation $\mathcal{H}_T : H^{1,1/2}_{0;0,}(Q) \to H^{1,1/2}_{0;,0}(Q)$ it turns out that the bilinear form

$$\int_0^T \int_\Omega \partial_t u\, \mathcal{H}_T v\, dx\, dt$$

is indeed symmetric and $H^{1/2}_{0,}(0,T;L^2(\Omega))$ elliptic, while $\langle \nabla_x u, \nabla_x \mathcal{H}_T u\rangle_{L^2(Q)}$ is positive semi–definite, see [6] for more details on coercive space–time finite element methods, and [7] for an efficient realization of the modified Hilbert transformation.

In order to characterize the mapping properties of the heat boundary integral operators, instead of the homogeneous Dirichlet boundary value problem (1) we now consider Dirichlet problem for the homogeneous heat equation,

$$\partial_t u - \Delta_x u = 0 \text{ in } Q, \quad u = g \text{ on } \Sigma, \quad u(0) = 0 \text{ in } \Omega. \tag{4}$$

When using a bounded extension $u_g \in H^{1,1/2}_{;0,}(Q)$ of the given Dirichlet datum $g \in H^{1/2,1/4}(\Sigma)$ we can reformulate the Dirichlet problem (4) as in (1), and hence we can apply the above results to establish the associated Dirichlet to Neumann map, and to characterize the spatial normal derivative on Σ as

$$\|\partial_{n_x} u\|^2_{[H^{1/2,1/4}_{,0}(\Sigma)]'} \le \|u\|^2_{H^{1/2}_{0,}(0,T;L^2(\Omega))} + \|\nabla_x u\|^2_{L^2(Q)}. \tag{5}$$

Note that $[H^{1/2,1/4}_{,0}(\Sigma)]'$ is the adjoint of the Dirichlet trace space of $H^{1,1/2}_{;,0}(Q)$ of functions which are zero at the final time. When using the norm equivalence

$$\|u\|_{H^{1/2}_{0,}(0,T;L^2(\Omega))} \simeq \|\nabla_x u\|_{L^2(Q)}$$

for functions satisfying the homogeneous heat equation, see, e.g., [1], we can now prove, as in the case of the Laplace operator, the ellipticity of the single layer boundary integral operator V, i.e., when replacing $\|u\|_{H^{1/2}_{0,}(0,T;L^2(\Omega))}$ by $\|\nabla_x u\|_{L^2(Q)}$. However, when replacing $\|\nabla_x u\|_{L^2(Q)}$ by $\|u\|_{H^{1/2}_{0,}(0,T;L^2(\Omega))}$ this then results in the ellipticity of $\mathcal{H}_T V$. Note that the boundary element trace spaces $H^{1/2,1/4}(\Sigma)$ and $H^{-1/2,-1/4}(\Sigma)$ do not take care of the initial and final zero conditions, but the underlying domain spaces $H^{1,1/2}_{0,}(Q)$ and $H^{1,1/2}_{,0}(Q)$ do. In particular this is important when analysing the non–symmetric coupling of space–time finite and boundary element methods.

Although the use of the modified Hilbert transformation $\mathcal{H}_T$ in combination with the heat single layer boundary integral operator V requires a more detailed consideration, in particular from a computational point of view, we expect more insight in the properties of the heat boundary integral operators. This will be the topic of a forthcoming publication, [8].

References

[1] M. Costabel: Boundary Integral Operators for the Heat Equation. Integral Equations and Operator Theory 13 (1990) 498–552.

[2] S. Dohr, K. Niino, O. Steinbach: Space–time boundary element methods for the heat equation. In: Space–Time Methods. Applications to Partial Differential Equations, (U. Langer, O. Steinbach eds.), Radon Series on Computational and Applied Mathematics, vol. 25, de Gruyter, Berlin, pp. 1–60, 2019.

[3] F.-J. Sayas: The validity of Johnson–Nédélec's BEM-FEM coupling on polygonal interfaces. SIAM J. Numer. Anal. 47 (2009) 3451–3463.

[4] O. Steinbach: A note on the stable one–equation coupling of finite and boundary elements. SIAM J. Numer. Anal. 49 (2011) 1521–1531.

[5] O. Steinbach: Space–time finite element methods for parabolic problems. Comput. Meth. Appl. Math. 15 (2015) 551–566.
[6] O. Steinbach, M. Zank: Coercive space-time finite element methods for initial boundary value problems. Electron. Trans. Numer. Anal., accepted (2020).
[7] O. Steinbach, M. Zank: A note on the efficient evaluation of a modified Hilbert transformation, submitted, 2019.
[8] O. Steinbach: On the mapping properties of boundary integral operators for the heat equation, in preparation.

Pseudodifferential equations in polyhedral domains II: hp approximation and graded meshes

Jakub Stocek
(joint work with H. Gimperlein, E. P. Stephan)

Starting from the regularity results in the talk by H. Gimperlein, this talk discusses the numerical approximation of boundary problems involving nonlocal operators, such as the integral fractional Laplacian. The article [4] surveys recent progress in their numerical analysis.

For elliptic differential boundary value problems in polyhedral domains, explicit singular expansions of their solutions give rise to h and hp discretizations with optimal convergence rates for finite [2] and boundary element methods [11]. In recent work [9, 10], corresponding results have been obtained for the fractional Laplacian and, in [7], for a class of nonlocal transmission problems.

We consider the numerical approximation of the integral fractional Laplacian, defined for a Schwartz function u on $\mathbb{R}^n$ by

$$(-\Delta)^s u(x) = c_{n,s}\, P.V. \int_{\mathbb{R}^n} \frac{u(x)-u(y)}{|x-y|^{n+2s}} dy, \qquad (s \in (0,1)).$$

Here $P.V.$ denotes the Cauchy principal value and $c_{n,s} = \frac{2^{2s} s \Gamma\left(\frac{n+2s}{2}\right)}{\pi^{\frac{n}{2}}}$. The operator $(-\Delta)^s : \widetilde{H}^s(\mathbb{R}^n) \to H^{-s}(\mathbb{R}^n)$ is a pseudodifferential operator of order $2s$.

The corresponding fractional Dirichlet problem in a domain $\Omega \subset \mathbb{R}^n$ is given by

$$\begin{aligned} (-\Delta)^s u &= f \text{ in } \Omega, \\ u &= 0 \text{ in } \Omega^C = \mathbb{R}^n \setminus \overline{\Omega}\ , \end{aligned} \tag{1}$$

and its weak formulation is given by: Find $u \in \widetilde{H}^s(\Omega)$ such that for all $v \in \widetilde{H}^s(\Omega)$

$$\frac{c_{n,s}}{2} \iint_{\mathbb{R}^n \times \mathbb{R}^n} \frac{(u(x)-u(y))(v(x)-v(y))}{|x-y|^{n+2s}} dx\ dy = \int_{\mathbb{R}^n} f(x) v(x)\ dx\ . \tag{2}$$

We discuss the Galerkin discretization of (2) by piecewise polynomials $V_h^p \subset \widetilde{H}^s(\Omega)$ of degree p: Find $u_h \in V_h^p$ such that for all $v \in V_h^p$

$$\frac{c_{n,s}}{2} \iint_{\mathbb{R}^n \times \mathbb{R}^n} \frac{(u_h(x)-u_h(y))(v_h(x)-v_h(y))}{|x-y|^{n+2s}} dx\ dy = \int_{\mathbb{R}^n} f(x) v_h(x)\ dx\ . \tag{3}$$

For $f \in H^{-s}(\Omega)$ there exists a unique solution $u \in \widetilde{H}^s(\Omega)$ to (2) and a unique solution $u_h \in V_h^p$ to (3).

For a polygon $\Omega \subset \mathbb{R}^2$ and sufficiently smooth right hand side f, we obtain a precise decomposition of the solution u near the boundary into edge and corner singular functions and a smooth remainder:

Theorem 1. *The solution of* (2) *has the form:*

$$u = u_{\text{reg}} + \sum_{e \in E} u^e + \sum_{v \in V} u^v + \sum_{v \in V} \sum_{e \in E(v)} u^{ev}. \tag{4}$$

Here $u^e(x)$ admits an asymptotic expansion near the edge e with leading part $u^e(x) \sim \operatorname{dist}(x,e)^s$, $u^v(x)$ admits an asymptotic expansion near the vertex v with leading part $u^v(x) \sim \operatorname{dist}(x,v)^\lambda$, and u^{ev} admits a related asymptotic expansion for the edge-vertex singularity. The remainder term u_{reg} is of higher regularity.

The decomposition follows from an extension of the boundary problem to $\mathbb{R}^3_+$, as popularized by Caffarelli and Silvestre [5]. The resulting local, degenerate mixed boundary value problem in the upper half space $\mathbb{R}^3_+$ allows to study the solution u using classical techniques for mixed boundary problems [6].

We present a careful study of the corner exponent λ generalizing classical results for screen problems for the ordinary Laplacian $-\Delta$ which correspond to $s = \frac{1}{2}$, e.g. in [12]. λ relates to the lowest eigenvalue for a perturbed Laplace-Beltrami operator on S^2_+ with mixed Dirichlet and Neumann boundary conditions. We discuss finite element approximations of λ, as well as highly-accurate semi–analytical approximations, as well as qualitative analytical bounds. In particular, we prove that $\max\{0, s-\frac{1}{2}\} < \lambda < 2s$. The upper and lower bounds are sharp: $\lambda \to \max\{0, s-\frac{1}{2}\}$ as the opening angle at the vertex tends to 2π, while $\lambda \to 2s$ as the opening angle tends to 0.

Theorem 1 allows to derive quasi-optimal convergence rates for Galerkin approximations of the fractional Laplacian, for the h-version on β-graded meshes and hp-versions. In 2d it turns out that the approximation error is dominated by the edge, not corner singularities, a consequence of the above-mentioned bound $\lambda > \max\{0, s - \frac{1}{2}\}$.

Our main approximation result for graded meshes generalises work for convex polyhedral domains by Acosta and Borthagaray [1]:

Theorem 2 ([9])**.** *Let $u \in \widetilde{H}^s(\Omega)$ be a solution to* (1) *and $\Pi_h u$ be the best approximation by p.w. linear functions on a β-graded mesh in the $\widetilde{H}^s(\Omega)$ norm.*
Then for $\beta > 2(2-s)$

$$\|u - \Pi_h u\|_{\widetilde{H}^s(\Omega)} \leq C_{\beta,\varepsilon} h^{\min\{\beta/2, 2-s\}-\varepsilon}.$$

For the hp-method our main theorem generalises results by Bespalov and Heuer for boundary integral equations [3]:

Theorem 3 ([10]). *Let $u \in \widetilde{H}^s(\Omega)$ be a solution to (1) and $\Pi_{h,p}u$ be the best approximation by piecewise polynomial functions on a quasi-uniform mesh $\mathcal{T}_h$. Then,*

$$\|u - \Pi_{h,p}u\|_{\widetilde{H}^s(\Omega)} \leq Ch^{\frac{1}{2}}p^{-1}(1 + \log(ph^{-1}))^{\beta},$$

where $\beta \in \mathbb{N}$ relates to the edge and corner behaviour.

The exponential convergence of the *hp*-method on geometrically graded meshes is the content of current work.

Beyond the approximation results, the talk discussed the details of the implementation of *hp*-version finite elements for the integral fractional Laplacian. It illustrated the theoretical results by numerical experiments, to be published in [9, 10].

References

[1] G. Acosta, J. P. Borthagaray, *A fractional Laplace equation: regularity of solutions and finite element approximations*, SIAM Journal on Numerical Analysis 55 (2017), 472–495.

[2] I. Babuška, *Finite element method for domains with corners*, Computing 6 (1970), 264–273.

[3] A. Bespalov, N. Heuer, *The hp-version of the boundary element method with quasi-uniform meshes in three dimensions*, ESAIM: M2AN 5 (2008), 821–849.

[4] J. P. Borthagaray, W. Li, R. H. Nochetto, *Linear and Nonlinear Fractional Elliptic Problems*, arXiv:1906.04230.

[5] L. Caffarelli, L. Silvestre, *An Extension Problem Related to the Fractional Laplacian*, Communications in Partial Differential Equations 32 (2007), 1245–1260.

[6] M. Dauge, *Elliptic boundary value problems in corner domains*, Lecture Notes in Mathematics 1341, Springer Verlag, 1988.

[7] G. Estrada-Rodriguez, H. Gimperlein and J. Stocek, *Nonlocal interface problems: Modelling, regularity, finite element approximation*, preprint (2020).

[8] H. Gimperlein, N. Louca, R. Mazzeo, in preparation.

[9] H. Gimperlein, E. P. Stephan and J. Stocek, *Corner Singularities for the Fractional Laplacian and Finite Element Approximation*, preprint (2020).

[10] H. Gimperlein, E. P. Stephan and J. Stocek, in preparation.

[11] J. Gwinner, E. P. Stephan, *Advanced Boundary Element Methods – Treatment of Boundary Value, Transmission and Contact Problems*, Springer Series in Computational Mathematics 52, Springer, 2018.

[12] J. A. Morrison, J. A. Lewis, *Charge Singularity at the Corner of a Flat Plate*, SIAM Journal on Applied Mathematics 31 (1976), 233–250.

Quadrature for Parabolic Space-Time Galerkin BEM

Johannes Tausch

Boundary integral formulations of parabolic PDEs involve layer operators on the lateral boundary Σ of the space-time domain Q. For instance, the single layer operator of the heat equation is given by

$$\mathcal{V}q(\mathbf{x}, t) = \int_{\Sigma} E(\mathbf{x} - \mathbf{y}, t - \tau)q(\mathbf{y}, \tau)\, d\Sigma_{y,\tau}, \quad (\mathbf{x}, t) \in \Sigma,$$

where the heat kernel is

$$E(\mathbf{x}-\mathbf{y},t-\tau)=\begin{cases}\frac{1}{(4\pi(t-\tau))^{d/2}}\exp\left(-\frac{|\mathbf{x}-\mathbf{y}|^2}{4(t-\tau)}\right), & t>\tau,\\ 0, & t\le\tau.\end{cases}$$

There are two choices for the construction of finite element spaces for the Galerkin discretization

(1) A tensor product of a finite element space on the boundary surface and a finite element space on the time interval.
(2) A space of piecewise polynomials on a triangulation of Σ. Since a parabolic PDE has a time and space variables, the triangulation consists of triangles in two, and tetrahedra in three spatial dimensions.

The first choice is easier to implement and has been analyzed in [1]. The second choice has received some recent interest [2] and enables space-time adaptivity and moving geometries with changes of topology. In either case, the numerical realization of Galerkin method involves computing possibly singular integrals. In the context of layer potentials for elliptic operators it is well known how to obtain singularity removing transformations which lead to efficient quadrature rules [4]. For parabolic operators discretized with tensor product meshes a similar methodology was developed in [3].

The goal of this work is to introduce these transformations for the case of a triangulation of Σ. If Σ_x, Σ_y are two patches on the space-time boundary, then the task is to compute integrals of the form

$$I=\int_{\Sigma_x}\int_{\Sigma_y}E(\mathbf{x}-\mathbf{y},t-\tau)\psi(\mathbf{x},\mathbf{y},t,\tau)\,d\Sigma_{y,\tau}\,d\Sigma_{x,t}\,. \tag{1}$$

Here $\psi(\mathbf{x},\mathbf{y},t,\tau)$ is a smooth function that incorporates contributions of the shape functions and the kernel has singularities if Σ_x and Σ_y coincide, have a common vertex, edge or, in the case of three spatial dimensions, have a common face.

The patches Σ_x and Σ_y can be parametrized by the standard simplex

$$\sigma^{(n)}=\{\,\widehat{\mathbf{x}}\,:\,0\le\widehat{x}_n\le\cdots\le\widehat{x}_1\le 1\}$$

using an affine transformation. Thus integral (1) becomes

$$I=\int\limits_{\sigma^{(n)}}\int\limits_{\sigma^{(n)}}k(\widehat{\mathbf{x}},\widehat{\mathbf{y}})\,d\widehat{\mathbf{y}}\,d\widehat{\mathbf{x}}. \tag{2}$$

The integration domain $\sigma^{(n)}\times\sigma^{(n)}$ is a complex polytope in $2n$ dimension which is the convex hull of the vertices

$$\mathbf{e}_{i,j}=\begin{bmatrix}\mathbf{e}_i\\ \mathbf{e}_j\end{bmatrix},\quad i,j\in\{0,\ldots,n\},$$

where the $\mathbf{e}_i$'s denote the vertices of the standard simplex $\sigma^{(n)}$

$$\mathbf{e}_0 = \begin{bmatrix} 0 \\ 0 \\ \vdots \\ 0 \end{bmatrix} \quad \mathbf{e}_1 = \begin{bmatrix} 1 \\ 0 \\ \vdots \\ 0 \end{bmatrix} \quad \mathbf{e}_2 = \begin{bmatrix} 1 \\ 1 \\ \vdots \\ 0 \end{bmatrix} \quad \dots \; \mathbf{e}_n = \begin{bmatrix} 1 \\ 1 \\ \vdots \\ 1 \end{bmatrix}.$$

The polytope $\sigma^{(n)} \times \sigma^{(n)}$ is then divided into simplices in $\mathbb{R}^{2n}$ using the planes $x_1 = y_1, \dots, x_n = y_n$

$$\sigma^{(n)} \times \sigma^{(n)} = \bigcup_{k=1}^{N_n} S_k \,.$$

We obtain $N_2 = 6$ and $N_3 = 20$. The next step is to introduce the singular and non-singular variables. For two spatial dimensions ($n = 2$) we set

$s = 2:$	$s = 3:$	$s = 4:$
$z_1' = y_1 - x_1,$	$z_1' = y_1 - x_1,$	$z_1' = x_1,$
$z_2' = y_2 - x_2,$	$z_2' = x_2,$	$z_2' = x_2,$
$\breve{z}_1 = x_1,$	$z_3' = y_2,$	$z_3' = x_1,$
$\breve{z}_2 = x_2,$	$\breve{z}_1 = x_1,$	$z_4' = x_2,$

depending on whether Σ_x and Σ_y are identical (s=2), have a common edge (s=3) or a common vertex (s=4). Here, s is the number of singular variables. Proceeding analogously for three spatial dimensions implies that the number of singular variables is $s \in \{3, 4, 5, 6\}$.

The simplices S_k are again images of simplices in $\mathbf{z}$-coordinates, the latter simplices can be mapped by a second linear transformation to the standard simplex $\sigma^{(2n)}$. By construction, the singular variables are mapped on the s-dimensional standard simplex $\sigma^{(s)}$. The domain for the remaining variables is a simplex in $\mathbb{R}^{2n-s}$ whose vertices depend linearly on the singular variables. Since the latter variables do not enter the kernel, they only appear as polynomials and can be integrated analytically. Thus integral (2) appears as

$$I_k = \int_{\sigma^{(s)}} \frac{1}{\mathbf{b} \cdot \mathbf{w}'^{\frac{n}{2}}} E\left(\frac{|B\mathbf{w}'|}{\mathbf{b} \cdot \mathbf{w}'^{\frac{1}{2}}}\right) \psi(\mathbf{w}') \, d\mathbf{w}'. \tag{3}$$

where $\psi(\cdot)$ is a polynomial, and B and $\mathbf{b}$ represent the coefficients of the transformation that maps $\mathbf{w}'$ to $\mathbf{x} - \mathbf{y}$ and $t - \tau$. This integral is singular at $\mathbf{w}' = 0$ which suggests to use the Duffy-like transform

$$\mathbf{w}' = \begin{bmatrix} \xi^2 \\ \xi^2 \mathbf{w} \end{bmatrix} \quad \text{where } \mathbf{w} \in \sigma^{(s-1)},$$

which has Jacobian ξ^{2s-1}. Then

$$t - \tau = \mathbf{b}' \cdot \mathbf{w} = \xi^2 \left(b_0 + b_1 w_1 + \cdots + b_{s-1} w_{s-1}\right) := \xi^2 \, \beta(\mathbf{w}),$$

and integral (3) becomes

$$I_k = \int_0^1 \int_{\sigma^{(s-1)}} \frac{\xi^{2s-1-n}}{\beta(\mathbf{w})^{\frac{n}{2}}} E\left(\xi \frac{c(\mathbf{w})}{\beta(\mathbf{w})^{\frac{1}{2}}}\right) \psi(\xi^2 \mathbf{w})\, d\mathbf{w}\, d\xi. \tag{4}$$

Note that the smallest power of ξ in the numerator occurs when $n = 2$ and $s = 2$. In this case $2s - 1 - n = 1$, so the singularity at $\xi = 0$ gets canceled by this power. However, this does not prove that the integrand will always be a smooth function. In particular, the integrand is singular when the quantity $t - \tau$ (and hence $\beta(\mathbf{w})$) changes signs when Σ_x and Σ_y overlap in the time variable.

Recall that the function $E(\cdot)$ is continued by zero when $\beta(\mathbf{w}) \leq 0$, thus we have to integrate integral (4) only over the intersection of $\sigma^{(s-1)}$ with the half-space $H^+ = \{\mathbf{w} : \beta(\mathbf{w}) \geq 0\}$, i.e., the domain

$$T := \sigma^{(s-1)} \cap H^+.$$

We will now describe the geometry of T in more detail. We set $d = s - 1$ and re-name the vertices of $\sigma^{(d)}$ to $\mathbf{v}_i$ such that

$$\mathbf{v}_i \in H^+, \quad i \in \{0, \ldots, \widehat{d}\},$$
$$\mathbf{v}_{\widehat{d}+j} \in H^-, \quad j \in \{1, \ldots, \widetilde{d}\}.$$

Here, H^- defines the complementary half-space. Since a simplex has an edge between any pair of vertices, there are intersection points $\mathbf{v}_{i,j}$ with the plane H^0 on the edges between $\mathbf{v}_i$ and $\mathbf{v}_{\widehat{d}+j}$. For convenience, we also denote the vertices $\mathbf{v}_i$ by $\mathbf{v}_{i,0}$. It is then easy to verify that the vertices of T are the convex hull of the points $\mathbf{v}_{i,j},\ i = 0 \ldots \widehat{d},\ j = 0 \ldots \widetilde{d}$, which motivates us to define the transform

$$\mathbf{w} = \phi(\widehat{\mathbf{w}}, \widetilde{\mathbf{w}}) = \sum_{i,j} \mathbf{v}_{i,j}\, \phi_i(\widehat{\mathbf{w}}) \phi_j(\widetilde{\mathbf{w}}). \tag{5}$$

Here ϕ_i denote the linear Lagrange polynomials of the standard simplex, i.e., $\phi_i(\mathbf{e}_j) = \delta_{i,j}$. Since $0 \leq \phi_i \leq 1$ and $\sum_i \phi_i = 1$ it follows that ϕ maps $\sigma^{(\widehat{d})} \times \sigma^{(\widetilde{d})}$ into T. The following result states that the map ϕ is also onto.

Theorem 1. *If the plane H^0 does not contain any of the vertices of $\sigma^{(d)}$ then T is combinatorially equivalent to $\sigma^{(\widehat{d})} \times \sigma^{(\widetilde{d})}$ and equation* (5) *defines a bijective map between $\sigma^{(\widehat{d})} \times \sigma^{(\widetilde{d})}$ and T.*

We do not give a careful proof of this result here. We only mention that the idea is to arrange the vertices $\mathbf{e}_{i,j}$ in and $\mathbf{v}_{i,j}$ into two rectangular arrays. The faces of each polytope are obtained by canceling rows and columns from the array. Thus there is a one-to-one correspondence of all faces. Further, beginning with the lowest-dimension, we see that ϕ in (5) maps bijectively between the corresponding faces.

Returning to the affine function $\beta(\mathbf{w})$, we see that

$$\beta(\mathbf{w}) = \sum_{i,j} \beta(\mathbf{v}_{i,j}) \phi_i(\widehat{\mathbf{w}}) \phi_j(\widetilde{\mathbf{w}}) = \sum_i \beta(\mathbf{v}_{i,0}) \phi_i(\widehat{\mathbf{w}})(1 - \widetilde{w}_1)$$

Here, the last step follows from the fact that β vanishes on the vertices on H^0 and that $\phi_0(\widetilde{\mathbf{w}}) = 1 - \widetilde{w}_1$. Now introduce another Duffy transform

$$\widetilde{\mathbf{w}} = \begin{bmatrix} 1-\zeta \\ (1-\zeta)\breve{\mathbf{w}} \end{bmatrix} \quad \text{where } \breve{\mathbf{w}} \in \sigma^{(\breve{d}-1)}.$$

Thus $\zeta = 1 - \widetilde{w}_1$ and integral(4) becomes

$$I_k = \int_0^1 \int_0^1 \int_{\sigma^{(\widehat{d})}} \int_{\sigma^{(\breve{d}-1)}} \frac{\xi}{\zeta} E\left(\frac{\xi}{\zeta}\psi_1(\zeta, \widehat{\mathbf{w}}, \breve{\mathbf{w}})\right) \psi_2\left(\xi, \zeta, \widehat{\mathbf{w}}, \breve{\mathbf{w}}\right) \, d\widehat{\mathbf{w}} d\breve{\mathbf{w}} \, d\zeta d\xi$$

where $\psi_1 > 0$ is smooth and ψ_2 is a polynomial. To handle the ratio ξ/ζ we introduce the following two transform which map $(\lambda, \mu) \in [0,1]^2$ to two triangles in the (ξ, ζ) plane which add up to $[0,1]^2$,

$$(a) \begin{bmatrix} \xi \\ \zeta \end{bmatrix} = \begin{bmatrix} \lambda\mu \\ \lambda \end{bmatrix}, \quad \text{and} \quad (b) \begin{bmatrix} \xi \\ \zeta \end{bmatrix} = \begin{bmatrix} \lambda \\ \lambda\mu \end{bmatrix}$$

Since the Jacobian contributes an additional factor of λ we find that I_k is the sum of

$$I_k^{(a)} = \int_0^1 \int_0^1 \int_{\sigma^{(\widehat{d})}} \int_{\sigma^{(\breve{d}-1)}} E\Big(\mu\psi_1\left(\lambda, \mu, \widehat{\mathbf{w}}, \breve{\mathbf{w}}\right)\Big) \psi_2\left(\lambda, \mu, \widehat{\mathbf{w}}, \breve{\mathbf{w}}\right) \, d\widehat{\mathbf{w}} d\breve{\mathbf{w}} \, d\lambda d\mu$$

$$I_k^{(b)} = \int_0^1 \int_0^1 \int_{\sigma^{(\widehat{d})}} \int_{\sigma^{(\breve{d}-1)}} \frac{1}{\mu} E\left(\frac{1}{\mu}\psi_1\left(\lambda, \mu, \widehat{\mathbf{w}}, \breve{\mathbf{w}}\right)\right) \psi_2\left(\lambda, \mu, \widehat{\mathbf{w}}, \breve{\mathbf{w}}\right) \, d\widehat{\mathbf{w}} d\breve{\mathbf{w}} \, d\lambda d\mu$$

These integrands are smooth and can be treated using standard quadrature rules.

References

[1] M. Costabel, *Boundary integral operators for the heat equation* Integral Equations Operator Theory, **13**, (1990) 498-552

[2] S. Dohr, J. Zapletal, G. Of, M. Merta and M. Kravčenko, *A parallel space time boundary element method for the heat equation* Comput. Math. Appl., **77** (2019), 2852-2866

[3] N. Mason and J. Tausch, *Quadrature for parabolic Galerkin BEM with moving surfaces* Comput. Math. Appl., **78** (2019), 1-14

[4] S. Sauter and C. Schwab, *Randelementmethoden: Analyse, Numerik und Implementierung schneller Algorithmen*, Teubner, Stuttgart, 2004

Boundary integral equations and boundary element methods for eigenvalue problems in acoustics and electromagnetics

Gerhard Unger

We analyze boundary integral equations and boundary element methods for eigenvalue problems in acoustics [6, 8] and electromagnetics [3, 9]. The cavity eigenvalue problem and the scattering resonance for an impenetrable and a penetrable scatterer are considered. The proposed boundary integral formulations for these eigenvalue problems are boundary integral formulations of the first kind and are based on the same boundary integral equations and boundary integral operators as those for the related source problems. Boundary integral formulations of eigenvalue problems always lead to nonlinear eigenvalue problems with respect to the eigenvalue parameter even if the original eigenvalue problem is a linear one. The reason for that is that the eigenvalue parameter occurs nonlinearly in the fundamental solution of the involved partial differential operator. However, as described below, the discretized eigenvalue problems may be transformed to equivalent linear eigenvalue problems by the contour integral method.

The considered boundary integral formulations of the eigenvalue problem are eigenvalue problems for holomorphic Fredholm operator-valued functions. For such kind of eigenvalue problems a comprehensive spectral theory exists [7]. Moreover, abstract results on the convergence for the approximation of such kind of eigenvalue problems are available [4, 5]. In particular, these convergence results are valid for the conforming Galerkin approximation of eigenvalue problems for holomorphic operator-valued functions if the occurring operators satisfy a Gåding's inequality. We have applied these convergence results in [8] to Galerkin boundary element approximations of acoustic eigenvalue problems and in [6] to coupled FEM-BEM formulations of vibro-acoustic eigenvalue problems, and we have shown that quasi-optimal error estimates are achieved. For electromagnetic eigenvalue problems the occurring boundary integral operators satisfy only a generalized Gårding's inequality. In such a case additional properties of the approximation spaces are required in order to guarantee convergence. In [2] sufficient conditions for the convergence of a conforming Galerkin approximation for such kind of eigenvalue problems are derived in an abstract setting. In [9] we have shown that these conditions are satisfied for the Galerkin approximation of boundary integral formulations of electromagnetic eigenvalue problems when classical boundary elements of Raviart-Thomas or Brezzi–Douglas–Marini type are used.

The Galerkin approximation of boundary integral formulations of eigenvalue problems result in eigenvalue problems for holomorphic matrix-valued functions for which commonly the contour integral method [1] is applied. The contour integral method is a reliable method for the approximation of all eigenvalues which lie inside of a given contour in the complex plane, and for the approximation of the corresponding eigenvectors. The method is based on the contour integration of the inverse of the occurring matrix-valued function of the eigenvalue problem and utilizes that the eigenvalues are poles of it. By contour integration a reduction

of the eigenvalue problem for a holomorphic matrix-valued function to an equivalent linear matrix eigenvalue problem is possible such that the eigenvalues of the linear eigenvalue problem coincide with the eigenvalues of the nonlinear eigenvalue problem inside the contour. For the practical application of this method an efficient approximation of the contour integral over the inverse of the underlying matrix-valued function of the eigenvalue problem is necessary. This can be achieved for example by the composite trapezoidal rule which requires the solution of several linear systems involving boundary element matrices related to the eigenvalue problem.

In photonics and plasmonics there is currently an intensive discussion in which respect eigenvalues and eigenmodes related to scattering problems can be used to describe the scattering behavior of a scatterer in given frequency range. In mathematical terms this leads to the question of modal expansion and of the modal approximation of the solution operator of scattering problems. We use boundary integral equation methods together with the analytic Fredholm theory to tackle this question. The solution operator of scattering problems can be described, when using appropriate boundary integral operators, as the inverse of a holomorphic Fredholm operator-valued function, which is a meromorphic operator-valued function. The Keldysh theorem [7] for holomorphic Fredholm operator-valued functions provides for any simple connected bounded domain in the complex plane with smooth boundary a representation of the principal part of the inverse of such kind of functions in terms of its eigenvalues which lie inside the domain and in terms of the corresponding eigenmodes. Numerical experiments in [3] show that at least for well separated eigenvalues this principal part can be utilized to achieve good approximations of scattering properties over a whole frequency range of interest. However, one of the central questions is still open, namely: under which condition it is possible to represent the solution operator of scattering problems purely in terms of the eigenvalues and eigenmodes.

References

[1] Beyn, W.J.: An integral method for solving nonlinear eigenvalue problems. Linear Algebra Appl. **436**(10), 3839–3863 (2012).

[2] Halla, M.: Analysis of radial complex scaling methods for scalar resonance problems in open systems. Ph.d. thesis, TU Vienna (2019)

[3] U. Hohenester, G. Unger, A. Trügler, *Novel Modal Approximation Scheme for Plasmonic Transmission Problems*, Phys. Rev. Lett. **121**, (2018), 246802.

[4] O. Karma, Approximation in eigenvalue problems for holomorphic Fredholm operator functions. I. *Numer. Funct. Anal. Optim.*, **17(3-4)**, (1996), pp. 365–387 .

[5] O. Karma, Approximation in eigenvalue problems for holomorphic Fredholm operator functions. II. *Numer. Funct. Anal. Optim.*, **17(3-4)**, (1996), pp. 389– 408.

[6] A. Kimeswenger, O. Steinbach, and G. Unger, *Coupled finite and boundary element methods for fluid-solid interaction eigenvalue problems*, SIAM J. Numer. Anal. **52**(5) (2014), 2400–2414.

[7] Kozlov, V., Maz′ya, V.: Differential Equations with Operator Coefficients with Applications to Boundary Value Problems for Partial Differential Equations. Springer-Verlag, Berlin (1999)

[8] O. Steinbach and G. Unger, *Convergence analysis of a Galerkin boundary element method for the Dirichlet Laplacian eigenvalue problem*, SIAM J. Numer. Anal. **50** (2012), 710–728.
[9] G. Unger, Convergence analysis of a Galerkin boundary element method for electromagnetic eigenvalue problems, Berichte aus dem Institut für Numerische Mathematik, 17/2, TU Graz, 2017.

A New Approach to Time Domain Boundary Integral Equations for the Wave Equation

Carolina Urzúa-Torres
(joint work with Olaf Steinbach)

Let $\Omega \subset \mathbb{R}^n$ $(n = 1, 2, 3)$ be a bounded interval for $n = 1$, or a bounded Lipschitz domain for $n \geq 2$. Let $(0, T)$ be a time interval with finite time horizon $T > 0$. We define the space-time cylinder $Q := \Omega \times (0, T) \subset \mathbb{R}^{n+1}$, and its lateral boundary $\Sigma := \partial\Omega \times [0, T]$. As model problems, we consider both the *interior* Dirichlet initial boundary value problem for the wave equation

$$
(1) \qquad \begin{cases} \partial_{tt} u(x,t) - \Delta_x u(x,t) = 0 & \text{for } (x,t) \in Q, \\ u(x,t) = g(x,t) & \text{for } (x,t) \in \Sigma, \\ u(x,0) = 0 & \text{for } x \in \Omega, \\ \partial_t u(x,0) = 0 & \text{for } x \in \Omega, \end{cases}
$$

and its corresponding *exterior* counterpart in $\mathbb{R}^n \setminus \overline{Q}$.

Different strategies have been used to derive variational methods for time domain boundary integral equations for the wave equation (1). The more established and succesful ones include weak formulations derived via the Laplace transform, and also space-time energetic variational formulations, often referred as *energetic BEM* in the literature. These approaches started with the groundbreaking works of Bamberger and Ha Duong [2], and Aimi et al. [1], respectively. We refer the reader to [4, 5, 6] and the references therein for an overview and more recent developments on time dependent boundary integral equations for the wave equation.

In spite of their extensive use, the corresponding numerical analysis of these formulations is still incomplete and presents difficulties that are hard to overcome, if possible at all.

One of these difficulties is the fact that current approaches provide continuity and coercivity estimates which are not in the same space-time (Sobolev) norms. Indeed, there is a so-called *norm gap* arising from a loss of regularity in time of the related boundary integral operators. Yet, recent work by Joly and Rodríguez shows that these norm gaps are not present in 1D [6]. Moreover, to the best of the authors' knowledge, there is no proof nor numerical evidence that such loss of time regularity should hold for higher dimensions either. These two observations encourage us to believe that one may be able to prove sharper results using different mathematical tools.

On the other hand, current strategies do not provide the foundations for space-time boundary element methods, which are basically boundary element discretizations

where the time variable is treated simply as another space variable, in contrast to techniques such as time-stepping methods and convolution quadrature methods [7].

Space-time discretization methods offer an increasingly popular alternative, since they allow the treatment of moving boundaries, adaptivity in space and time simultaneously, and space-time parallelization. However, in order to exploit these advantages, one needs to have a complete numerical analysis of the corresponding Galerkin methods.

In this talk, we present a new approach to formulate boundary integral equations for the wave equation. Based on [8, 10], we work directly in the time domain and aim for a mathematical framework that overcomes the aforementioned difficulties and also paves the way to stable space-time FEM/BEM coupling.

For this, we begin by considering the Sobolev spaces used by Costabel in [3], which are defined on the *extended space-time cylinders* $Q_- := \Omega \times (-\infty, T)$ and $Q_+ := \Omega \times (0, \infty)$, and allow us to include the zero initial conditions $u(x, 0) = 0$ and $\partial_t u(x, 0) = 0$ for $x \in \Omega$. There we derive trace theorems, Green's formulas, representation formulas, boundary integral operators, and Calderón identities.

Next, we discuss how to exploit the tools from [8] to achieve an ellipticity estimate for the weakly singular boundary integral operator V arising from (1) in $1D$. This new estimate is in the natural energy trace space for V, i.e. it does not lose time regularity. The key piece for this result is a Hilbert-type transform studied in [8, 9] for the heat equation. We explain how this leads to the expected estimates in $1D$ and the connection of our work with the energetic BEM approach. Finally, we conclude by mentioning how we expect that these ideas extend to higher dimensions.

References

[1] A. Aimi, M. Diligenti, C. Guardasoni, and S. Panizzi, *A space-time energetic formulation for wave propagation analysis by BEMs*, Riv. Mat. Univ. Parma 7 (2008) 171–207.

[2] A. Bamberger, T. Ha Duong: *Formulation variationnelle pour le calcul de la diffraction d'une onde acoustique par une surface rigide*, Math. Methods Appl. Sci. 8 (1986) 598–608.

[3] M. Costabel: *Boundary Integral Operators for the Heat Equation*, Integral Equations and operator Theory 13 (1990) 498–552.

[4] M. Costabel: *Developments in boundary element methods for time-dependent problems.* In: Problems and Methods in Mathematical Physics (L. Jentsch, F. Tröltzsch eds.), Teubner Texte zur Mathematik, vol. 134, B. G. Teubner, Stuttgart, Leipzig (1994), pp. 17–32.

[5] T. Ha-Duong: *On retarded potential boundary integral equations and their discretisation.* In: Topics in computational wave propagation. Direct and inverse problems (M. Ainsworth, P. Davies, D. Duncan, P. Martin, B. Rynne, eds.), Lecture Notes in Computational Science and Engineering, vol. 31, Springer, Berlin (2003), pp. 301–336.

[6] P. Joly, J. Rodríguez: *Mathematical Aspects of Variational Boundary Integral Equations for Time Dependent Wave Propagation*, J. Integral Equations Appl., 29 (2017) 137–187.

[7] F.-J. Sayas: *Retarded ptentials and time domain boundary integral equations. A road map*, Springer Series in Computational Mathematics (2016).

[8] O. Steinbach, M. Zank: *Coercive space-time finite element methods for initial boundary value problems*, Electron. Trans. Numer. Anal., accepted (2020).

[9] O. Steinbach, M. Zank: *A note on the efficient evaluation of a modified Hilbert transformation*, submitted (2019).
[10] M. Zank: *Inf-sup stable space-time methods for time-dependent partial differential equations*, Dissertation, TU Graz (2019).

Reporter: Ralf Hiptmair

Participants

Prof. Dr. Francesco P. Andriulli
Dipartimento di Matematica
Politecnico di Torino
Corso Duca degli Abruzzi, 24
10129 Torino
ITALY

Dr. Martin Averseng
Centre INRIA Saclay
École Polytechnique
CMAP UMR 7640 CNRS
Route de Saclay
91128 Palaiseau Cedex
FRANCE

Prof. Dr. Steffen Börm
Lehrstuhl Scientific Computing
Institut für Informatik
Christian-Albrechts-Universität zu Kiel
Christian-Albrecht-Platz 4
24118 Kiel
GERMANY

Dr. Stéphanie Chaillat-Loseille
ENSTA - UMA ParisTech
Laboratoire POEMS
Bureau 2226
828, Boulevard des Maréchaux
91762 Palaiseau Cedex
FRANCE

Prof. Dr. Simon N. Chandler-Wilde
Department of Mathematics and Statistics
University of Reading
Whiteknights
P.O. Box 220
Reading RG6 6AX
UNITED KINGDOM

Dr. Xavier Claeys
Laboratoire Jacques-Louis Lions
Université Pierre et Marie Curie
Bureau 15-25-310
4 place Jussieu
75005 Paris Cedex
FRANCE

Dr. Marion Darbas
LAMFA CNRS 7352 - UMR
Université de Picardie Jules Verne
UFR de Sciences
33, rue Saint-Leu
80039 Amiens Cedex 1
FRANCE

Prof. Dr. Jürgen Dölz
Fachbereich Mathematik
Technische Universität Darmstadt
Dolivostraße 15
64293 Darmstadt
GERMANY

Dr. Victor Dominguez
Department of Mathematics and Computer Engineering
Universidad Pública de Navarra
Campus de Tudela
Avenida de Tarazona, s/n
31500 Tudela (Navarro)
SPAIN

Prof. Dr. Mahadevan Ganesh
Department of Applied Mathematics and Statistics
Colorado School of Mines
Chauvenet Hall 222
1500 Illinois Street
Golden, CO 80401-1887
UNITED STATES

Prof. Dr. Adrianna Gillman
Department of Applied Mathematics
University of Colorado, Boulder
Engineering Center, ECOT 335
Boulder, CO 80309-0526
UNITED STATES

Dr. Heiko Gimperlein
Maxwell Institute for Mathematical Sciences
and Department of Mathematics
Heriot-Watt University
Riccarton
Edinburgh EH14 4AS
UNITED KINGDOM

Prof. Dr. Helmut Harbrecht
Departement Mathematik und Informatik
Universität Basel
Spiegelgasse 1
4051 Basel
SWITZERLAND

Prof. Dr. Ralf Hiptmair
Seminar für Angewandte Mathematik
ETH - Zentrum
Rämistrasse 101
8092 Zürich
SWITZERLAND

Dr. Carlos F. Jerez-Hanckes
Faculty of Engineering and Sciences
Universidad Adolfo Ibáñez
Campus Peñalolén
Diagonal Las Torres 2700
Santiago, Région Metropolitana
CHILE

Dr. Frédérique Le Louër
Laboratoire de Mathématiques Appliquées
Université de Technologie de Compiègne
Département Génie Informatique
LMAC EA 2222, Bureau P 123
Sorbonne Universités
57, Avenue de Landshut
60203 Compiègne Cedex
FRANCE

Prof. Dr. Eric Michielssen
Electrical Engineering and Computer Science Department
The University of Michigan
3420 EECS
500 S. State Street
Ann Arbor MI 48109-2122
UNITED STATES

Prof. Dr. Dirk Praetorius
Institut für Analysis und Scientific Computing
Technische Universität Wien
E 101/4
Wiedner Hauptstrasse 8-10
1040 Wien
AUSTRIA

Prof. Dr. Sergej Rjasanow
Fachrichtung Mathematik
Universität des Saarlandes
Geb. E1.1, Rm 3.26
Postfach 151150
66041 Saarbrücken
GERMANY

Prof. Dr. Stefan A. Sauter
Institut für Mathematik
Universität Zürich
Winterthurerstrasse 190
8057 Zürich
SWITZERLAND

Prof. Dr. Martin Schanz
Institut für Baumechanik
Technische Universität Graz
Technikerstraße 4/II
8010 Graz
AUSTRIA

Dr. Euan A. Spence
Department of Mathematical Sciences
University of Bath
Claverton Down
Bath BA2 7AY
UNITED KINGDOM

Prof. Dr. Olaf Steinbach
Institut für Angewandte Mathematik
Technische Universität Graz
Steyrergasse 30
8010 Graz
AUSTRIA

Jakub Štoček
Department of Mathematics
Heriot-Watt University
Riccarton Campus
Edinburgh EH14 4AS
UNITED KINGDOM

Prof. Dr. Johannes Tausch
Department of Mathematics
Southern Methodist University
Clements Hall, 209 B
Dallas TX 75275-0156
UNITED STATES

Dr. Gerhard Unger
Institut für Angewandte Mathematik
Technische Universität Graz
Steyrergasse 30
8010 Graz
AUSTRIA

Dr. Carolina Urzúa-Torres
Mathematical Institute
University of Oxford
AWB
Woodstock Road
Oxford OX2 6GG
UNITED KINGDOM